ALKALI SILICA REACTIVITY OF BLENDED CLASS C AND CLASS F FLY ASH SYSTEMS

by

Ikechukwu K. Okechi, B.Eng.

A thesis submitted to the Graduate Council of
Texas State University in partial fulfillment
of the requirements for the degree of
Masters of Science
with a Major in Technology Management
August 2019

Committee Members:

Federico Aguayo, Chair

Yoo-Jae Kim

Anthony Torres

COPYRIGHT

by

Ikechukwu K. Okechi

2019

FAIR USE AND AUTHOR'S PERMISSION STATEMENT

Fair Use

Duplication Permission

DEDICATION

I would like to dedicate this to Almighty God, who answers prayers and never fails.

ACKNOWLEDGEMENTS

I would like to take this opportunity to express my appreciation and gratitude towards my parents, Richard Okechi and Theresa Okechi, for their loving support and encouragement.

My sincere appreciation also goes to my academic advisor, Dr. Federico Aguyao, for the academic and professional guidance he provided me during the course of my graduate studies. He was very patient with me and never declined to assist me whenever I consult him. I wouldn't have wished for any better advisor. I also want to appreciate Olvin Funez, Brent Vant Land, Desmond Davis and Maria Valdez for their immense support during my research.

I would also like to appreciate the members of my thesis committee, Dr. Yoo-Jae Kim, and Dr. Anthony Torres for their assistance and advice.

Lastly, I thank the faculty and staffs in the Department of Engineering Technology for their continuous support all through my studies.

TABLE OF CONTENTS

Page

ACKNOWLEDGEMENTS v

LIST OF TABLES x

LIST OF FIGURES xii

ABSTRACT xv

CHAPTER

1. INTRODUCTION 1

    1.1 Background 1
    1.2 Problem Statement 1
    1.3 Research Objective 3
    1.4 Research Significance 3
    1.5 Thesis Organization 4

2. LITERATURE REVIEW 5

    2.1 Fly Ash 5
        2.1.1 Fly ash background 5
        2.1.2 Recent changes to fly ash 9
    2.2 Hydration Mechanism of Fly Ash Concrete 14
    2.3 Fresh Properties of Fly Ash Concrete 16
    2.4 Hardened Properties of Fly Ash Concrete 19
    2.5 Alkali Silica Reaction 24
        2.5.1 Mechanisms of ASR 24
        2.5.2 Test methods to evaluate ASR of cementitious mixtures 26
        2.5.3 Mitigation and prevention of ASR with fly ash concrete 29

3. EXPERIMENTAL MATERIALS AND POCEDURES 32

3.1 Mechanical Properties.....32
3.1.1 Materials and mix proportion.....32
3.1.2 Apparatus 38
3.1.3 Procedure 38
3.1.3.1 Fresh propreties.....38
3.1.3.2 Splitting tensile strength 39
3.1.3.3 Compressive strength.....39
3.1.3.4 Elastic modulus.....40
3.1.3.5 Drying shrinkage.....40
3.2 Heat of Hydration using Isothermal Calorimetry 41
3.2.1 Materials and mix proportion.....41
3.2.2 Apparatus 45
3.2.3 Procedure 45
3.3 Alkali Silica Reactivity 47
3.3.1 Accelerated mortar bar test/ Mortar bar test 47
3.3.1.1 Materials and mix proportion.....47
3.3.1.2 Apparatus 50
3.3.1.3 Procedure 51
3.3.2 Concrete prism test (ASTM C1293).....51
3.3.2.1 Materials and mix proportion.....51
3.3.2.2 Apparatus 52
3.3.2.3 Procedure 53
3.3.3 Concrete exposure blocks 54
3.3.3.1 Materials and mix proportion.....54
3.3.3.2 Apparatus 54
3.3.3.3 Procedure 55

4. RESULTS AND DISCUSSIONS.....58

4.1 Mechanical Properties....58
4.1.1 Fresh properties....58
4.1.2 Compressive strength....58
4.1.3 Splitting tensile strength....64
4.1.4 Elastic modulus....69
4.1.5 Drying shrinkage....73
4.1.6 Summary of mechanical testing....78
4.2 Heat of Hydration using Isothermal Calorimetry....79
4.2.1 Hydration of blended fly ash paste mixtures....80
4.2.1.1 Influence of blended fly ash systems in paste mixtures at 5°C....80
4.2.1.2 Influence of blended fly ash systems in paste mixtures at 23°C....83
4.2.1.3 Influence of blended fly ash systems in paste mixtures at 38°C....86
4.2.2 Hydration of blended fly ash mortar mixtures....89
4.2.2.1 Influence of blended fly ash systems in mortar mixtures at 5°C....89
4.2.2.2 Influence of blended fly ash systems in mortar mixtures at 23°C....92
4.2.2.3 Influence of blended fly ash systems in mortar mixtures at 38°C....95
4.2.3 Summary of heat of hydration testing....98
4.3 Alkali Silica Reactivity....99
4.3.1 Accelerated mortar bar test/ Mortar bar test....100
4.3.2 Concrete prism test (ASTM 1293)....107
4.3.3 Concrete exposure blocks....109
4.3.4 Summary of ASR testing....114

5. CONCLUSIONS AND RECOMMENDATIONS....116

5.1 Mechanical Properties....116
5.1.1 Compressive strength....116
5.1.2 Splitting tensile strength....117
5.1.3 Elastic modulus....118
5.1.4 Drying shrinkage....118
5.2 Heat of Hydration....119
5.3 Alkali Silica Reactivity....120
5.3.1 Accelerated mortar bar test/ Mortar bar test....120
5.3.2 Concrete prism test....121
5.3.3 Concrete exposure blocks....122
5.4 Recommendation for Future Work....122
REFERENCES....123

LIST OF TABLES

Table **Page**

1. Chemical and Physical Properties of Cement 32
2. Chemical Properties of Fly Ash 33
3. Physical Properties of Aggregates for Mechanical Property Tests 34
4. Testing Matrix for Mechanical Properties 36
5. Mix Proportion for Mechanical Properties Mixtures in kg/m^3 37
6. Testing Matrix for Paste Mixture 42
7. Testing Matrix for Mortar Mixtures 43
8. Mix Proportion for Paste Mixtures 44
9. Mix Proportion for Mortar Mixtures 45
10. Physical Properties of Reactive River Sand 48
11. Mix Proportion for Accelerated Mortar Bar Test 50
12. Mix Proportion for the Concrete Prism Test and Concrete Exposure Blocks 52
13. Environmental Conditions during Test Period (WeatherUnderground, 2019) 57
14. Fresh Properties Tests Results 58
15. Compressive Strength Test Results in MPa 59
16. Splitting Tensile Strength Result in MPa 65
17. Modulus of Elasticity Test Results in GPa 69
18. Drying Shrinkage Results for all Mixtures in Percent 75

19. Heat of Hydration for Binary Paste Mixtures at 5°C 80

20. Heat of Hydration for Ternary Paste Mixtures at 5°C 81

21. Heat of Hydration for Binary Paste Mixtures at 23°C 83

22. Heat of Hydration for Ternary Paste Mixtures at 23°C 84

23. Heat of Hydration for Binary Paste Mixtures at 38°C 86

24. Heat of Hydration for Ternary Paste Mixtures at 38°C 87

25. Heat of Hydration for Binary Mortar Mixtures at 5°C 90

26. Heat of Hydration for Ternary Mortar Mixtures at 5°C.....91

27. Heat of Hydration for Binary Mortar Mixtures at 23°C 93

28. Heat of Hydration for Ternary Mortar Mixtures at 23°C.....94

29. Heat of Hydration for Binary Mortar Mixtures at 38°C 96

30. Heat of Hydration for Ternary Mortar Mixtures at 38°C.....97

31. Fresh Properties Tests Results for ASR Concrete Mixtures.....100

32. Accelerated Mortar Bar Test Expansion Data for Binary Mixtures 101

33. Accelerated Mortar Bar Test Expansion Data for Ternary Mixtures 101

34. One Year Expansion Data for Concrete Prism Test 107

35. One Year Expansion Data for Concrete Exposure Blocks 110

LIST OF FIGURES

Figure **Page**

1. Schematic illustration of the mechanism of ASR in concrete 25

2. Sieve Analysis for River Sand 34

3. Sieve Analysis for Limestone Rock.....35

4. (1) Bench Mixer and 4 ounce Containers (2) Isothermal Calorimeter and Computer System.....47

5. Sieve Analysis for Reactive River Sand 49

6. (1) Storage Container as Prescribed in ASTM C1293 (2) Storage Environment as prescribed in ASTM C1293 53

7. (1) Interior View of 406 x 406 x 406mm (16 x 16 x 16 in) Mold (2) Exterior View of 406 x 406 x 406mm (16 x 16 x 16 in) Mold (3) Concrete Blocks After Casting and Demolding 55

8. Outdoor Exposure Site Located in San Marcos, Texas 57

9. Compressive Strength for Binary Mixture at w/cm of 0.40.....59

10. Compressive Strength for Binary Mixtures at w/cm of 0.45 60

11. Compressive Strength for Ternary Mixtures at w/cm of 0.40 62

12. Compressive Strength for Ternary Mixtures at w/cm of 0.45 63

13. Splitting Tensile Strength for Binary Mixture at w/cm of 0.4.....65

14. Splitting Tensile Strength for Binary Mixtures at w/cm of 0.45 66

15. Splitting Tensile Strength for Ternary Mixtures at w/cm of 0.4.....66

16. Splitting Tensile Strength for Ternary Mixtures at w/cm of 0.45.....67

17. Modulus of Elasticity for Binary Mixture at w/cm of 0.4 70

18. Modulus of Elasticity for Binary Mixture at w/cm of 0.45 70

19. Modulus of Elasticity for Ternary Mixture at w/cm of 0.4.....71

20. Modulus of Elasticity for Ternary Mixture at w/cm of 0.45.....71

21. Percentage Drying Shrinkage for Binary Mixture at w/cm of 0.4.....73

22. Percentage Drying Shrinkage for Ternary Mixture at w/cm of 0.4 74

23. Percentage Drying Shrinkage for Fly Ash Class C Binary Mixtures at w/cm of 0.45 76

24. Percentage Drying Shrinkage for Fly Ash Class F Binary Mixtures at w/cm of 0.45 77

25. Percentage Drying Shrinkage for Ternary Mixtures at w/cm of 0.45.....77

26. Heat of Hydration for Binary Paste Mixtures at 5^{o}C 81

27. Heat of Hydration for Ternary Paste Mixtures at 5^{o}C 82

28. Heat of Hydration for Binary Paste Mixtures at 23^{o}C 84

29. Heat of Hydration for Ternary Paste Mixtures at 23^{o}C 85

30. Heat of Hydration for Binary Paste Mixtures at 38^{o}C 87

31. Heat of Hydration for Ternary Paste Mixtures at 38^{o}C 88

32. Heat of Hydration for Binary Mortar Mixtures at 5^{o}C 90

33. Heat of Hydration for Ternary Mortar Mixtures at 5^{o}C.....91

34. Heat of Hydration for Binary Mortar Mixtures at 23^{o}C 93

35. Heat of Hydration for Ternary Mortar Mixtures at 23^{o}C.....94

36. Heat of Hydration for Binary Mortar Mixtures at 38^{o}C 96

37. Heat of Hydration for Ternary Mortar Mixtures at 38^{o}C.....97

38. Accelerated Mortar Bar Test Results for Class C Fly Ash Binary Mixtures at 20% Replacement.....102

39. Accelerated Mortar Bar Test Results for Class F Fly Ash Binary Mixtures at 20% Replacement.....102

40. Accelerated Mortar Bar Test Results for Class C fly ash Binary Mixtures at 30% Replacement.....103

41. Accelerated Mortar Bar Test Results for Class F Fly Ash Binary Mixtures at 30% Replacement.....103

42. Accelerated Mortar Bar Test Results for Ternary Mixtures Involving Fly Ash C2 and F1 105

43. Accelerated Mortar Bar Test Results for Ternary Mixtures Involving Fly Ash C2 and F2 105

44. Accelerated Mortar Bar Test Results for Ternary Mixtures Involving Fly Ash C2 and F3 106

45. Concrete Prism Test Expansion for Binary Mixtures 108

46. Concrete Prism Test Expansion for Ternary Mixtures 108

47. Exposure Blocks Expansion for Binary Mixtures 110

48. Exposure Blocks Expansion for Ternary Mixtures.....111

49. Rate of Crack Observed on Each Block 113

ABSTRACT

This study presents an assessment of the reactivity and performance of blended systems containing Class C and Class F fly ashes, including fly ashes produced from blended coal sources (bituminous and lignite). Seven fly ashes comprising of three Class F and four Class C with varied calcium and alumina content were obtained from Texas and used in this study. The three Class F fly ashes were designated as F1, F2, and F3, while the four Class C fly ashes were designated as C1, C2, C3, and C4. The Class F fly ash F2 was produced from two different coal sources (bituminous and lignite). These fly ashes were tested to ascertain: the heat of hydration when used as partial replacement for cement, ability to improve mechanical properties and mitigate alkali-silica reaction (ASR). Mortar and concrete mixtures were produced. These mixtures involved binary blends of Class C and Class F fly ashes at 20 and 30% cement replacements, and ternary blends at 10/20%, 20/10% and 15/15% cement replacements for Class C and Class F fly ashes respectively. The following test were performend: compressive strength, splitting tensile strength, elastic modulus, drying shrinkage, heat of hydration using isothermal calorimetry, ASR mitigation using the accelerated mortar bar test (ASTM C1260/C1567) and the concrete prism test (ASTM C1293). The long-term durability was also investigated with the use of large concrete exposure blocks. The results of the mechanical property tests showed that the binary and ternary mixtures involving the Class C fly ashes (C2 and C3) and the Class F fly ash (F2) outperformed other fly ashes in improving mechanical properties especially at early age (Day 7). The heat of hydration test results

showed that the binary and ternary mixtures of the Class C fly ash C2 and the Class F fly ash F2 generated more heat than that of Class F fly ash F1. Finally, the results of the ASR tests showed that the Class F fly ashes performed better than the Class C fly ashes in mitigating ASR. However, the Class F fly ash F1 was the most effective followed by the Class F Fly ashes F2 and F3. The effect of blending was also observed as the ternary mixtures of the Class C and Class F fly ashes were able to keep expansion within the 0.04% limit at year one in the concrete prism test (ASTM C1293) and large concrete exposure blocks.

1. INTRODUCTION

1.1 Background

Concrete is a mixture of fine aggregate, cement, coarse aggregate and water. Compared to other construction materials such as: stone, asphalt, timber, steel, brick, etc., concrete stands out as the most used construction material (Mindess, Young, & Darwin, 2003). One of the unique characteristics of concrete is the ability to be cast into any desired shape and size. This attribute accounts for its wide application (Mindess, Young, & Darwin, 2003). Cement is an important component of concrete that helps bind the other components together. Although cement remains an indispensable component of concrete, the high temperature required for its production and the high amount of greenhouse gas (CO_2) emitted during cement production persist as drawbacks to its usage (García-Lodeiro, Palomo, & Fernández-Jiménez, 2007). The advent and use of mineral admixtures such as: slag, calcined shale, silica fume, calcined clay and fly ash in concrete has not only helped to alleviate these drawbacks, but has also produced concrete of high performance and durability (Chen, 2016).

1.2 Problem Statement

Fly ash is one of the products of coal combustion with immense application in cement and concrete production. The addition of fly ash to concrete has shown to impart tremendous benefits in concrete both in its plastic and hardened state. One of the benefits of adding fly ash to concrete is to mitigate ASR (Ahmaruzzaman, 2010). However, the quality of fly ash produced by electric power generating plants depends mainly on the coal source, as well as the combustion environment and the mineral constituents

(Folliard, Hover, Harris, Ley, & Naranjo, 2009). According to Ramme and Tharaniyil, ASTM C618 Classified fly ash based on the coal source as either Class C or Class F. A high calcium fly ash (Class C) is usually produced from burning lignite or subbituminous coal, while low calcium fly ash (Class F) is usually produced from burning bituminous coal or anthracite (Ramme & Tharaniyil, 2013). In the United States, the quantity and rank of coal produced differs across coal producing states. The state of Wyoming, which was reported by the United States Energy Information Administration (EIA) as the highest producer of coal in 2006 has mainly deposits of sub-bituminous coal. Whereas Texas, which was reported by EIA as the fifth largest producer of coal in 2006 has both deposits of bituminous and sub-bituminous coal (Folliard et al., 2009). According to Folliard et al., out of 102.7 million short tons of coal used in 2003 for generating electricity in Texas, 54% was from Wyoming, 44% from Texas mines and 2% from Colorado. Since fly ash is a by-product, most electrical power generating plant places little or no attention on the rank of coal burnt to produce fly ash. This negligence in the rank of coal burnt introduces variation in the properties of fly ash produced making it difficult to characterize how it may perform in concrete, especially its long-term durability. In addition, many of the electric power generating plants in the country have either converted fully to burning subbituminous coal and/or have been placed offline completely due to the increasing regulation from the Environmental Protections Agency (EPA). More recently, Texas electric power plants have been blending various coals sources (lignite and bituminous blends) to meet environmental regulation, while also attempting to produce quality fly ash for use in concrete. However, very little research has been done to determine how they may perform in fresh and hardened concrete. Thus,

there is a need to evaluate and characterize their performance through short-term and long-term testing.

1.3 Research Objective

The objective of this research is to evaluate the reactivity and performance of blended systems containing Class C and Class F fly ashes, including fly ashes produced from blended coal sources (bituminous and lignite) in improving the mechanical properties of concrete including compressive strength, tensile strength, elastic modulus, and drying shrinkage, as well as mitigating alkali-silica reaction (ASR) through the accelerated mortar bar test (ASTM C1260/C1567), concrete prism test (ASTM C1293) and the long-term durability with large concrete exposure blocks.

1.4 Research Significance

1. To generate short and long-term data for ASR of blended systems containing Class C and Class F fly ashes, as well as fly ashes produced from blended coal sources.
2. To generate data that will guide the use of blended systems containing Class C and Class F fly ashes, as well as fly ashes produced from blended coal sources in achieving certain desired mechanical and durability properties of concrete.
3. To reduce the cost of producing concrete by partially replacing cement with fly ash.
4. To help reduce the emission of the greenhouse gas "CO_2" resulting from the production of cement by reducing the quantity of cement required for producing quality concrete.

1.5 Thesis Organization

The first section of this report is the introduction. It is comprised of a background discussion on concrete, the statement of problem under review, the objective of this research, the significance of this research and organization of this research report. The second section of this report presents a literature review on fly ash, hydration mechanism of fly ash, fresh properties of fly ash concrete, hardened properties of fly ash concrete, and alkali silica reaction. The third section is the experimental materials and procedures. This section provides a detailed account of the materials, mix proportion, apparatus and procedures employed in carrying out the various laboratory and field research. The fourth section of this report presents the results and discussion of all laboratory and field tests carried out in this research, while the fifth section gives the overall conclusions for this research based on findings.

2. LITERATURE REVIEW

2.1 Fly Ash

2.1.1 Fly ash background.

Fly ash is produced by electric power plants that burn pulverized coal to generate electricity. The burning of coal in electric power production plants produces two forms of ashes. One is fine and light enough to be transported by flue gases to the top of the combustion chamber where they are collected, while the other drops to the bottom and sides of the combustion chamber (Folliard et al., 2009). The ash that drops to the bottom and sides of the combustion chamber is known as bottom ash, while that which is transported to the top of the combustion chamber by flue gases is known as fly ash (Folliard et al., 2009). The electrical power industry used the term fly ash for the first time in 1930, but an all-inclusive information of its possible use in concrete in North America was reported for the first time in the year 1937 (Ramezanianpour, 2014). Meanwhile, the first major application of fly ash was in the construction of the Hungry Horse Dam reported in the year 1948 (Ramezanianpour, 2014). Subsequently, fly ash has continued to gain more acceptance and application as several studies continues to substantiate its usage, hence, offering a solution to the environmental pollution caused by its disposal. A review carried out by Ahmaruzzaman on the utilization of fly ash, validates that fly ash can be used as follows: mine back fill, road sub-base, concrete production, zeolite synthesis, a low-cost adsorbent for the removal of organic compounds, dyes, and heavy metals (Ahmaruzzaman, 2010).

The physical, chemical and mineralogical characteristics of fly ash depends on the nature of the coal burnt and the process of burning and retrieving the fly ash generated (Folliard et al., 2009). Coal is a transformed stratified rock originating from the decay of dead vegetation. The transformation from dead vegetation to coal takes place sequentially over a long period as follows: from the dead vegetation to peat then lignite, sub-bituminous coal, bituminous coal, and anthracite (Folliard et al., 2009). According to ASTM C618-19 Classification, fly ash can either be Class F or Class C. Class F fly ash has pozzolanic properties and is typically produced by burning bituminous coal or anthracite. Whereas, Class C fly ash possess both pozzolanic and cementitious properties and is typically produced from burning lignite or subbituminous coal (ASTM International, 2019).

Physically, fly ash comprises of particles of different sizes and shapes. Most of the particles are regular with either a spherical or rounded shape, while others are irregular or angular and contains agglomerates, quartz and other unburned particles (Marinković & Dragaš, 2018). Fly ash particles are either in solid or hollow form and generally possess a glassy smooth surface, though variation still exist between various types of fly ash. This shape and surface quality of fly ash accounts for the increased workability achieved with less water in fly ash concrete (Marinković & Dragaš, 2018). Fly ash possess a particle size in a range that could be less than 1µm to more than 100µm and a specific gravity that is between 1.9 to 2.8 (Rashad, 2015). The specific surface area of fly ash range from 170 to 1000 m^2/kg and it also possess various colors such as: black, gray, and tan, which is determined by the quantity of unburned carbon in the fly ash (Ahmaruzzaman, 2010).

The chemical constituents of fly ash are mainly iron oxide (Fe_2O_3), calcium oxide (CaO), alumina (Al_2O_3) and silica (SiO_2). Other chemical constituents of fly ash are sodium oxide (Na_2O), magnesium oxide (MgO), titanium oxide (TiO_2), Sulfur oxide (SO_3), potassium oxide (K_2O) and unburned carbon (C) (Ramezanianpour, 2014). The chemical composition of fly ash is dependent on the coal that produced it as well as the burning conditions of the boiler (Aughenbaugh, Stutzman, & Juenger, 2016). Class F fly ash, which is produced by burning anthracite and bituminous coal contains low calcium oxide (CaO), but high amount of alumina (Al_2O_3) and silica (SiO_2). Whereas, Class C fly ash, which is produced by burning lignite and sub-bituminous coal contains lower alumina (Al_2O_3) and silica (SiO_2), but high amount of calcium oxide (CaO) (Marinković & Dragaš, 2018). The rate of cooling of fly ash particles results to the formation of either glassy particles or crystalline particles. A rapid cooling results to the formation of glassy particles which accounts for 50-90% of the mass of fly ash, while a slow cooling results to the formation of crystalline particles which accounts for 5-50% of the mass of fly ash (Aughenbaugh et al., 2016; Kruse et al., 2013). The reactivity of fly ash depends largely on its glassy and crystalline phases. The combustion of low calcium coal results in the formation of aluminosilicate glass which is found more in Class F Fly ashes. Whereas, the combustion of high calcium coal results in the formation of calcium aluminosilicate glass which is that main constituent of Class C that makes it more reactive than Class F (Kruse et al., 2013). Fly ash in its crystalline phase consist of both reactive and stable minerals such as: ettringite, opaline, hematite, mullite, quartz, gypsum, feldspar, anhydrite and spinel (Pandey & Singh, 2010).

Fly ash has become a valuable material for use in cement and concrete production due to the tremendous benefits it offers. Some of the benefits that can be derived from using fly ash in concrete production are: good workability in concrete at lower water content, reduction in the cost of producing cement or concrete, reduced bleeding, lower evolution of heat in mass concrete thereby preventing cracking at early ages, improved mechanical and durability properties, improved packing in concrete, reduced permeability and prevention of chemical attack (Ahmaruzzaman, 2010). The benefits derived from fly ash depends on the type and dosage used. For instance, Class F fly ash has low calcium oxide (CaO), or calcium content compared to Class C fly ash and offers more resistance to sulfate attack and ASR at lower replacement levels compared to Class C fly ash (Latifee, 2016). Class F fly ash brings about late compressive strength development in concrete especially at high cement replacement due to its slow rate of reaction, whereas Class C fly ash reacts faster and promotes early strength development in concrete (M. D.A. Thomas, Shehata, Shashiprakash, Hopkins, & Cail, 1999). Latifee (2016) carried out extensive testing on three categories of fly ash; Class C, Class F and intermediate Class in order to verify if the dosage of fly ash is more significant than type of fly ash and also confirm if lime content in fly ash varies proportionally to its effect on ASR mitigation. Each category had three different types of fly ash making it a total of nine fly ashes. The flow from Class F, through intermediate to Class C portrays the increase in lime content (CaO) with Class F as the lowest with lime content less than 8%, intermediate between 18% and 20%, and Class C above 20%. These fly ashes were used at replacement levels of 15%, 25%, and 35% and were tested using the Miniature Concrete Prism Test which produced result within 56days and is regarded as reliable as

ASTM C1293 (Latifee, 2016). The results showed that the dosage of fly ash was more significant for high lime fly ashes than low lime fly ashes. It also showed that the ASR expansion increased linearly as the lime content of the fly ashes increased from Class F through intermediate to Class C (Latifee, 2016).

2.1.2 Recent changes to fly ash.

Coal has been one of the world's major source of electric energy. It was recorded that coal accounted for 25% of the world's energy supply in 2006, which amounted to 3090 million tons of oil equivalent (Shaheen, Hooda, & Tsadilas, 2014). The global adoption of coal as a source of electric energy has resulted to the production of huge amount of coal fly ash. It was reported that the estimated global annual production of coal ash was about 600 million tons and fly ash accounts for 75-80% of the total, which is roughly 500 million tons (Ahmaruzzaman, 2010; Rashad, 2015). However, this estimated amount of fly ash produced globally continues to increase concurrently with global demand for energy. A more recent estimate of the total global fly ash production was about 750 million tons, which is 250 million tones more than the previous estimate (Shaheen et al., 2014). One major problem associated with the production of fly ash is environmental pollution. According to a fly ash production and utilization data for 2005, India was recorded as the country that generates the highest amount of fly ash at 118 million tons/year but utilizes only 38% of the produced fly ash. Following India are other countries like China, which generates 100 million tons/year and utilizes 45%, United States generates 75 million tons/year and utilizes 65%, Germany generates 40 million tons/year and utilizes 85%, UK generates 15 million tons/year and utilizes 50%, whereas Denmark, Netherlands, Italy generates 2 million tons/year and utilizes 100% (Shaheen et

al., 2014). The unused fly ash and other coal combustion residues produced from these countries are usually disposed in large storage ponds or landfills as waste (Shaheen et al., 2014). However, this method of disposing coal ash still raises a lot of concern as there are chances that it could still find its way into the environment due to lack of proper management (Ritter, 2016).

In the U.S., the EPA has continued to initiate regulatory measures to mitigate the issue of environmental pollution from the emissions and solid waste emanating from coal power plants. Some of the enacted rules of EPA as regards to coal combustion emissions and waste disposal are: the removal of toxic substances from coal combustion emissions, lining of new and old coal ash storage ponds, continuous inspection of all coal ash impoundments to ensure structural stability and avoid percolation of pollutants to groundwater level, cleaning of contaminated sites, encourage the beneficial use of fly ash only in cases of encapsulated application like in concrete and not in exposed application like soil stabilization, etc. ("Fly Ash Supply," 2010; Mele, 2018; Ritter, 2016). These stringent rules by the EPA has impacted negatively on both utility companies and other industries that depend on coal combustion products. Some utility companies seem to be considering other cheaper alternatives like the use of natural gas ("Where Has the Fly Ash Gone?," 2012).

The quality and quantity of fly ash produced for construction purposes have also been affected by the regulatory measures enacted by EPA. For instance, the availability of Class F fly ash has become an issue of concern in Texas. Class F fly ash is heavily used by Texas Department of Transportation to mitigate sulfate attack, ASR, and control temperature in mass concrete structures ("Fly Ash Supply," 2010). Most power plants in

Texas usually produce Class F fly ash by burning either Texas lignite coal or a blend of Texas lignite coal and Powder River Basin coal (PRB) which has high lime content. However, some of these power plants that produce Class F fly ash in Texas now produces Class C fly ash as they have switched to burning either blends with higher amount of PRB or 100% PRB so as to reduce cost and maintain emission standards ("Fly Ash Supply," 2010). In addition to the decline in the availability of Class F fly ash is the issue of fly ash quality. In order to prevent the emission of mercury, and gases like sulfur and nitrogen oxide, chemical substances like activated carbon and ammonia are injected into the flue gas to trap these substances from being emitted and end up being captured with the fly ash. This activated carbon in the fly ash could be a problem if entrained air is needed in concrete, but the ammonia could only be a problem if used in enclosed structures with limited flow of air ("Fly Ash Supply," 2010).

In a quest to extend solutions to the challenges in the production, disposal and availability of fly ash, researchers have made some remarkable breakthroughs that could be implemented as a solution to such challenges. The use of remediated and reclaimed fly as is one of such solutions. Reclaiming and remediating fly ash simply refers to the act of retrieving fly ash from storage ponds and landfills and remediating the fly ash to meet standard specifications (Diaz-Loya, Juenger, Seraj, & Minkara, 2017). This is achieved through processes like dredging, dewatering, drying, milling, air classification and storing (Diaz-Loya et al., 2017). Diaz-Loya et al. (2017) compared the characterization and performance data of a reclaimed and remediated fly ash that was originally produced between the 70s and 80s with a currently produced fly ash from the same power plant in accordance to ASTM C618. The results showed the following: slight differences in

chemical and physical properties but more similarity in mineralogical properties between the reclaimed and current fly ash, equivalent contribution of strength from both fly ashes, reclaimed fly ash remained pozzolanic as verified using thermogravimetric analysis, both fly ashes were effective in reducing the heat of hydration of cement paste as verified using isothermal calorimetry, and finally both were also effective in reducing the risk of alkali silica reaction as verified in accordance to ASTM 1567 (Diaz-Loya et al., 2017).

Another emerging practice in the industry that has helped mitigate the issue of declining availability of Class F and also meet certain requirement that has to do with the application of fly ash and other supplementary cementitious material (SCM) is blending. According to ASTM C1697-18, SCM is defined as "a slag cement or pozzolan that contributes to the properties of concrete or mortar through hydraulic or pozzolanic activity, or both". Most SCMs are waste generated from industrial activities, thus, their use in concrete offers both economic and environmental benefits (Folliard et al., 2009). Cement blending with fly ash or other SCMs can be done during production at the cement production plant or during the production of concrete. Cement is blended with either one, two or three SCMs and are termed binary, ternary and quaternary blends respectively (Antiohos, Papadakis, Chaniotakis, & Tsimas, 2007). The goal of blending one to three SCMs with cement is to produce cement and concrete of certain desirable characteristics by bringing in the various attributes and ability of each SCMs into play in the cement or concrete mix and allowing the deficiencies of one SCM to be compensated by the other (Antiohos et al., 2007). According to ASTM C1697 -18, the blend proportion for blended supplementary materials can be confirmed by ascertaining the chemical composition of the blended supplementary materials and its constituents (ASTM C1697-

18). The shortcomings of both Class C and F fly ashes are compensated by the act of blending. Blending helps to obtain a mixture of fly ash with a favorable calcium content and improved resistance to sulfate attack and alkali silica reaction (Dhole, Thomas, Folliard, & Drimalas, 2011). There are some documented researches on the use of either Class C or Class F fly ash or a blend of these fly ashes and other supplementary cementing materials in producing mortar and concrete with high performance and strength as well as resistance to sulfate attack and alkali silica reaction. Dhole et al. (2011) investigated the use of ternary, quaternary blends of six Class C fly ashes, Class F fly ash, silica fume, and ultra-fine fly ash in resisting sulfate attack. This was done in accordance to ASTM C1012 for a duration of 18 months. The results showed that Class C fly ash mixtures offered lower resistance to sulfate attack compared to Class F fly ash mixtures. However, ternary mixtures of Class C fly ash and either Class F fly ash or silica fume offered better resistance to sulfate attack. The Class C fly ash and Ultra-fine fly ash mixtures at 10% replacement offered a very high resistance to sulfate attack (Dhole et al., 2011). Erdem and Kirca investigated the effect of using binary blends over ternary blends in producing high strength concretes. In other to achieve their aim, a mixture of portland cement and silica fume was used in the binary blends whereas the ternary blends were achieved using either fly ash or slag. By varying the binder content for every mixture, a total of 80 high strength concrete mixtures were produced. The result showed that the binary blends with silica fume improved concrete compressive strength at all ages. Also, the ternary blends showed the possibility of obtaining higher strengths than the binary blends when the appropriate replacement levels are chosen (Erdem & Kirca, 2008).

2.2 Hydration Mechanism of Fly Ash Concrete

Cement hydration is an exothermic reaction that take place when cement is mixed with water. This reaction begins as water comes in contact with the aluminates and silicates constituent of cement to form hydration products such as: calcium silicate hydrate (C-S-H) which is known as the binder in cement-based materials, tricalcium aluminate hydrate (C_3AH) and calcium hydroxide ($Ca(OH)_2$) (Neville, 2011). The rate at which hydration occurs in cement depends on the mineralogical composition of the cement (Monteagudo, Moragues, Gálvez, Casati, & Reyes, 2014). The hydration reaction is more intense with more evolution of heat and shorter setting time in cements with high tricalcium aluminate (C_3A) and low tricalcium silicate (C_3S), but less intense with less evolution of heat and longer setting time in cements with low tricalcium aluminate (C_3A) and high tricalcium silicate (C_3S) (Monteagudo et al., 2014). However, cement hydration is positively affected if cement is partially replaced with fly ash (Zeng, Li, Fen-chong, & Dangla, 2012). When cement is replaced with fly ash at the same water to cementitious material ratio (w/cm), more water becomes available for hydration and hence promoting the degree of hydration. At the same time, the cement hydration process is also accelerated as the fly ash adsorbs Ca^{2+} and thus making more sites available for the precipitation of cement and alkali (Kocak & Nas, 2014; Zeng et al., 2012). Fly ash in an alkaline environment reacts with calcium hydroxide and other products of hydration to form more calcium silicate hydrate (C-S-H) and calcium-aluminate-silicate-hydrate (C-A-S-H) phases also known as zeolite phases (Tang et al., 2016).

There are several ways of determining the progress of cement hydration. This includes measuring: the heat evolved during hydration, the amount of $Ca(OH)_2$ in the

paste, the amount of chemically combined water, the specific gravity of the paste, the amount of hydrated cement present and indirectly from the strength of hydrated paste (Neville, 2011). These ways of determining the progress of cement hydration are usually achieved through experimental methods such as: backscattered electron (BSE) image analysis, thermogravimetric analysis (TGA), and X-ray diffraction analysis (XRD) (Neville, 2011; Zeng et al., 2012). Also, the extent of pozzolanic reaction is determined using experimental methods such as: selective dissolution method, thermogravimetric analysis (TGA), and X-ray diffraction analysis (XRD) (Zeng et al., 2012). Many researchers have employed these experimental methods in their investigations on cement hydration and pozzolanic reactions. Zang et al. (2015) used thermogravimetric analysis (TGA) in their study to ascertain the reaction extent of cement hydration and fly ash pozzolanic reaction in fly ash cement paste. TGA was chosen because of its reliability in measuring the quantity of calcium hydroxide and amount of non-evaporable water in blended cement pastes (Zeng et al., 2012). Tang et al. (2016) used an innovative method known as non-contact impedance measurement as well as TGA, XRD and scanning electron microscopy (SEM) to investigate the hydration process of fly ash blended cement (Tang et al., 2016). Deboucha et al. (2017) investigated the degree of hydration of cement paste containing limestone filler and blast furnace slag by estimating the chemically bound water using thermogravimetric analysis. They also suggested a direct way of assessing the quantity of mineral admixtures in a hydration reaction using modified TGA (Deboucha, Leklou, Khelidj, & Oudjit, 2017).

Another method that is used to determine the rate of heat production and the developed heat of cement hydration is isothermal calorimetry (Wadsö, 2001). This

method involves the use of an isothermal calorimeter to measure at constant temperature the rate of heat production also known as thermal power and the rate of heat production per gram of cement also known as specific thermal power (Wadsö, 2001). The isothermal calorimeter is designed to measure heat flow from samples by conducting away from the samples the heat produced thereby maintaining the isothermal condition of the samples (Wadsö, 2001). ASTM C1679-19 describes the procedure and apparatus for measuring the thermal power of blended and unblended cement pastes and mortars using an isothermal calorimeter (ASTM International, 2019). Xiong and Van Breugel used isothermal calorimetry at 20, 30 and 40^{o}C with w/cm ratios of 0.6 and 0.4 to investigate the kinetics of Portland cement and blast furnace slag cement. Their aim was to determine the apparent activation energy (E_a) which is used in numerical simulations of the processes of cement hydration to ascertain the effect of temperature in the rate of cement hydration reactions. The activation energy was obtained both experimentally and through numerical simulations and was confirmed to be in agreement. Results also showed that the activation energy (E_a) relied on the temperature, water/cement ratio and degree of hydration (Xiong & Van Breugel, 2001).

2.3 Fresh Properties of Fly Ash Concrete

Fresh concrete properties refer to those attributes exhibited by concrete when it is in plastic state. These fresh properties of concrete largely determine the properties of the final hardened concrete (Mindess et al., 2003). Terms like consistency, mobility, flowability, pumpability, compactibility, finishability, harshness, etc. are used in describing certain qualities exhibited by fresh concrete. However, these terms can still be referred to as the workability of fresh concrete (Mindess et al., 2003; Neville, 2011).

According to ASTM C125-19, workability is defined as: "that property of freshly mixed concrete that affects the ease with which it can be mixed, placed, consolidated, and struck off". Workability is affected by temperature, water content, time, mix proportion, aggregate property, cement property, and admixtures (Mindess et al., 2003). Water is a major requirement for workability. However, a good workability can only be achieved if a balance is attained as to the right amount of water required alongside other constituent of concrete to achieve a desired workability (Neville, 2011). The workability of concrete is usually improved without adding more water by incorporating fly ash. This improvement in workability is as a result of the lubricating effect from the smooth spherical particles of fly ash (Ramezanianpour, 2014). The workability of concrete can be assessed using tests like slump test, compacting factor test, flow test, vebe test, remolding test, flow table test, etc. But the most commonly used of all is the slump test (Neville, 2011).

Slump test is described in ASTM C143/C143M-15a. According to ASTM C143/C143M-15a, slump test is carried out using a mold that is shaped like the frustum of a cone and is made with either metal or plastic that is resistant to cement paste attack. The standard dimensions for the height, diameter of top and bottom circular ends of the frustum are given as 12±1/8 inches, 4±1/8 inches, and 8±1/8 inches respectively (ASTM International, 2015). The test is carried out by filling the firmly fixed mold with concrete in three layers. Each layer should be around one-third the volume of the mold and must be rammed 25 times using a steel rod of 16mm diameter. After filling the mold to the top, the rod is used to strike off the surface of the concrete before raising the mold gradually in a vertical direction within 5±2 seconds. The slump is obtained by measuring the

vertical height from the top of the mold to the center of the displaced concrete specimen. The prescribed time for the entire test is $2^1/_2$ minutes (ASTM International, 2015).

Other tests carried out on fresh concrete are air content test and unit weight. The air content of concrete can be determined using any of these three methods: volumetric, gravimetric, and pressure method. However, the pressure method is the most commonly used of the three and is described in ASTM C231/C231M-17a. Whereas volumetric and gravimetric methods are described in ASTM C173/C173M-16 and ASTMC138/C138M-17a respectively (Mindess et al., 2003). According to ASTM C231/C231M-17a, the pressure method is performed using an air meter that comprises of a cylindrical measuring bowl with a capacity of at least 6.0L ($0.2ft^3$) and a cover assembly that is designed to have a pressure tight fit with the measuring bowl as well as clamps, air valves, bleeder valves, petcocks for bleeding off or introducing water and a meter for direct reading of air content. The way the concrete is placed and rodded in the measuring bowl is similar to the slump test. Although certain steps like tapping the sides of the measuring bowl with mallet, adding water through the petcocks, reading air content directly from a dial etc. are peculiar to the air content test (ASTM International, 2017). The unit weight of fresh concrete also known as density of fresh concrete is described in ASTMC138/C138M-17a. It is determined by measuring the weight of concrete required to fill a container with known volume and this is usually done before the air content test by measuring the weight of the concrete filled measuring bowl before carrying out the air content test (Mindess et al., 2003).

2.4 Hardened Properties of Fly Ash Concrete

As concrete transforms from a plastic workable material to a hardened mass, its properties also change. Hardened concrete possesses mechanical and durability properties such as compressive strength, tensile strength, shrinkage, elastic property, creep, electrical, thermal, and transport properties etc. (Kovler & Roussel, 2011). The properties of hardened concrete are dependent on some factors which either undermine or improve its performance. For instance, the compressive strength of concrete which is perceived as the most vital property of concrete depends on factors like water-cement ratio, compaction, age, mode of curing, temperature, aggregate type and size, cement type, amount and type of admixture etc. (Neville, 2011).

The addition of fly ash in concrete affects the compressive strength as well as other hardened concrete properties (Ramezanianpour, 2014). Fly ash addition results to a reduction in the quantity of cement and the amount of water required for hydration thus leading to an increase in compressive strength of the resulting concrete (Ramezanianpour, 2014). Certain physical, chemical and reactivity properties of fly ash influence the rate at which strength is gained in concrete. Class C fly ash reacts faster and hence leads to early strength development in concrete whereas Class F reacts slower and results in late strength development in concrete (M. D.A. Thomas et al., 1999). The act of increasing the fineness of fly ash used in concrete by grinding also increases the compressive strength and other mechanical properties of concrete (Aydin, Karatay, & Baradan, 2010).

The test method for the compressive strength of cylindrical concrete specimens is described in ASTM C39/C39M-18. According to ASTM C39/C39M-18, the compressive

strength test should be carried out using a power operated machine with enough capacity and capable of sustaining a continuous load rate of 0.25±0.05MPa/s (35±7psi/s) without shock. This test involves applying an axial load to a cylindrical concrete specimen and maintaining the prescribed loading rate until the specimen fails. The maximum load applied is usually displayed on a dial or digital indicator and is used to calculate the compressive strength by dividing it with the cross-sectional area of the specimen (ASTM International, 2018). The test method for the splitting tensile strength of cylindrical concrete specimens is described in ASTM C496/C496M-17. The same test machine used in the compressive strength test is also used for the splitting tensile strength test. However, the splitting tensile strength involves applying a constant load along the diameter and length of the cylindrical concrete specimen at a steady rate of range 0.7 to 1.4 MPa/min (100 to 200 psi/min) until the concrete fails due to the induced tensile stresses along the plain of the load applied (ASTM International, 2017). The tensile strength is calculated using the maximum load alongside other parameters as stated in section 9.1 of ASTM C496/C496M-17. The test method for the static modulus of elasticity of concrete in compression is described in ASTM C 469/C469M-14. The same testing machine used for the compressive strength test can be used for the static modulus of elasticity test. Though, the modulus of elasticity test involves attaching to the cylindrical concrete specimen a compressometer capable of reading the deformation (strain) of the specimen while a compressive load is been applied at a steady rate of 250±50 kPa (35±7psi/s) until the maximum applied load for the modulus of elasticity is reached (ASTM International, 2014). In order to calculate the elastic modulus, these two readings are to be recorded without interruptions; the load at a longitudinal strain of 50

microstrain and the longitudinal strain at the maximum load which is 40% of the ultimate load of specimens in the same category (ASTM International, 2014). The formula for calculating the modulus of elasticity is stated in Section 7.1 of ASTM C 469/C469M-14. The test method for the change in length (drying shrinkage) of concrete and mortar specimens that is not attributed to external forces or changes in temperature is described in ASTM C157/C157M-17 ((ASTM International, 2017). This method involves placing cured concrete and mortar specimens in a controlled environment like the drying room described in section 5.4 of ASTM C157/C157M-17 and continue to measure them using a length comparator to ascertain their length as they age (ASTM International, 2017). The length change is calculated using the formula in section 12.2 of ASTM C 157/C157M-17.

Due to the rising use of fly ash in concrete, a lot of researchers have investigated the effect of adding fly ash to the mechanical and durability properties of concrete. Naik, Singh and Ramme investigated the effect of blended fly ash on the mechanical and durability properties of concrete. This research involved the use of Type I cement without fly ash as control, 35% replacement of cement with ASTM Class C fly ash and 40% replacement of cement with both Class C and Class F fly ash. The ternary blends involving Class C and Class F were proportioned as 75%/25%, 50%/50%, 25%/75% for Class C and Class F respectively. Mechanical properties tests such as compressive strength, tensile strength, modulus of elasticity, and flexural strength were carried out on concrete samples produced using the mix proportions enumerated above. Durability properties were ascertained using tests like abrasion resistance, drying shrinkage, electrical prediction of chloride ion penetration, and salt scaling resistance. The results for both the mechanical and durability properties tests showed that the ternary blends of

Class C and Class F were either better or similar to the mixtures containing cement without fly ash (control) and the binary blends of Class C and cement (Naik, Singh, & Ramme, 1998). Wang and Park investigated the compressive strength development of high-volume fly ash concrete using numerical procedure. This procedure involved the use of a combined hydration model in evaluating the degree of reaction of cement, fly ash, cement and fly ash interactions, phase volume fractions, and Calcium Silicate Hydrate (CSH) as a function of curing age. In addition to the hydration model, a strength model was also adopted to ascertain the compressive strength of hardened high-volume fly ash concrete using the Calcium Silicate Hydrate (CSH) content. Following the results of the numerical procedure used in this research, these conclusions were made: the compressive strength of control concrete is more than that of the fly ash blended concrete at early age, concrete with low volume fly ash (15-25%) can exceed the control concrete at late age, the compressive strength of high volume fly ash concrete (45-55%) with high water to cementitious material ratio cannot exceed the control concrete at late age, and the compressive strength of high volume fly ash concrete (45-55%) with low water to cementitious material ratio can exceed the control concrete at late age (Wang & Park, 2015). Shaikh and Supit investigated the effect of ultrafine fly ash on the compressive strength and durability properties of high-volume Class F concrete. This research was done using: Portland cement concrete without fly ash as control, ultrafine fly ash at 8% and 12% cement replacement, high volume Class F fly ash concrete without ultrafine fly ash at 40% and 60% cement replacement, high volume Class F fly ash concrete at 32% and 52% cement replacement with ultrafine fly ash of 8% cement replacement to go with each percentage replacement of high volume Class F fly ash. Concrete specimens

produced from the different mix proportions were tested to ascertain their compressive strengths at 3, 7, 28, 56 and 90 days. In addition, durability properties like: chloride induced corrosion, chloride ion penetration, porosity, water sorptivity, chloride diffusivity, volume of permeable voids were also ascertained at ages 28 and 90 days. The results showed that the introduction of 8% ultrafine fly ash improved the compressive strength of the control concrete and the high-volume Class F fly ash concrete both at early age and later age. Also, the introduction of the 8% ultrafine fly ash improved all tested durability properties of the high-volume Class F fly ash compared to the control concrete (Shaikh & Supit, 2015). Saha investigated the effect of Class F fly ash on the durability properties of concrete. Five different mix proportions were used in this study. This includes a control mix without fly ash and other mixtures that contains Class F fly ash at 10%, 20%, 30%, and 40% cement replacement. Compressive strength test and other durability tests like: sorptivity, drying shrinkage, permeable void, and chloride permeability were carried out on concrete specimens after different curing periods. The results showed that the fly ash samples exhibited lower compressive strength than the control samples at early age. However, the compressive strength of the fly ash samples increased over a longer period due to pozzolanic reaction. Also, the results of the durability property tests showed improved durability in the fly ash concrete compared to the control (Saha, 2018). Nath and Sarker investigated the effect of fly ash on the durability properties of high strength concrete. Test specimens were produced using Portland cement without fly ash as control and mixtures involving Class F fly ash at 30% and 40% total cementitious material content. The mixtures were produced using both varying water to cementitious material ratio and a constant water to cementitious material

ratio. Compressive strength, sorptivity, drying shrinkage and rapid chloride permeability tests were carried out on test specimens. The results showed a reduction in the 28-day strength of fly ash concrete at constant water to cementitious material ratio. However, with w/b ratio 0.31 and 40% fly ash, a high strength concrete with a 28 days compressive strength of 60 MPa was achieved. The fly ash concrete showed reduction in drying shrinkage at the same 28-day design strength as the control. There was also a significant reduction in sorptivity and chloride ion permeation due to the addition of fly ash (Nath & Sarker, 2011).

2.5 Alkali Silica Reaction

2.5.1 Mechanism of ASR

Alkali-silica reaction is a reaction that leads to the failure of concrete. This reaction involves reactive silica and alkalis in the pores of concrete both emanating from the aggregate and cement constituent of concrete respectively. The reaction between the silica content of the aggregate and the alkali from the cement produces a hydrophilic gel that is innocuous on its own but can be detrimental to concrete when it absorbs water and swells to cause cracking in concrete (Latifee, 2016). According to Ichikawa's proposed model on the mechanism of ASR, the reaction starts when the alkali in the pore solution of concrete attacks the surface of the reactive aggregate and converts it to alkali silicate. This reaction leads to the consumption of hydroxide ions (OH^-) and dissolution of calcium ions (Ca^{2+}) which reacts with the alkali silicate surface to form a reaction rim that is made up of calcium alkali silicate. The calcium alkali silicate (reaction rim) allows more alkalis into the aggregate but does not allow alkali silicate out of it. This leads to

more formation of alkali silicate to a point that it generates enough internal pressure to crack the reaction rim as well as the cement paste surrounding the aggregate (Ichikawa, 2009). Figure 1 shows a schematic diagram of the process as proposed by Ichikawa.

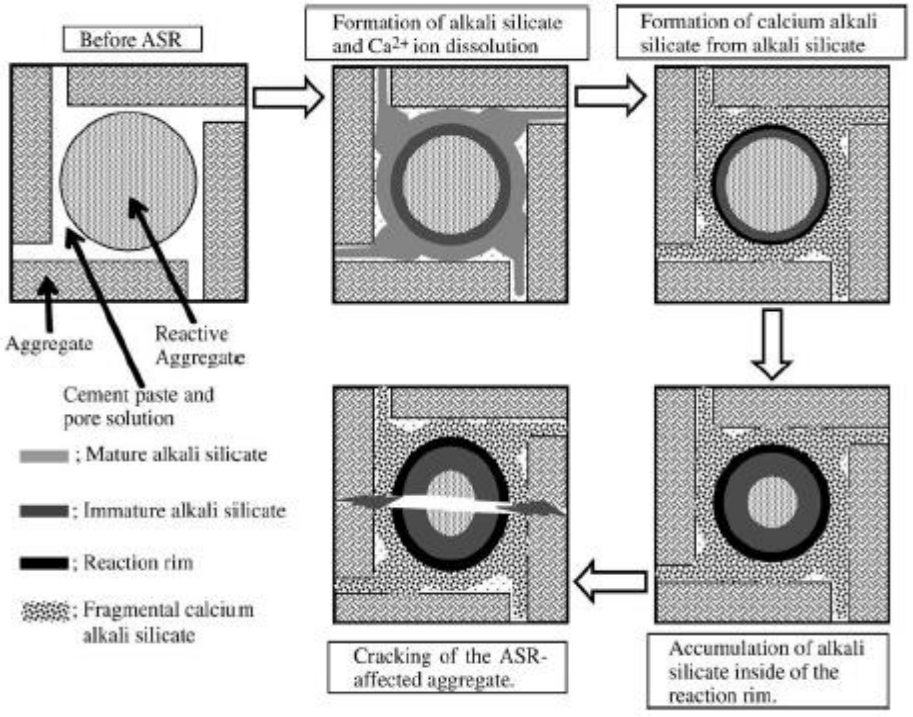

Figure 1. Schematic illustration of the mechanism of ASR in concrete. Adapted From "Alkali-Silica Reaction, Pessimum effects and Pozzolanic Effect," by T. Ichikawa, 2009, *Cement and Concrete Research, 39*, p.718.

Tom Stanton is recognized as the person who discovered ASR (Mather, 1999). He asserted that the failure was due to expansions associated with the reaction between the alkalis content of cement paste and some reactive types of silica in the aggregate. Though there are other forms of reactive silica, Stanton focused on only opal and chert as types of reactive silica (Mindess et al., 2003). According to Mindess et al., Stanton highlighted the

following as factors controlling alkali-silica expansion: quantity of reactive silica, nature of reactive silica, quantity of alkali, size of reactive material and quantity of moisture. For ASR expansion to take place in concrete, certain conditions must be met. Some of the conditions are: the availability of sufficient alkalis from the cement, the presence of aggregates that contain reactive forms of silica, and sufficient moisture (Latifee, 2016). Alkali silica reaction can be controlled by controlling the conditions necessary for its occurrence. This means that controlling conditions like the amount of reactive silica, alkali concentration, and moisture would consequently prevent alkali silica reaction in concrete (Mindess et al., 2003).

2.5.2 Test methods to evaluate ASR of cementitious mixtures

Certain standard test methods can be used in detecting the potential for alkali silica reaction as well as verifying the capability of some additional materials in mitigating ASR. These methods have their shortcomings that either pose a challenge in their usage or render them completely unsuitable. The Mortar Bar Test (ASTM C227) was one of those methods that was used in the past for testing the potential for alkali silica reaction in concrete. However, this test is no longer in use because of the following shortcomings: alkali leaching, failure to substantiate the potential of various rocks to react with alkali, and the right amount of alkali required to instigate the expansion with an aggregate (M. Thomas, Fournier, Folliard, Ideker, & Shehata, 2006). Another test that is like the Mortar Bar Test (ASTM C227) is the Pyrex Mortar Test (ASTM C441). The major difference between the Mortar Bar Test (ASTM C227) and Pyrex Mortar Test (ASTM C441) is the use of Pyrex glass as aggregate in Pyrex Mortar Test (ASTM C441) (M. Thomas et al., 2006). The Accelerated Mortar Bar Test (ASTM C1567) is one

method used currently to detect the likelihood for harmful alkali silica reaction of aggregate in combination with hydraulic cement and other supplementary cementitious materials (SCMs) within 16 days using mortar bars of 25 x 25mm (1x1 inch) cross section (ASTM International, 2013). This method involves certain procedures that includes submerging the mortar bars in a 1 molar solution of Sodium Hydroxide (NaOH) and then measure them at intervals to assess the expansion due to ASR (ASTM International, 2013). Expansions which are less than 0.10% at 16 days after casting for a combination of aggregate and cementitious material are likely going to produce an acceptable expansion in concrete. Meanwhile, expansions which are greater than 0.10% at 16 days after casting indicates a potential harmful expansion (ASTM International, 2013). Another method similar to the accelerated mortar bar method (ASTM C1567) is the mortar bar method (ASTM C1260). The difference between ASTM C1567 and ASTM 1260 is that ASTM C1260 is used to detect the potential for alkali silica reaction of aggregate in combination with hydraulic cement without adding any supplementary cementitious material. Also, expansions in the mortar bar method (ASTM C1260) are considered unharmful if they are less than 0.10% at 16 days after casting and harmful if they are greater than 0.20% after casting. Whereas, expansions between 0.10% and 0.20% are typically considered moderately reactive and thus, requires more confirmation (ASTM International, 2014). Due to the extremely harsh alkaline solution used in conducting the accelerated mortar bar test (ASTM C1567) and the mortar bar test (ASTM C1260), some aggregate with good field performance are considered as reactive, hence making these tests less reliable for rejecting aggregates (M. Thomas et al., 2006). The

Concrete Prism Test (ASTM C1293) is used as a confirmatory test when the accelerated mortar bar test and mortar bar test are inadequate (ASTM International, 2018).

The Concrete Prism Test (ASTM C1293) is another method used to determine the vulnerability of either an aggregate or a combination of aggregate and other mineral admixtures in expansions due to alkali silica reaction by measuring the length change in concrete prisms of size 75 x 75mm (3 x 3 inches) cross section over a period of 12-24 months (ASTM C1293-18a). This method involves increasing the alkali content (Na_2O_{eq}) of the concrete mix to 1.25% of cement mass by adding a solution of 50% w/w Sodium Hydroxide (NaOH) to the mixture (ASTM International, 2018). For the Concrete Prism Test (ASTM C1293), the aggregate under investigation can be considered as potentially reactive if the average expansion of the concrete prisms is greater than or equal to 0.04% at 12 months (ASTM International, 2018). If the expansion is less than 0.04% and the aggregate is combined with one or more supplementary cementitious material (SCM), then it can be reasonably concluded that the amount of SCM added is the minimum required to avoid excessive expansion (ASTM International, 2018). The main issues with the Concrete Prism Test are alkali leaching and the time it takes to complete the test (Latifee & Rangaraju, 2015). However, the Concrete Miniature Prism Test serves to solve the issues with the Concrete Prism Test and the Accelerated Mortar Bar Test by providing reliable results on the reactivity of most aggregate at 56 days and slow reactive aggregate at 84 days (Latifee & Rangaraju, 2015). According to Latifee and Rangaraju (2015), the Concrete Miniature Prism Test involves: the use of coarse and fine aggregate sizes in the range of 12.5- 9.5mm and 9.5-4.75mm respectively, increasing the alkaline content of the concrete mix to 1.25% by cement mass, casting of concrete prisms of

dimension 50 x 50 x 285mm (2 x 2 x 11.85 in.), submerging prisms in water after initial readings and subjecting them to a steady temperature of 60^{o}C, taking zero readings and transferring prisms to 1M NaOH solution already conditioned at 60^{o}C after 24 hours, and taking subsequent readings at 3, 7, 10, 14, 21, 28, 42, 56, 70, and 84 days. Autoclave Mortar Bar Test is another test used in evaluating the efficacy of SCM's in preventing harmful expansions due to ASR by increasing the alkaline content of the mix to 3.5% by mass of cement (M. Thomas et al., 2006). This test involves storing mortar bars in a moist environment for two days after which they are transferred to an autoclave with temperature and pressure at 130^{o}C (266^{o}F) and 0.17MPa (25 psi) respectively (M. Thomas et al., 2006).

Researchers have also employed the use of large concrete exposure blocks subjected to natural conditions to determine the vulnerability of an aggregate or combination of aggregate and SCMs in expansions due to alkali silica reaction (Shafaatian, Akhavan , Maraghechi, & Rajabipour, 2013). Drimalas et al., investigated the efficacy of lithium salts in mitigating ASR by subjecting large concrete specimens to different natural climatic conditions (Drimalas et al., 2012). The use of large concrete blocks exposed to natural conditions helps to supplement laboratory investigations and give more credence to specifications that result from the findings of laboratory and field investigations (M. Thomas et al., 2006).

2.5.3 Mitigation and prevention of ASR with fly ash concrete

ASR can be mitigated through the use of mineral admixtures also known as SCMs. Example of such mineral admixtures are: silica fume, calcined clay, ground-

granulated blast furnace slag, fly ash and calcined shale (Folliard et al., 2009; Shafaatian et al., 2013). The ability of fly ash and other SCMs to reduce the alkali content of cement due to partial replacement as well as convert calcium hydroxide ($Ca(OH)_2$) through their pozzolanic reaction to Calcium Silicate Hydrate (C-S-H), affirms their efficacy in resisting sulfate attack and mitigating alkali silica reaction (Kadasamy & Shehata, 2014; Skaropoulou, Sotiriadis, Kakali, & Tsivilis, 2013).

There are several investigations on the use of binary, ternary, and quaternary blends of fly ash and other SCMs to mitigate alkali silica reaction in concrete. In an attempt to proffer solution to the problem of alkali silica reaction caused by high alkali cement and alkali-silica reactive aggregates used in Iceland, Gudmundsson and Olafsson investigated the effectiveness of silica fume in preventing alkali silica reaction in concrete. Silica fume is available in Iceland as a by-product from ferrosilicon plants. Aside from blending silica fumes into the cement, other preventive measures like washing sea dredged materials, limited use of reactive materials and change in the criteria for reactive material were adopted in preventing alkali-silica reaction. The results of the standardized test ASTM C227 and C1260 showed that silica fume was effective in preventing alkali-silica reaction in concrete. Also, a field observation of concrete made with the same silica fume blend, for 20 years showed no sign of alkali-silica reaction (Gudmundsson & Olafsson, 1999). In an attempt to seek solutions to the problem of reduced early strength concrete caused by a replacement level of fly ash or slag for ASR resistance as suggested in their initial research, Lane and Ozyildirim decided to evaluate concretes produced using binary and ternary blends of OPC, Silica fume, fly ash or slag and reactive construction aggregates peculiar to Virginia. The concretes produced were

tested for ASR resistance, strength and electrical resistance. The results showed that concrete produced using ternary blends with low replacement levels of fly ash or slag can be used to prevent low early strength problems and increase ASR resistance due to their high electrical resistance (Lane & Ozyildirim, 1999). Kandasamy and Shehata investigated the efficacy of ternary blends containing slag and high calcium fly ash in mitigating alkali silica reaction in concrete. They compared the efficacy of the binary blends involving either of slag or high calcium fly ash with that of the ternary blends at the same SCM content. This was done using the alkali leaching test, concrete prism and accelerated mortar bar test. The result showed that the ternary blends offered no substantial advantage in ASR mitigation compared to the binary blends at the same total SCM content (Kadasamy & Shehata, 2014).

3. EXPERIMENTAL MATERIALS AND PROCEDURES

3.1 Mechanical Properties

3.1.1 Materials and mix proportion

A type I Portland cement was used for all mechanical property mixes. This cement was obtained from a local Central Texas cement producer and was referred in this entire work as PC-1. Table 1 shows the physical and chemical properties of the cement.

Table 1. Chemical and Physical Properties of Cement

Chemical Analysis %		
Item (%)	Test Results	Spec. Limit
MgO	1.2	6.0 max.
SO3	3.3	3.5 max.
Loss on Ignition	2.4	3.5 max.
Insoluble residue	0.49	1.5 max.
CO2	1.36	
Limestone	3.4	5.0 max.
CaCO3 in limestone	80.7	70 min.
Total Alkali as Na_2O	0.78	
Physical Test		
Air content of mortar (volume %)	9	12 max.
Blaine fineness (m2/kg)	382	260 min.
Mesh 325 (45 microns) % through	94.7	
Autoclave expansion (%)	0.07	0.80 max.
Time of setting - Vicat test (minutes)		
Initial- not less than or more than	84	45 - 375
Final	220	
Compressive strength		
1-day, minimum MPa	18.6	
3-day, minimum MPa	30.7	12
7-day, minimum MPa	37.8	19
28-day, minimum MPa	43.7	
False set (OPTIONAL)	77	50 min.

Seven fly ashes comprising of three Class F and four Class C with varied calcium and alumina content were obtained from Texas and used in this entire study. The three Class

F and four Class C fly ashes were referred to as FA-F1, FA-F2, FA-F3 and FA-C1, FA-C2, FA-C3, FA-C4 respectively. The FA represents Fly Ash and the F# and C# represents the class and a designation number from 1 to 4. The significance between the designation number being the chemical properties of the Fly Ash, as seen in Table 2. However, it should be noted that only five fly ashes (FA-F1, FA-F2, FA-C1, FA-C2, and FA-C3) were used for the mechanical property tests. These fly ashes were selected to reduce the quantity of mixtures produced for this test by using representative samples that depicts the variation in chemical properties of fly ash as shown in Table 2. One of the Class F fly ashes (FA-F2) was produced by burning 80% Powder River Basin (PRB) coal and 20% Lignite Coal. The Class F fly ashes FA-F1 and FA-F3 were produced by burning 100% lignite coal, while the Class C fly ashes FA-C1, FA-C2, FA-C3 and FA-C4 were produced by burning 100% PRB coal. Table 2 shows the chemical properties of the seven fly ashes used in this study.

Table 2. Chemical Properties of Fly Ash

	FA-F1	**FA-F2**	**FA-F3**	**FA-C1**	**FA-C2**	**FA-C3**	**FA-C4**	**ASTM C618 LIMITS (%)**	
	(%)	**(%)**	**(%)**	**(%)**	**(%)**	**(%)**	**(%)**	**CLASS C**	**CLASS F**
Silicon Oxide SiO_2	65.8	45.3	49.4	36.1	35.0	37.2	41.0		
Aluminum Oxide Al_2O_3	18.3	20.6	22.0	14.8	17.5	17.1	17.8		
Iron Oxide (Fe_2O_3)	1.2	4.7	12.6	4.3	4.1	4.5	3.8		
SUM (SiO_2+Al_2O_3+Fe_2O_3)	85.3	70.5	84.1	55.3	56.6	58.8	62.7	50 min	50 min
Sulfur Trioxide (SO_3)	0.2	0.7	0.8	1.3	1.0	0.8	1.3	5.0 max	5.0 max
Calcium Oxide	3.9	13.3	3.0	27.2	26.1	25.7	20.7	>18.0	18 max
Magnesium Oxide (MgO)	0.8	3.9	1.0	5.5	4.1	4.1	3.6		
Sodium Oxide (Na_2O)	3.4	1.3	0.7	2.2	2.0	1.8	1.9		
Potassium Oxide (K_2O)	2.2	0.8	1.5	0.3	0.4	0.5	0.6		
Phosphorus Oxide (P_2O_5)	0.0	0.3	0.2	0.6	0.9	0.7	0.7		

The fine and coarse aggregates used were fine river sand and crushed limestone rock sourced from a local quarry in Texas. Table 3 shows the physical properties of the fine river sand and crushed limestone rock while the sieve analysis are shown in Figure 2 and Figure 3 respectively.

Table 3. Physical Properties of Aggregates for Mechanical Property Tests

Aggregates	**Bulk specific gravity (OD)**	**Bulk specific gravity (SSD)**	**Apparent specific gravity**	**Absorption (%)**	**Dry rodded unit weight (kg/m^3)**
River Sand	2.60	2.62	2.65	0.66	1786.33
Limestone Rock	2.52	2.58	2.68	2.44	1574.89

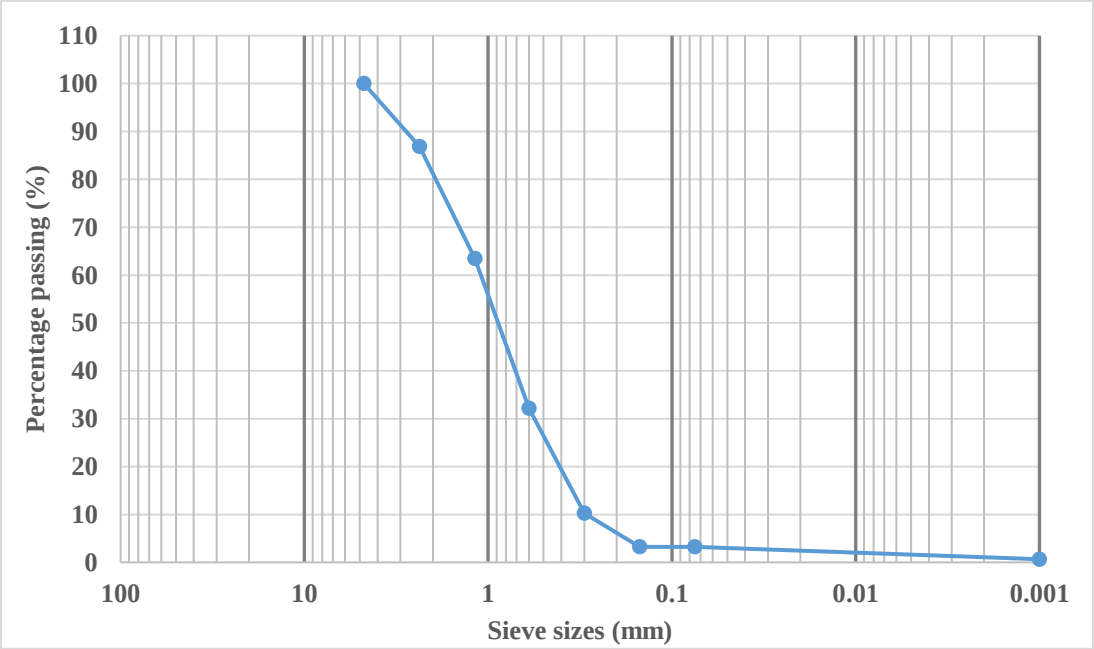

Figure 2. Sieve Analysis for River Sand

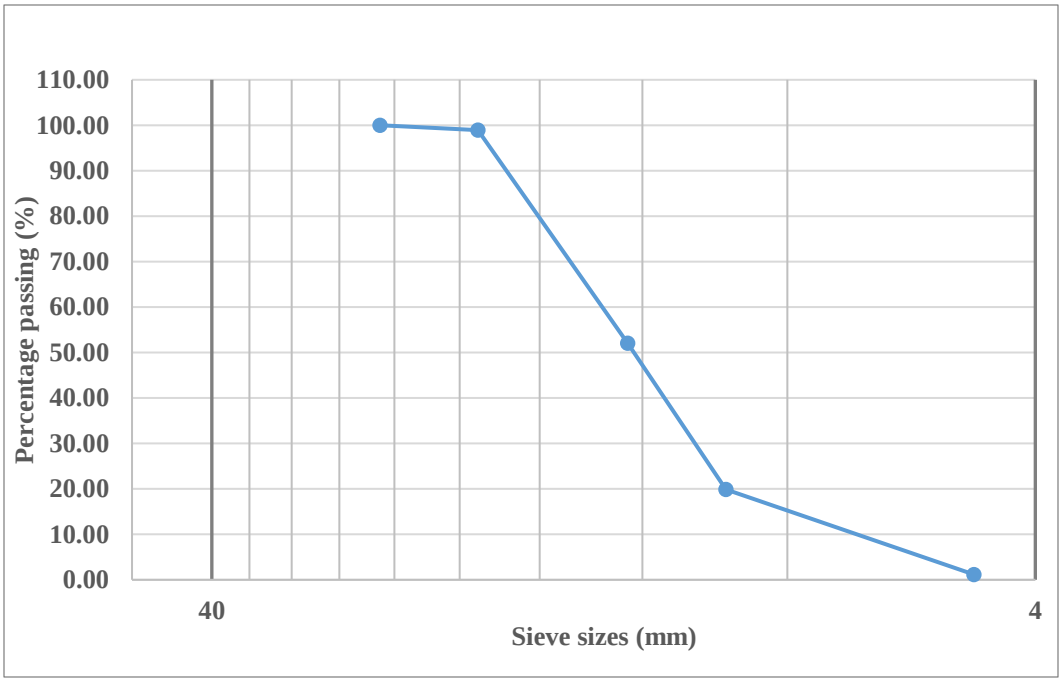

Figure 3. Sieve Analysis for Limestone Rock

The mechanical properties tests had a total of 20 mixtures which includes a control mix referred to as PC-1, three Class C fly ash binary mixes (PC-1+FA-C1, PC-1+FA-C2, and PC-1+FA-C3) each at 30% cement replacement, two Class F fly ash binary mixes (PC-1+FA-F1 and PC-1+FA-F2) each at 20% cement replacement and six ternary blends involving one of the Class C fly ashes (FA-C2) and either of the two Class F fly ashes FA-F1 and FA-F2 at alternating replacement levels of 10/20%, 15/15% and 20/10% while still maintaining a total of 30% cement replacement for each ternary mix. Apart from the binary blends PC-1+FA-C1, PC-1+FA-C3, PC-1+FA-F1 and PC-1+FA-F2 which were produced using a w/cm ratio of 0.45, all other blends (binary and ternary) including control were produced using w/cm ratios of 0.40 and 0.45. This was done to limit the quantity of mixtures produced and also aid comparison of mechanical properties

at w/cm ratios of 0.4 and 0.45. The testing matrix and mix proportions for mechanical properties are shown in Table 4 and 5 respectively.

Table 4. Testing Matrix for Mechanical Properties

Mixture	**W/CM**		**Class C Fly Ash @ 30% Replacement**			**Class F Fly Ash @ 20% Replacement**		**Blended Class C and Class F Fly Ash @ 30% Target Replacement**	
	0.4	0.45	FA-C1	FA-C2	FA-C3	FA-F1	FA-F2	FA-C2+F1	FA-C2+F2
PC-I	✓	✓							
PC-I+FA-C1*		✓	✓						
PC-I+FA-C2	✓	✓		✓					
PC-I+FA-C3*		✓			✓				
PC-I+FA-F1*		✓				✓			
PC-I+FA-F2*		✓					✓		
PC-I+FA-C2+FA-F1 (20%C2/10%F1)	✓	✓						✓	
PC-I+FA-C2+FA-F1 (15%C2/15%F1)	✓	✓						✓	
PC-I+FA-C2+FA-F1 (10%C2/20%F1)	✓	✓						✓	
PC-I+FA-C2+FA-F2 (20%C2/10%F2)	✓	✓							✓
PC-I+FA-C2+FA-F2 (15%C2/15%F2)	✓	✓							✓
PC-I+FA-C2+FA-F2 (10%C2/20%F2)	✓	✓							✓
* w/cm=0.45 ONLY									

Table 5. Mix Proportion for Mechanical Properties Mixtures in kg/m^3

Mixtures	w/cm	Cement	Rock	Sand	Water	FA-C1	FA-C2	FA-C3	FA-F1	FA-F2
PC-I	0.40	390	1100	687	156	-	-	-	-	-
PC-I	0.45	335	1136	711	151	-	-	-	-	-
PC-I+FA-C1(30%)	0.45	234	1125	703	151	100	-	-	-	-
PC-I+FA-C2(30%)	0.40	273	1086	679	156	-	117	-	-	-
PC-I+FA-C2(30%)	0.45	234	1125	703	151	-	100	-	-	-
PC-I+FA-C3(30%)	0.45	234	1125	703	151	-	-	100	-	-
PC-I+FA-F1 (20%)	0.45	267	1129	705	151	-	-	-	67	
PC-I+FA-F2 (20%)	0.45	267	1129	705	151	-	-	-	-	67
PC-I+FA-C2+FA-F1(20%C2/10%F1)	0.40	273	1086	679	156	-	78	-	39	-
PC-I+FA-C2+FA-F1(20%C2/10%F1)	0.45	234	1125	703	151	-	67	-	33	-
PC-I+FA-C2+FA-F1(15%C2/15%F1)	0.40	273	1086	679	156	-	59	-	59	-
PC-I+FA-C2+FA-F1(15%C2/15%F1)	0.45	234	1125	703	151	-	50	-	50	-
PC-I+FA-C2+FA-F1(10%C2/20%F1)	0.40	273	1086	679	156	-	39	-	78	-
PC-I+FA-C2+FA-F1(10%C2/20%F1)	0.45	234	1125	703	151	-	33	-	67	-
PC-I+FA-C2+FA-F2(20%C2/10%F2)	0.40	273	1086	679	156	-	78	-	-	39
PC-I+FA-C2+FA-F2(20%C2/10%F2)	0.45	234	1125	703	151	-	67	-	-	33
PC-I+FA-C2+FA-F2(15%C2/15%F2)	0.40	273	1086	679	156	-	59	-	-	59
PC-I+FA-C2+FA-F2(15%C2/15%F2)	0.45	234	1125	703	151	-	50	-	-	50
PC-I+FA-C2+FA-F2(10%C2/20%F2)	0.40	273	1086	679	156	-	39	-	-	78
PC-I+FA-C2+FA-F2(10%C2/20%F2)	0.45	234	1125	703	151	-	33	-	-	67

All concrete mixtures for determination of mechanical properties were produced in accordance to ASTM C192/C192M-18. The cementitious materials (cement and fly ash) were loaded separately into the mixer during mixing. Fresh property tests such as slump, air content and unit weight were carried out on each mix. Sixteen cylinders of dimension 100 x 200mm (4 x 8 inches) and three prisms of dimension 75 x 75 x 281.25mm (3 x 3 x 11.25 inches) were produced for each mix. This amounted to 60 prisms produced for

drying shrinkage test and 320 cylinders produced for compressive strength, elastic modulus, and tensile strength test. The concrete cylinders and prisms were demolded and transferred to a moist room at 23^0C and > 95% RH for curing after being cast and left in their mold for 24 hours.

3.1.2 Apparatus

The apparatus used for the determination of fresh properties and mechanical properties of concrete are as follows: slump cone and base plate for the determination of slump of fresh concrete as described in section 5.1 of ASTM C143/C143M-15a, a straight steel tamping rod of diameter $^5/_8 \pm ^1/_6$ inches (16±2 mm), an air meter for the determination of air content using pressure method as described in section 4.1.2 of ASTM C231/C231M-17a, bulb syringe, scoop, measuring tape, mallet, trowel, rectangular strike-off plate, balance, vibrating table, concrete mixer, compression testing machine with digital indicator, compressometer for determination of elastic modulus, capping plates and alignment devices, melting pots for sulfur mortar as described in ASTM C617/C617M-15, a drying room that conforms to the requirements of section 5.4 of ASTM C157/C157M-17, length comparator for measuring length change, gauge studs, 100 x 200mm (4 x 8 inches) cylindrical plastic molds, and 75 x 75 x 281.25mm (3 x 3 x 11.25 inches) steel molds.

3.1.3 Procedure

3.1.3.1 ***Fresh properties.*** The slump test was carried out in accordance to ASTM C143/C143M-15a. A metallic slump cone with base plate was used for the slump test. Air content test was done using the pressure method in accordance to ASTM C231/C231M-

17a. This involved the use of an air meter which comprises of a cylindrical measuring bowl and a cover assembly as explained in section 4.1.2 of ASTM C231/C231M-17a. The capacity of the cylindrical measuring bowl was 7.08 x $10^{-3}m^3$ ($0.25ft^3$) and the cover assembly was fitted with clamps, pressure gauge, petcocks for introducing water, main air valve, air bleeder valve, air chamber and hand pump. The unit weight test was carried out in accordance to ASTM C138/C138M-17a.

3.1.3.2 ***Splitting tensile strength.*** This test was carried out in accordance to ASTM C496/C496M-17. Four cylindrical concrete specimens of dimension 100 x 200mm (4 x 8 inches) were produced from each of the twenty concrete mixtures prepared for the determination of mechanical properties. These four concrete cylinders were used to determine the splitting tensile strength at day 28 and 91. Two concrete cylinders were tested at each age (day 28 and 91).

3.1.3.3 ***Compressive strength.*** The compressive strength was determined in accordance to ASTM C39/C39M-18. Unbonded caps were attached to concrete specimens to ensure an even distribution of load during the test. Twelve cylindrical concrete specimens of dimension 100 x 200mm (4 x 8 inches) were produced from each of the twenty concrete mixtures prepared for the determination of mechanical properties. Three cylindrical concrete specimens were tested at day 1, 7, 28 and 91 respectively. However, the determination of compressive strength at ages 28 and 91 was done together with the determination of elastic modulus at the same ages in accordance to ASTM C469/C469M-14.

3.1.3.4 ***Elastic modulus.*** The determination of elastic modulus was done in accordance to ASTM C469/C469M-14. Three cylindrical concrete specimens were used to determine the elastic modulus alongside the compressive strength at ages 28 and 91. Two cylinders out of the three tested for each age (28 and 91) were sulfur capped in accordance to ASTM C617 as prescribed in ASTM C469/C469M-14. The concrete cylinder which was not sulfur capped was first tested for strength with unbonded caps and the ultimate load was recorded. A compressometer was attached to the second cylinder which was sulfur capped and used to read the longitudinal strain (deformation) of the specimen when the cylinder was subjected to compressive loading. The applied load and longitudinal strain were recorded at 40 microstrain and 40% of the ultimate load of the first cylindrical concrete specimen respectively. These values were recorded for three consecutive trials. The second sulfur capped concrete cylinder was later loaded to failure and 40% of its ultimate load was used in testing the third sulfur capped cylinder which went through the same process before it was finally loaded to failure.

3.1.3.5 ***Drying shrinkage.*** The drying shrinkage test was done in accordance to ASTM C157/C157M-17. Three concrete prisms of dimension 75 x 75 x 281.25mm (3 x 3 x 11.25 inches) were produced from each of the twenty concrete mixtures prepared for the determination of mechanical properties. The concrete prisms were demolded 24 hours after casting and transferred to a moist curing room where they were cured for 6 days. The concrete prisms were transferred to a drying room after the curing period and initial comparator readings were taken in the drying room. Subsequent readings were taken in the drying room at day 4, 7, 14, 28, 56, 84, 112, and 224.

3.2 Heat of Hydration using Isothermal Calorimetry

3.2.1 Materials and mix proportion

Type I Portland cement was used for all heat of hydration mixtures. The physical and chemical properties of the cement are shown on Table 1. Two Class F fly ashes and one Class C fly ash referred in this study as FA-F1, FA-F2 and FA-C2 respectively were used as SCMs. The physical and chemical properties of the three fly ashes are shown on Table 2. Fine river sand was used to produce the mortar mixtures and the physical properties and sieve analysis of the fine sand are shown on Table 3 and Figure 2 respectively. The heat of hydration test was carried out using isothermal calorimetry. Paste and mortar mixtures were produced and tested at three different temperatures (23^{o}C, 5^{o}C, and 38^{o}C). The water to cementitious material ratio for the paste and mortar mixtures were 0.42 and 0.45 respectively. Whereas, the sand to cement ratio for the mortar mixtures was 2.25 to 1. The paste and mortar mixtures comprised of two samples of the control mix, two samples for each of the two Class F fly ash binary mixes (PC-1+FA-F1 and PC-1+FA-F2) at 30% cement replacement, two samples of the Class C fly ash binary mix (PC-1+FA-C2) at 30% cement replacement, and two samples for each of the ternary blends involving one of the Class C fly ashes (FA-C2) and either of the two Class F fly ashes FA-F1 and FA-F2 at alternating replacement levels of 10%/20%, 15%/15% and 20%/10% while still maintaining a total of 30% cement replacement for each ternary mix. The testing matrix for the paste and mortar mixtures are given in Table 6 and 7 respectively. The testing matrix for the mortar mixture was the same as the paste mixture except for the addition of fine sand in all mortar mixtures. The mix proportion for the paste and mortar mixtures are given in Table 8 and 9 respectively.

Table 6. Testing Matrix for Paste Mixture

Mix No.	Sample	Cement Type	Fine Aggregate	Fly Ash 1	Fly Ash 2
1	A	PC-Type I	-	N/A	-
	B	PC-Type I	-	N/A	-
2	A	PC-Type I	-	30% -F1	-
	B	PC-Type I	-	30% -F1	-
3	A	PC-Type I	-	30%-F2	-
	B	PC-Type I	-	30%-F2	-
4	A	PC-Type I	-	30% -C2	-
	B	PC-Type I	-	30% -C2	-
5	A	PC-Type I	-	20%-F1	10%-C2
	B	PC-Type I	-	20%-F1	10%-C2
6	A	PC-Type I	-	15%-F1	15%-C2
	B	PC-Type I	-	15%-F1	15%-C2
7	A	PC-Type I	-	10%-F1	20%-C2
	B	PC-Type I	-	10%-F1	20%-C2
8	A	PC-Type I	-	20%-F2	10%-C2
	B	PC-Type I	-	20%-F2	10%-C2
9	A	PC-Type I	-	15%-F2	15%-C2
	B	PC-Type I	-	15%-F2	15%-C2
10	A	PC-Type I	-	10%-F2	20%-C2
	B	PC-Type I	-	10%-F2	20%-C2

Table 7. Testing Matrix for Mortar Mixtures

Mix No.	Sample	Cement Type	Fine Aggregate	Fly Ash 1	Fly Ash 2
1	A	PC-Type I	River Sand	-	-
	B	PC-Type I	River Sand	-	-
2	A	PC-Type I	River Sand	30% -F1	-
	B	PC-Type I	River Sand	30% -F1	-
3	A	PC-Type I	River Sand	30%-F2	-
	B	PC-Type I	River Sand	30%-F2	-
4	A	PC-Type I	River Sand	30% -C2	-
	B	PC-Type I	River Sand	30% -C2	-
5	A	PC-Type I	River Sand	20%-F1	10%-C2
	B	PC-Type I	River Sand	20%-F1	10%-C2
6	A	PC-Type I	River Sand	15%-F1	15%-C2
	B	PC-Type I	River Sand	15%-F1	15%-C2
7	A	PC-Type I	River Sand	10%-F1	20%-C2
	B	PC-Type I	River Sand	10%-F1	20%-C2
8	A	PC-Type I	River Sand	20%-F2	10%-C2
	B	PC-Type I	River Sand	20%-F2	10%-C2
9	A	PC-Type I	River Sand	15%-F2	15%-C2
	B	PC-Type I	River Sand	15%-F2	15%-C2
10	A	PC-Type I	River Sand	10%-F2	20%-C2
	B	PC-Type I	River Sand	10%-F2	20%-C2

Table 8. Mix Proportion for Paste Mixtures

Mixture	**Sample**	**River Sand (g)**	**Type I Cement (g)**	**FA-F1 (g)**	**FA-F2 (g)**	**FA-C2 (g)**	**Water (g)**
PC	A	-	52.8	-	-	-	22.2
	B	-	52.8	-	-	-	22.2
PC+FA-F1	A	-	36.9	15.84	-	-	22.2
	B	-	36.9	15.84	-	-	22.2
PC+FA-F2	A	-	36.9	-	15.84	-	22.2
	B	-	36.9	-	15.84	-	22.2
PC+FA-C2	A	-	36.9	-	-	15.84	22.2
	B	-	36.9	-	-	15.84	22.2
PC+FA-F1+FA-C2 (20%/10%)	A	-	36.9	10.56	-	5.28	22.2
	B	-	36.9	10.56	-	5.28	22.2
PC+FA-F1+FA-C2 (15%/15%)	A	-	36.9	7.92	-	7.92	22.2
	B	-	36.9	7.92	-	7.92	22.2
PC+FA-F1+FA-C2 (10%/20%)	A	-	36.9	5.28	-	10.56	22.2
	B	-	36.9	5.28	-	10.56	22.2
PC+FA-F2+FA-C2 (20%/10%)	A	-	36.9	-	10.56	5.28	22.2
	B	-	36.9	-	10.56	5.28	22.2
PC+FA-F2+FA-C2 (15%/15%)	A	-	36.9	-	7.92	7.92	22.2
	B	-	36.9	-	7.92	7.92	22.2
PC+FA-F2+FA-C2 (10%/20%)	A	-	36.9	-	5.28	10.56	22.2
	B	-	36.9	-	5.28	10.56	22.2

Table 9. Mix Proportion for Mortar Mixtures

Mixture	Sample	River Sand (g)	Type I Cement (g)	FA-F1 (g)	FA-F2 (g)	FA-C2 (g)	Water (g)
PC	A	118.8	52.8	-	-	-	23.7
	B	118.8	52.8	-	-	-	23.7
PC+FA-F1	A	118.8	36.9	15.84	-	-	23.7
	B	118.8	36.9	15.84	-	-	23.7
PC+FA-F2	A	118.8	36.9	-	15.84	-	23.7
	B	118.8	36.9	-	15.84	-	23.7
PC+FA-C2	A	118.8	36.9	-	-	15.84	23.7
	B	118.8	36.9	-	-	15.84	23.7
PC+FA-F1+FA-C2 (20%/10%)	A	118.8	36.9	10.56	-	5.28	23.7
	B	118.8	36.9	10.56	-	5.28	23.7
PC+FA-F1+FA-C2 (15%/15%)	A	118.8	36.9	7.92	-	7.92	23.7
	B	118.8	36.9	7.92	-	7.92	23.7
PC+FA-F1+FA-C2 (10%/20%)	A	118.8	36.9	5.28	-	10.56	23.7
	B	118.8	36.9	5.28	-	10.56	23.7
PC+FA-F2+FA-C2 (20%/10%)	A	118.8	36.9	-	10.56	5.28	23.7
	B	118.8	36.9	-	10.56	5.28	23.7
PC+FA-F2+FA-C2 (15%/15%)	A	118.8	36.9	-	7.92	7.92	23.7
	B	118.8	36.9	-	7.92	7.92	23.7
PC+FA-F2+FA-C2 (10%/20%)	A	118.8	36.9	-	5.28	10.56	23.7
	B	118.8	36.9	-	5.28	10.56	23.7

3.2.2 Apparatus

The apparatus used for the determination of heat of hydration of paste and mortar mixtures are as follows: pipette, spatula, bench mixer, scale, graduated cylinder, a piece of 2mm binding wire, oven, four ounce plastic containers with lids, environmental chamber, isothermal calorimeter and a computer system for data entry and collection.

3.2.3 Procedure

The determination of heat of hydration for paste and mortar mixtures using isothermal calorimetry was carried out in accordance to ASTM C1679-17. This test was done at three different temperatures (23^{o}C, 5^{o}C, and 38^{o}C) for both paste and mortar

mixtures. The isothermal calorimeter was designed to be operated via an installed computer software which was used to input and retrieve information from the calorimeter. The computer system was used for setting the testing temperatures, entering required details of test samples and retrieving the test result at the end. The calorimeter was situated in a room with temperature at 23±4^{o}C but was transferred to an environmental chamber which was set at a temperature of 5^{o}C while testing the mortar mixtures at 5^{o}C. The paste mixtures were prepared by weighing out the cementitious materials in four-ounce containers (two containers per mix) followed by the addition of water before mixing with a bench mixer. The mortar mixtures were prepared in the same vein except for the addition of river sand, hand mixing of the entire constituent (cement, fly ash and river sand) with a spatula before adding water and mixing with the bench mixer. While mixing with the bench mixer, a piece of 2mm binding wire was used to stir the samples in the container to ensure a proper mix. The weights of the constituent of each mix followed by the time at which water was added and the total weight after mixing with the bench mixer were recorded for all mixes and entered into the computer system to aid the final determination of heat of hydration by the system. The containers with samples were placed in the calorimeter immediately after mixing and weighing. Each test ran for 48 hours and the results were automatically recorded and saved by the system.

1

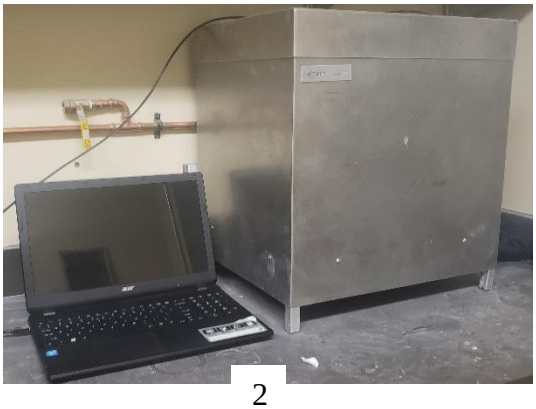

2

Figure 4. (1) Bench Mixer and 4 ounce Containers (2) Isothermal Calorimeter and Computer System

3.3 Alkali Silica Reactivity

In order to ascertain the ability of blended fly ash systems to mitigate ASR in concrete, mortar bars of dimension 25 x 25 x 250mm (1x 1 x 11.25 in) and concrete prisms of dimension 75 x 75 x 250mm (3 x 3 x 11.25 in) were tested in accordance to ASTM C1567 (Accelerated Mortar Bar Test), ASTM C1260 (Mortar Bar Test) and ASTM C1293 (Concrete Prism Test). Also, concrete blocks were made from the same mix used for casting the concrete prisms and subjected to natural conditions to investigate their long-term durability. Fresh property tests like slump, air content, and unit weight were carried out for all concrete mixtures in accordance to ASTM C143/C143M, ASTM C231/C231M, and ASTM C138/C138M respectively.

3.3.1 Accelerated mortar bar test / Mortar bar test

3.3.1.1 ***Materials and mix proportion*****.** A type I Portland cement with an alkali content of 0.78 Na_2O_{eq} was used in this test. The physical and chemical properties of the cement are shown on Table 1. Seven fly ashes comprising of three Class F and four Class C fly ashes

were used in this test. The three Class F and four Class C fly ashes were referred to as FA-F1, FA-F2, FA-F3 and FA-C1, FA-C2, FA-C3, FA-C4 respectively. The chemical properties of the seven fly ashes are given in Table 2. A reactive siliceous river sand was used as fine aggregate in this test. This sand was sieved as prescribed in ASTM C1260 (2014)/ASTM C1567 (2013) and 10%, 25%, 25%, 25% and 15% of samples retained in sieve number 8, 16, 30, 50 and 100 respectively were collected to make up the 2.25 parts of aggregate to 1 cement part required for each mortar mix. The physical properties and sieve analysis for the reactive river sand are given in Table 10 and Figure 5 respectively.

Table 10. Physical Properties of Reactive River Sand

Aggregates	**Bulk specific gravity (OD)**	**Bulk specific gravity (SSD)**	**Apparent specific gravity**	**Absorption (%)**	**Dry rodded unit weight (kg/m^3)**
Reactive River Sand	2.56	2.59	2.63	0.96	1732.51

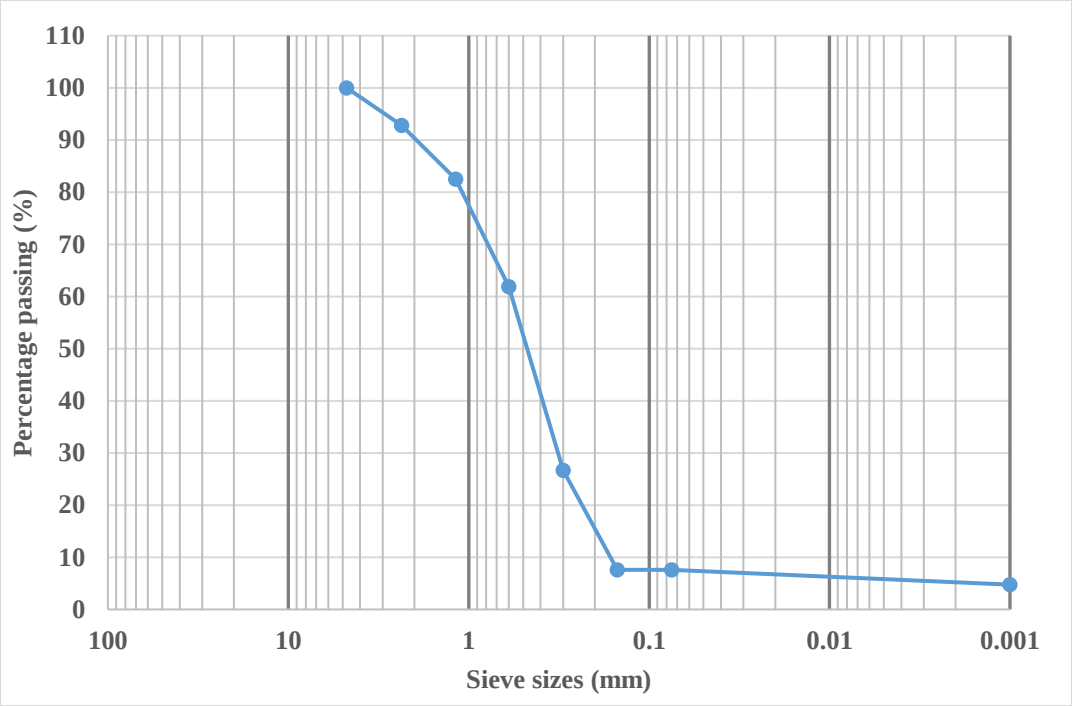

Figure 5. Sieve Analysis for Reactive River Sand

Sodium hydroxide pellets were used in producing the 1N sodium hydroxide solution required for this test. The control was produced in accordance to the Mortar Bar Test (ASTM C1260) with type I Portland cement as the only cementitious material, but the rest of the mixes were produced in accordance to the Accelerated Mortar Bar Test (ASTM C1567) which involved the addition of fly ash to partially replace cement. A total of 24 mixtures were produced for this test. This comprises of a control mix, seven binary mixtures involving the seven fly ashes used in this test at 20% cement replacement, another seven binary mixtures of the same seven fly ashes at 30% replacement and nine ternary mixtures involving the Class C fly ash C2 and each of the Class F fly ashes (F1, F2 and F3) at replacement levels of 20%/10%, 15%/15% and 10%/20% while still

maintaining a total of 30% cement replacement for each of the ternary mix. The mix proportion for this test is given in Table 11

Table 11. Mix Proportion for Accelerated Mortar Bar Test

Mixtures	**% Fly Ash**		**Cement**	**Reactive Fine Sand**	**Water**	**Fly Ash Class C**	**Fly Ash Class F**
	Class C	**Class F**	**(g)**	**(g)**	**(g)**	**(g)**	**(g)**
PC-1	Control		586.70	1320.00	299.25	-	-
PC-1+FA-C1	20	-	469.36	1320.00	244.10	117.34	-
PC-1+FA-C1	30	-	410.69	1320.00	216.52	176.01	-
PC-1+FA-C2	20	-	469.36	1320.00	244.10	117.34	-
PC-1+FA-C2	30	-	410.69	1320.00	216.52	176.01	-
PC-1+FA-C3	20	-	469.36	1320.00	244.10	117.34	-
PC-1+FA-C3	30	-	410.69	1320.00	216.52	176.01	-
PC-1+FA-C4	20	-	469.36	1320.00	244.10	117.34	-
PC-1+FA-C4	30	-	410.69	1320.00	216.52	176.01	-
PC-1+FA-F1	-	20	469.36	1320.00	244.10	-	117.34
PC-1+FA-F1	-	30	410.69	1320.00	216.52	-	176.01
PC-1+FA-F2	-	20	469.36	1320.00	244.10	-	117.34
PC-1+FA-F2	-	30	410.69	1320.00	216.52	-	176.01
PC-1+FA-F3	-	20	469.36	1320.00	244.10	-	117.34
PC-1+FA-F3	-	30	410.69	1320.00	216.52	-	176.01
PC-1+FA-C2+FA-F1	20	10	410.69	1320.00	216.52	117.34	58.67
PC-1+FA-C2+FA-F1	15	15	410.69	1320.00	216.52	88.01	88.01
PC-1+FA-C2+FA-F1	10	20	410.69	1320.00	216.52	58.67	117.34
PC-1+FA-C2+FA-F2	20	10	410.69	1320.00	216.52	117.34	58.67
PC-1+FA-C2+FA-F2	15	15	410.69	1320.00	216.52	88.01	88.01
PC-1+FA-C2+FA-F2	10	20	410.69	1320.00	216.52	58.67	117.34
PC-1+FA-C2+FA-F3	20	10	410.69	1320.00	216.52	117.34	58.67
PC-1+FA-C2+FA-F3	15	15	410.69	1320.00	216.52	88.01	88.01
PC-1+FA-C2+FA-F3	10	20	410.69	1320.00	216.52	58.67	117.34

3.3.1.2 ***Apparatus.*** The apparatus used in this test are: electrically powered mortar mixer with paddle and mixing bowl as described in ASTM C305, tamper and trowel as specified by ASTM C109/C109M, containers for immersing bars as described in section

5.5 of ASTM C1260 (2014), oven, length comparator, and steel molds of dimension 25 x 25 x 250mm (1x 1 x 11.25 in).

3.3.1.3 ***Procedure.*** The Accelerated Mortar Bar Test and the Mortar Bar Test were carried out in accordance to ASTM C1567 (2013) and ASTM C1260 (2014) respectively. The mixing exercise was done in accordance to ASTM C305 and four mortar bars of dimension 25 x 25 x 250mm (1x 1 x 11.25 in) were cast for each mix. The initial comparator readings and zero readings were taken after demolding and before the mortar bars were transferred from water to 1N sodium hydroxide solution respectively. Subsequent readings were taken at day 3, 5, 7, 10, 14, 21, and 28.

3.3.2 Concrete prism test (ASTM C1293)

3.3.2.1 ***Materials and mix proportion.*** A type I Portland cement with an alkali content of 0.78 Na_2O was used in this test. The physical and chemical properties of the cement are shown on Table 1. Three fly ashes comprising of two Class F fly ashes (FA-F1 and FA-F2) and one Class C fly ash (FA-C2) were used in this test. The chemical properties of the three fly ashes are given in Table 2. Fine and coarse aggregates were used in this test. The coarse aggregate was crushed limestone rock sourced from a local quarry in Texas and the fine aggregate was a reactive siliceous river sand. The physical properties and sieve analysis of the coarse aggregates are given in Table 3 and Figure 3 respectively. Whereas, the physical properties and sieve analysis for the reactive siliceous river sand are given in Table 10 and Figure 4 respectively. Sodium hydroxide (NaOH) was also added to each concrete mix at an amount equal to 1.25% of the cement mass. This was done to increase the alkali content of the mixture.

A total of eight mixtures were produced for this test. This includes a control mix, three binary mixtures involving each of the three fly ashes (FA-F1, FA-F2 and FA-C2) at 30% cement replacement and four ternary mixtures involving the Class C fly ash C2 and each of the Class F fly ashes F1 and F2 at replacement levels of 10/20%, 15/15% and 20/10% while still maintaining a total of 30% cement replacement for each ternary mix. The mix proportion for the CPT test and that of the concrete exposure blocks are given in Table 12.

Table 12. Mix Proportion for the Concrete Prism Test and Concrete Exposure Blocks

Mixtures	**% Fly Ash**		**Cement**	**Reactive River Sand**	**Rock**	**Water**	**Fly Ash Class C**	**Fly Ash Class F**
	Class C	**Class F**	**(kg/m^3)**	**(kg/m^3)**	**(kg/m^3)**	**(kg/m^3)**	**(kg/m^3)**	**(kg/m^3)**
PC-1	Control		419.89	666.59	1066.54	187.67	-	-
PC-1+FA-C2	30	-	293.92	657.21	1051.54	188.06	125.97	-
PC-I+FA-F1	-	30	293.92	655.78	1049.25	188.06	-	125.97
PC-I+FA-F2	-	30	293.92	655.78	1049.25	188.06	-	125.97
PC-I+FA-C2+ FA-F1	20	10	293.92	655.78	1049.25	188.06	83.98	41.99
PC-I+FA-C2+ FA-F1	10	20	293.92	655.78	1049.25	188.06	41.99	83.98
PC-I+FA-C2+ FA-F2	20	10	293.92	655.78	1049.25	188.06	83.98	41.99
PC-I+FA-C2+ FA-F2	10	20	293.92	655.78	1049.25	188.06	41.99	83.98

3.3.2.2 ***Apparatus.*** The apparatus used in this test are: an electric powered concrete mixer, length comparator, storage containers as specified in ASTM C1293, tamper rods, trowels, absorbent material and perforated racks as specified in ASTM C1293, concrete mixer, gauge studs, steel molds of dimension 75 x 75 x 250mm (3 x 3 x 11.25 in), storage containers conforming to that prescribed in section 5.2 of ASTM C1293-18a, oven

capable of maintaining temperature at 38± 2ºC and conforms with the storage environment specified in ASTM C1293.

1

2

Figure 6. (1) Storage container as prescribed in ASTM C1293 (2) Storage environment as prescribed in ASTM C1293

3.3.2.3 ***Procedure.*** The Concrete Prism Test was carried out in accordance to ASTM C1293-18a. Four prisms of dimension 75 x 75 x 250mm (3 x 3 x 11.25 in) were produced from each mix for this test. The prisms were demolded after 24 hours and initial comparator readings were taken. Afterwards, the prisms were transferred to a moist curing room where they were cured for 6 days. The 7 days comparator reading were taken after curing and the prisms were placed in storage containers as specified in ASTM C1293-18a. They were four prisms in each storage container representing one mix. All containers were stored in a storage environment with temperature maintained at 38 ± 2ºC. Subsequent comparator readings were taken at the ages of 28 days, 56 days, 3 months, 6 months, 9 months, and 12 months. The containers were removed from the oven and

transferred to a temperature-controlled environment as specified in ASTM C1293-18a for a period of 16±4 hours before the readings were taken.

3.3.3 Concrete exposure blocks

3.3.3.1 ***Materials and mix proportion.*** The same materials (cement, fly ash, rocks, reactive siliceous river sand, and NaOH) and mix proportion used in the Concrete Prism Test were used for the Concrete Exposure Blocks. The properties of the cement and fly ashes are given in Table 1 and Table 2 respectively. The physical properties and sieve analysis of the coarse aggregates are given in Table 3 and Figure 3 respectively. Whereas, the physical properties and sieve analysis for the reactive siliceous river sand are given in Table 10 and Figure 4 respectively. The exposure blocks were cast from the same eight mixes that was used to produce the prisms for the Concrete Prism Test. One block was cast from each mix which amounted to eight blocks. The mix proportion for this test was the same as that used for the Concrete Prism Test and is given in Table 12.

3.3.3.2 ***Apparatus.*** The apparatus used in this test are: poker vibrator, molds capable of forming concrete blocks of dimension 406.4 x 406.4 x 406.4mm (16 x 16 x 16 in), concrete mixer, trowel, hand-held length comparator.

1 2 3

Figure 7. (1) Interior View of 406 x 406 x 406mm (16 x 16 x 16 in) Mold (2) Exterior View of 406 x 406 x 406mm (16 x 16 x 16 in) Mold (3) Concrete Blocks After Casting and Demolding

3.3.3.3 ***Procedure***. The Concrete Exposure Blocks were produced and tested in accordance to ASTM C 1293-18a. Wooden molds were fabricated to enable the casting of blocks of dimension 406 x 406 x 406mm (16 x 16 x 16 in). One concrete block was produced from each mix. The molds were designed to accommodate 20 pieces of 5 inches long bolts, four on each surface except the bottom surface. Each bolt was designed to have a tiny hole at the end to enable length measurement using a hand-held length comparator. The bolts on each side surface were positioned in such a way that they protruded slightly from the concrete block after casting with two bolts aligning horizontally and the other two vertically. The horizontal and vertical distance between bolts were 254mm (10 in) for two of the side surfaces and 203mm (8 in) for the other two side surfaces. However, the four bolts at the top surface were positioned like the vertices of a square. This distance between the top bolts was 254mm (10 in). Pictures of the mold and block are given in Figure 6. Concrete was poured into the molds in roughly three equal layers. Each layer was compacted with a poker vibrator after which a trowel was

used to smoothen the surface to ensure that the concrete flushed with the top of the mold. The molds were covered with their lids and left for 24 hours for setting and hardening to take place before demolding. The concrete blocks were cured for 6 days in the laboratory by covering them with wet burlap materials and plastic bags to prevent loss of moisture. The blocks were checked continuously within the 6 days to see if the burlap material needed wetting. The first comparator readings were taken in the laboratory at age 7 using the hand-held length comparator. The initial lengths between the vertical and horizontal bolts were measured for all side surfaces. Likewise, the lengths between the top surface bolts were measured in a manner that looks as if the sides of a square are been measured. The blocks were later moved from the laboratory to an exposure site (open field) where they remained permanently throughout the test. Subsequent measurements were taken in the same manner at the exposure sites at temperatures between 20^{o}C and 26^{o}C (68^{o}F and 78^{o}F). This was done at the ages of 28 days, 56 days, 3 months, 6 months, 9 months, and 12 months. Figure 8 and Table 13 shows a picture of the exposure site and environmental conditions during the test period respectively.

Figure 8. Outdoor Exposure Site Located in San Marcos, Texas

Table 13. Environmental Conditions during Test Period (WeatherUnderground, 2019)

Temperature, ºC (ºF)	-4 – 43 (25 – 109)
RH, %	10 – 100
Annual Precipitation, Inches	989.02

4. RESULTS AND DISCUSSIONS

4.1 Mechanical Properties

4.1.1 Fresh properties

The results of the fresh property tests (slump, air content and unit weight) for all mechanical properties mixtures are given in Table 14.

Table 14. Fresh Properties Tests Results

Mixture	**% Fly Ash**		**w/cm = 0.40**			**w/cm = 0.45**		
	C	**F**	**Slump (mm)**	**Air Content (%)**	**Unit Weight (kg/m^3)**	**Slump (mm)**	**Air Content (%)**	**Unit Weight (kg/m^3)**
PC-1	Control		6.35	2.20	2411.67	12.70	2.30	2373.23
PC-I+FA-C1	30		-	-	-	57.15	1.80	2366.82
PC-I+FA-C2	30		57.15	2.00	2392.45	25.40	2.10	2359.13
PC-I+FA-C3	30		-	-	-	31.75	2.00	2356.57
PC-I+FA-F1	-	20	-	-	-	50.80	2.00	2343.75
PC-I+FA-F2	-	20	-	-	-	38.10	1.90	2362.98
PC-I+FA-C2+FA-F1	20	10	82.55	2.50	2389.89	44.45	1.30	2411.67
PC-I+FA-C2+FA-F1	15	15	69.85	1.10	2347.60	50.80	1.40	2352.72
PC-I+FA-C2+FA-F1	10	20	50.80	2.20	2368.10	57.15	2.00	2395.01
PC-I+FA-C2+FA-F2	20	10	63.50	1.50	2388.60	25.40	1.50	2396.29
PC-I+FA-C2+FA-F2	15	15	31.75	1.70	2393.73	19.05	1.70	2400.14
PC-I+FA-C2+FA-F2	10	20	69.85	1.80	2402.70	12.70	1.50	2418.08

4.1.2 Compressive strength

The compressive strength test results for all mixtures are given in Table 15. The compressive strength for binary mixtures (cement and one fly ash) at w/cm ratios of 0.40 and 0.45 are represented graphically in Figure 9 and Figure 10 respectively.

Table 15. Compressive Strength Test Results in MPa

Mixture	**% Fly Ash**		**w/cm = 0.40**				**w/cm = 0.45**			
			Age (Days)				**Age (Days)**			
	C	F	Day 1	Day 7	Day 28	Day 91	Day 1	Day 7	Day 28	Day 91
PC-1	Control		56.7	82.8	80.1	93.8	41.5	64.3	69.1	79.8
PC-I+FA-C1	30	-	-	-	-	-	31.6	56.5	78.5	80.7
PC-I+FA-C2	30	-	42.0	76.4	86.8	101.0	30.1	61.7	79.1	91.9
PC-I+FA-C3	30	-	-	-	-	-	30.4	63.1	70.0	94.0
PC-I+FA-F1	-	20	-	-	-	-	34.9	56.5	62.8	77.4
PC-I+FA-F2	-	20	-	-	-	-	37.2	62.5	64.8	87.1
PC-I+FA-C2+FA-F1	20	10	41.4	67.2	77.1	97.1	36.3	56.0	78.1	88.9
PC-I+FA-C2+FA-F1	15	15	42.0	59.8	77.0	92.2	34.6	56.4	72.0	87.7
PC-I+FA-C2+FA-F1	10	20	35.4	52.2	69.5	89.0	28.3	42.8	62.4	73.0
PC-I+FA-C2+FA-F2	20	10	38.8	70.0	83.6	98.6	32.7	64.2	81.7	98.0
PC-I+FA-C2+FA-F2	15	15	40.9	70.7	87.7	105.4	33.7	64.4	80.5	90.2
PC-I+FA-C2+FA-F2	10	20	38.1	58.5	73.8	95.1	37.4	72.7	90.1	102.5

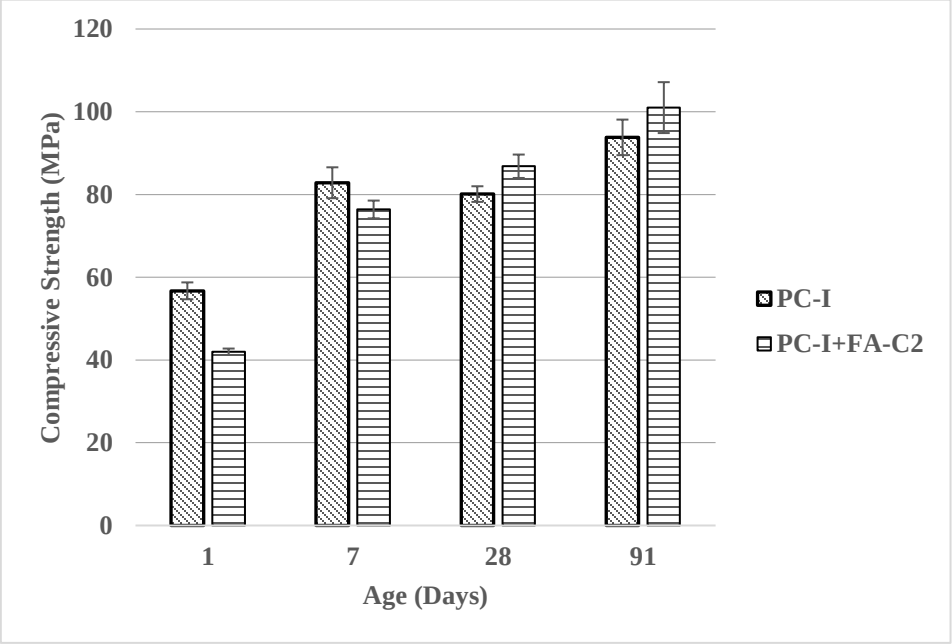

Figure 9. Compressive Strength for Binary Mixture at w/cm of 0.40

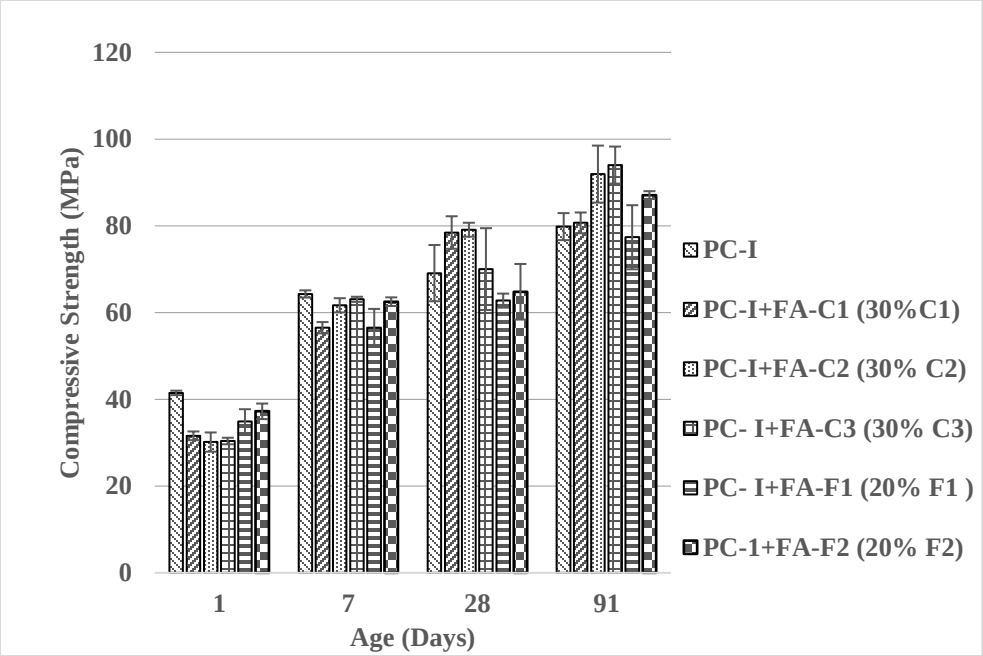

Figure 10. Compressive Strength for Binary Mixtures at w/cm of 0.45

The result shows the effect of w/cm ratio on the compressive strength of concrete as all mixtures tested at w/cm ratio of 0.4 exhibited higher compressive strengths compared to their corresponding compressive strengths at a w/cm ratio of 0.45. The results on Figure 9 and 10 showed that the compressive strength of all binary mixtures and control at w/cm ratios of 0.45 and 0.40 increased as the curing age of the concrete increased. Though, the compressive strength of the binary mixture containing fly ash C2 at w/cm of 0.4 remained lower than the control mixture at the same w/cm ratio at day 1 and 7, it later became higher than the control mixture at day 28 and 91 due to pozzolanic reactions. Figure 10 showed that the compressive strength of the control concrete (PC-1) at w/cm ratio of 0.45 was higher than that of all binary mixtures at day 1 and 7. However, the compressive strength of the binary mixtures containing 30%C2, 30%C3 and 20%F2 were close to that of the control mix at day 7 and finally exceeded the control at day 91. This

early increase in strength at the age of 7 exhibited by the binary mixtures containing 30%C2, 30%C3 and 20%F2 are as a result of their high reactivity and CaO content. This result conforms with the statement made by M. D. A Thomas et al. concerning high and low CaO fly ashes (M. D.A. Thomas et al., 1999). Although this attribute is peculiar to Class C fly ashes, the Class F fly ash F2 which was produced by burning 80% PRB coal and 20% Lignite coal exhibited this same early strength gain due to its chemical properties which are somewhat intermediate of the other two Class F and four Class C fly ashes shown in Table 2. The compressive strength of the Class F fly ash binary mixture PC-1+FA-F2 at 20% cement replacement was higher than the Class F fly ash binary mixture PC-1+FA-F1 at the same cement replacement in all ages. This lower compressive strength of Class F fly ash binary mixture PC-1+ FA-F1 as compared to that of F2 (PC-1+FA-F2) was due to the low CaO content of the Class F fly ash F1. This is also in agreement with the results of M. D. A Thomas et al. (1999). Also shown on Figure 10 are the compressive strength of the binary mixtures containing the Class C fly ashes C1, C2, and C3 at 30% cement replacement which were higher than the control mixture at day 28 and 91. The binary mixture containing fly ash C2 at 30% replacement had the highest compressive strength among other mixtures at day 28 but was superseded by the binary mixture containing fly ash C3 at day 91. The higher compressive strength exhibited by the binary mixture containing fly ash C3 at day 91 is likely due to pozzolanic reaction. All fly ash binary mixtures exceeded the control at day 91 except the binary mixture with fly ash F1. However, the binary mixture containing F1 showed a continuous increase in strength as the age increased and most likely would continue to attain higher strengths at later ages due to pozzolanic reaction.

The compressive strength for the ternary mixtures at w/cm ratios of 0.4 and 0.45 are shown in Figure 11 and 12 respectively.

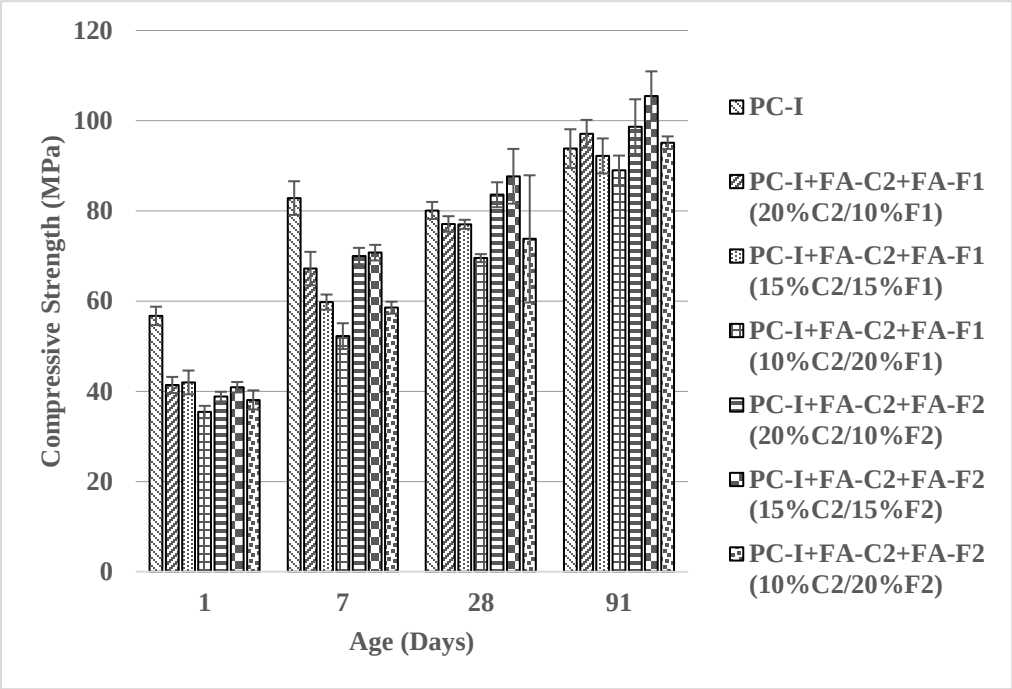

Figure 11. Compressive Strength for Ternary Mixtures at w/cm of 0.40

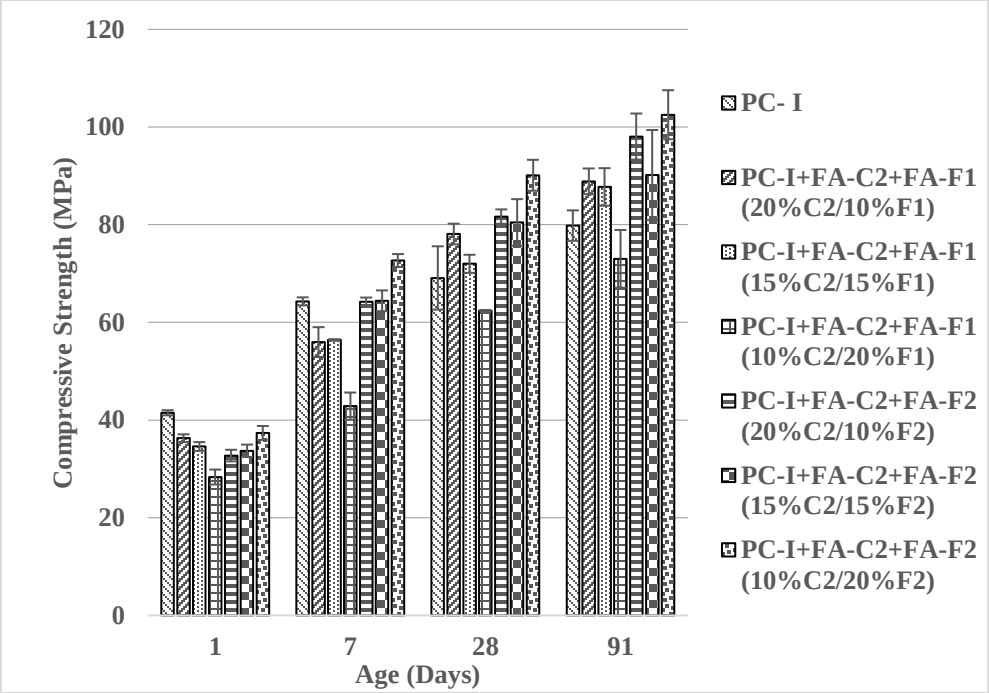

Figure 12. Compressive Strength for Ternary Mixtures at w/cm of 0.45

All ternary mixtures at w/cm ratios of 0.4 and 0.45 including the control mixtures increased as the age of the concrete increased. The compressive strength of the control concrete at w/cm ratios of 0.4 and 0.45 exceeded that of other ternary mixtures of the same w/cm ratios at day 1. However, at day 7 the compressive strength of the control concrete (64.3 MPa) at a w/cm ratio of 0.45 was exceeded by that of the ternary mixture containing 10%C2/20% F2 with a compressive strength of 72.7 MPa. Figure 12 showed that the ternary mixture involving 10%C2 /20%F2 at a w/cm ratio of 0.45 had the highest compressive strength compared to the control and other ternary mixtures at day 7, 28 and 91. This high strength of the ternary mixture involving 10%C2 /20%F2 was as a result of the high pozzolanic reactivity and early strength gain of the fly ashes C2 and F2. The compressive strength of all other ternary mixtures at a w/cm ratio of 0.45 exceeded that

of the control concrete at ages 28 and 91 except for the ternary mixture involving 10%C2 /20%F1. This was depicted on both Figure 11 and Figure 12 as the ternary mixture involving 10%C2 /20%F1 remained the lowest at all ages (1, 7, 28 and 91) compared to the control concrete and other ternary mixtures. The lower strength of the ternary mixture involving 10%C2 /20% F1 was likely as a result of the low CaO content of the Class F fly ash F1 which had a higher cement replacement level of 20% in the mix. For this same reason, the ternary mixtures containing C2 and F2 at all tested cement replacement levels and w/cm ratio of 0.45 outperformed those containing C2 and F1 at day 7, 28, and 91. The compressive strength of the control concrete at a w/cm ratio of 0.4 remained higher than that of the ternary mixtures at day 7. However, the compressive strength of the ternary mixtures involving 20%C2/10%F2 and 15%C2/15%F2 at w/cm ratio of 0.4 were higher than other ternary mixtures of the same w/cm ratio at day 28 and 91 with the ternary mixture involving 15%C2/15%F2 as the highest in both ages (day 28 and 91). This high compressive strength is due to the high reactivity and early strength gain of the fly ashes C2 and F2 as well as the replacement levels and w/cm ratio used.

4.1.3 Splitting tensile strength

The splitting tensile strength results are given in Table 16. The splitting tensile strength for fly ash binary mixtures at w/cm ratios of 0.4 and 0.45 are given in Figure 13 and Figure 14 respectively. Whereas, that for ternary mixtures at w/cm ratios of 0.4 and 0.45 are given in Figure 15 and Figure 16 respectively.

Table 16. Splitting Tensile Strength Result in MPa

Mixture	% Fly Ash		w/cm:	0.40		0.45	
	Class C	Class F	Age (Days):	28	91	28	91
PC-1	Control			7.21	8.46	6.02	6.81
PC-I+FA-C1	30	-		-	-	4.80	6.62
PC-I+FA-C2	30	-		7.43	7.60	4.85	7.96
PC-I+FA-C3	30	-		-	-	6.70	7.56
PC-I+FA-F1	-	20		-	-	5.81	7.45
PC-I+FA-F2	-	20		-	-	6.83	6.27
PC-I+FA-C2+FA-F1	20	10		5.48	6.86	7.13	6.82
PC-I+FA-C2+FA-F1	15	15		5.24	7.22	5.60	6.31
PC-I+FA-C2+FA-F1	10	20		6.59	5.56	5.58	5.43
PC-I+FA-C2+FA-F2	20	10		5.21	6.88	6.11	6.76
PC-I+FA-C2+FA-F2	15	15		4.38	7.03	4.10	7.41
PC-I+FA-C2+FA-F2	10	20		6.31	6.15	6.93	7.35

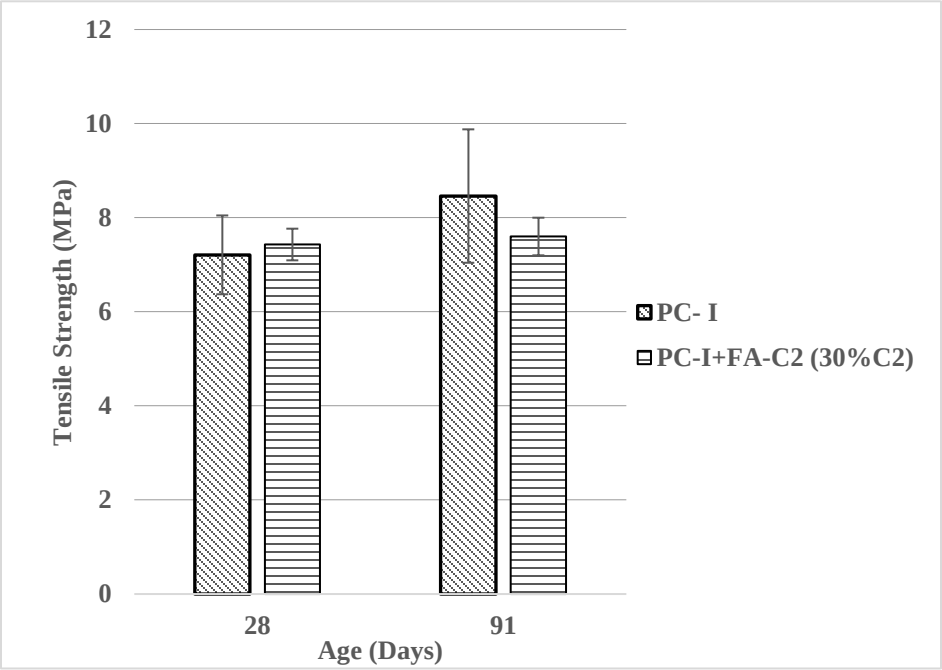

Figure 13. Splitting Tensile Strength for Binary Mixture at w/cm of 0.4

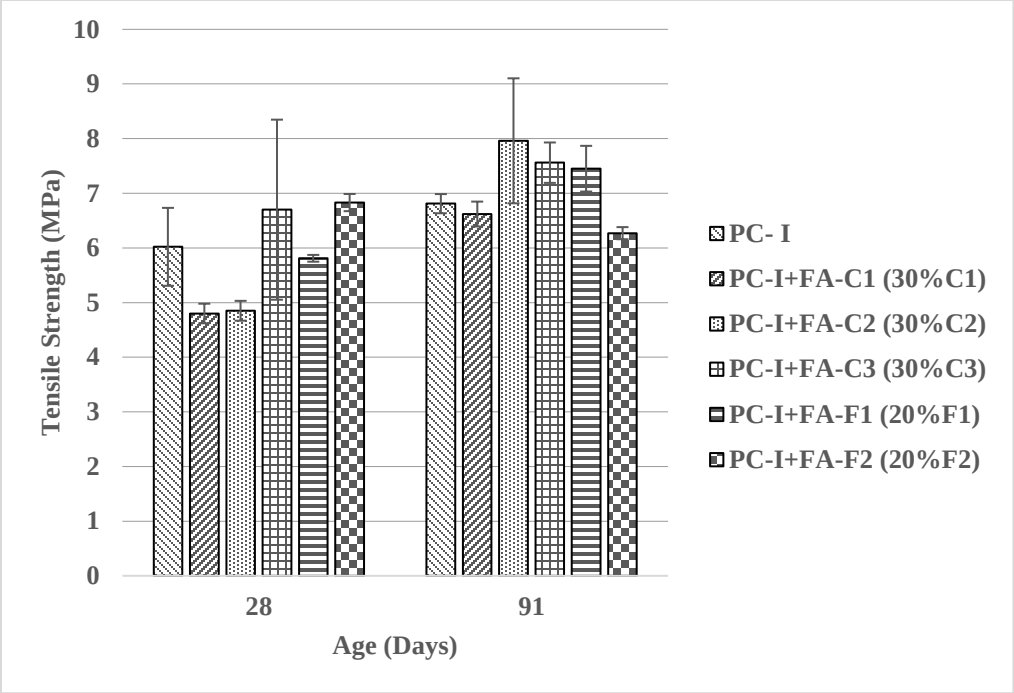

Figure 14. Splitting Tensile Strength for Binary Mixtures at w/cm of 0.45

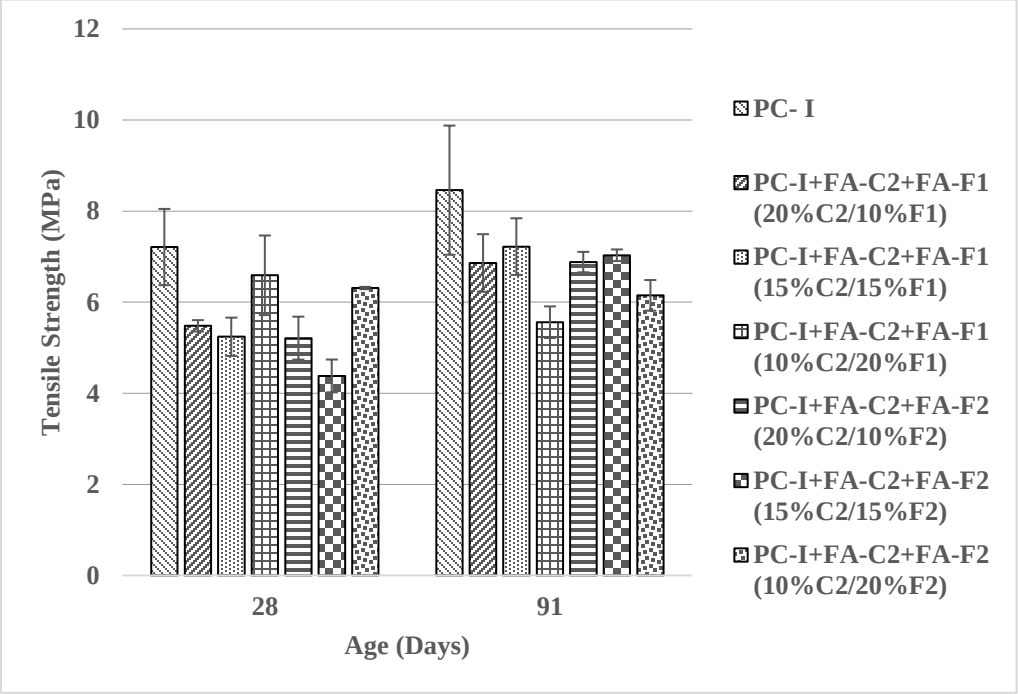

Figure 15. Splitting Tensile Strength for Ternary Mixtures at w/cm of 0.4

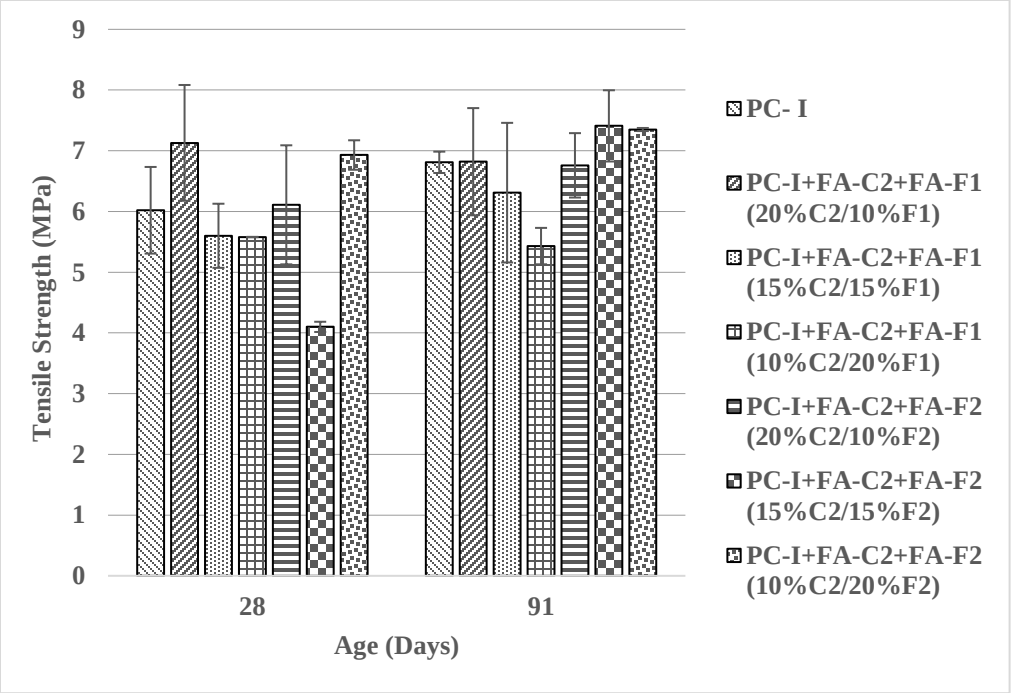

Figure 16. Splitting Tensile Strength for Ternary Mixtures at w/cm of 0.45

The controls and fly ash binary mixtures at w/cm ratios of 0.4 and 0.45 increased in tensile strength as their age increased from day 28 to 91 except for the binary mixture involving 20%F2 at w/cm ratio of 0.45 which exhibited a dramatic reduction in tensile strength at day 91. However, the splitting tensile strength for the binary mixture (PC-1+FA-C2) at 30% C2 replacement and w/cm ratio of 0.4 was higher than the control at day 28 but was exceeded by the control at day 91. This increased tensile strength of the control at day 91 and w/cm ratio of 0.4 was as a result of the improved tensile strength experienced in hydraulic cement concrete at lower w/cm ratio. The binary mixtures involving 30%C3 and 20%F2 at w/cm ratio of 0.45 had higher tensile strengths compared to the control at day 28. But at day 91, the binary mixtures involving 30%C2, 30%C3 and

20%F1 outperformed the control except for the binary mixture involving 30%C1. This observed performance in tensile strength from the fly ash binary mixtures at day 91 was as a result of improved microstructure due to pozzolanic reactions. The binary mixture with the highest tensile strength at day 91 and w/cm ratio of 0.45 was that with 30%C2 cement replacement. This high tensile strength was due to the pozzolanic effect of fly ash C2 in the mix.

As for the tensile strength of ternary mixtures at w/cm ratio of 0.40, the control outperformed all ternary mixtures at day 28 and 91. However, among the ternary mixtures at w/cm ratio of 0.4, the ternary mixture involving 10%C2/20%F1 was the highest in splitting tensile strength at day 28. Whereas the ternary mixture involving 15%C2/15%F1 was the highest in splitting tensile strength at day 91. The observed increase in splitting tensile strength in the ternary mixture involving 15%C2/15%F1 at day 91 was due to pozzolanic reaction of the fly ashes C2 and F1. There was also a dramatic reduction in splitting tensile strength displayed by ternary mixtures involving 10%C2/20%F1 and 10%C2/20%F2 at day 91. All ternary mixtures at w/cm ratio of 0.45 showed an increase in splitting tensile strength from day 28 to day 91 due to pozzolanic reactions except for the ternary mixture involving 20%C2/10%F1. The ternary mixtures involving 10%C2/20%F2 and 20%C2/10%F1 at a w/cm ratio of 0.45 performed better than other mixtures including the control at day 28. Whereas, the ternary mixtures involving 10%C2/20%F2 and 15%C2/15%F2 at a w/cm ratio of 0.45 outperformed other ternary mixtures at the same w/cm ratio including the control at day 91.

4.1.4 Elastic modulus

The elastic modulus test results are given in Table 17. The elastic modulus for fly ash binary mixtures at w/cm ratios of 0.4 and 0.45 are given in Figure 17 and Figure 18 respectively. Whereas, that for ternary mixtures at w/cm ratios of 0.4 and 0.45 are given in Figure 19 and Figure 20 respectively.

Table 17. Modulus of Elasticity Test Results in GPa

Mixture	**% Fly Ash**		**w/cm:**	**0.40**		**0.45**	
	C	**F**	**Age (Days):**	**28**	**91**	**28**	**91**
PC-1	Control			62.1	60.6	55.1	58.4
PC-I+FA-C1	30	-		-	-	61.2	61.1
PC-I+FA-C2	30	-		60.8	65.9	58.6	62.8
PC-I+FA-C3	30	-		-	-	54.6	63.3
PC-I+FA-F1	-	20		-	-	56.6	58.3
PC-I+FA-F2	-	20		-	-	58.6	63.9
PC-I+FA-C2+FA-F1	20	10		57.5	63.3	58.4	62.7
PC-I+FA-C2+FA-F1	15	15		57.9	61.4	57.2	60.0
PC-I+FA-C2+FA-F1	10	20		57.9	58.8	56.2	52.4
PC-I+FA-C2+FA-F2	20	10		61.9	64.7	61.7	66.1
PC-I+FA-C2+FA-F2	15	15		61.4	62.7	61.9	62.1
PC-I+FA-C2+FA-F2	10	20		60.4	62.9	61.3	62.5

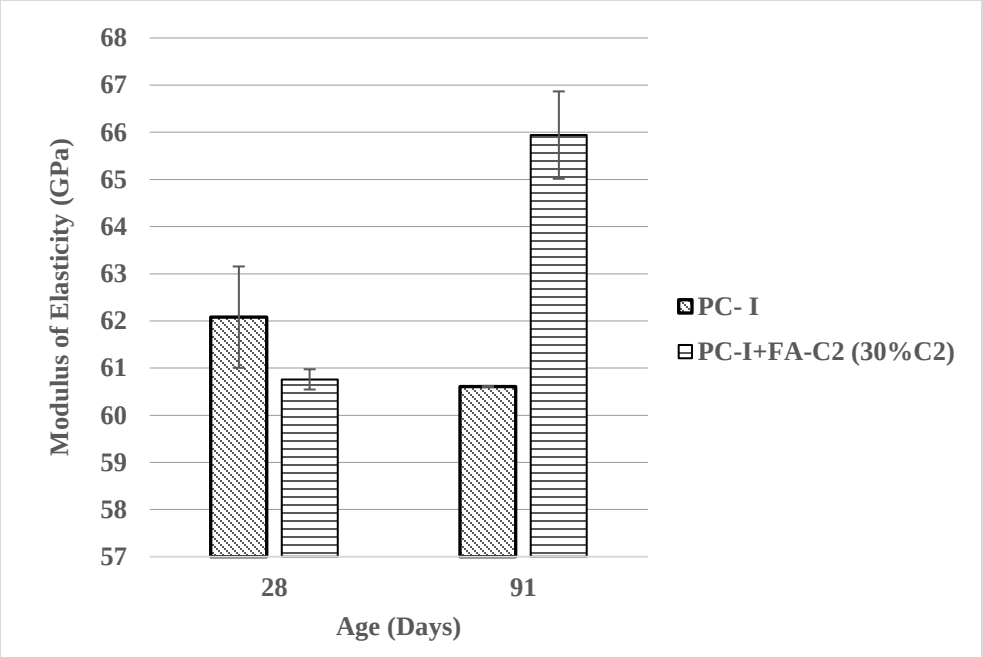

Figure 17. Modulus of Elasticity for Binary Mixture at w/cm of 0.4

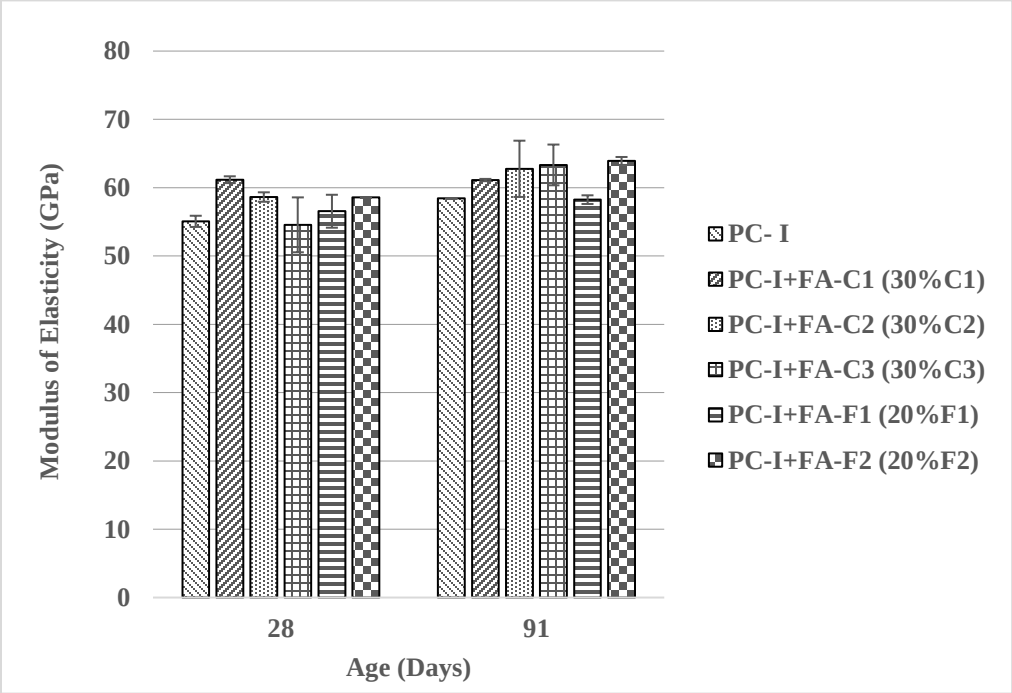

Figure 18. Modulus of Elasticity for Binary Mixture at w/cm of 0.45

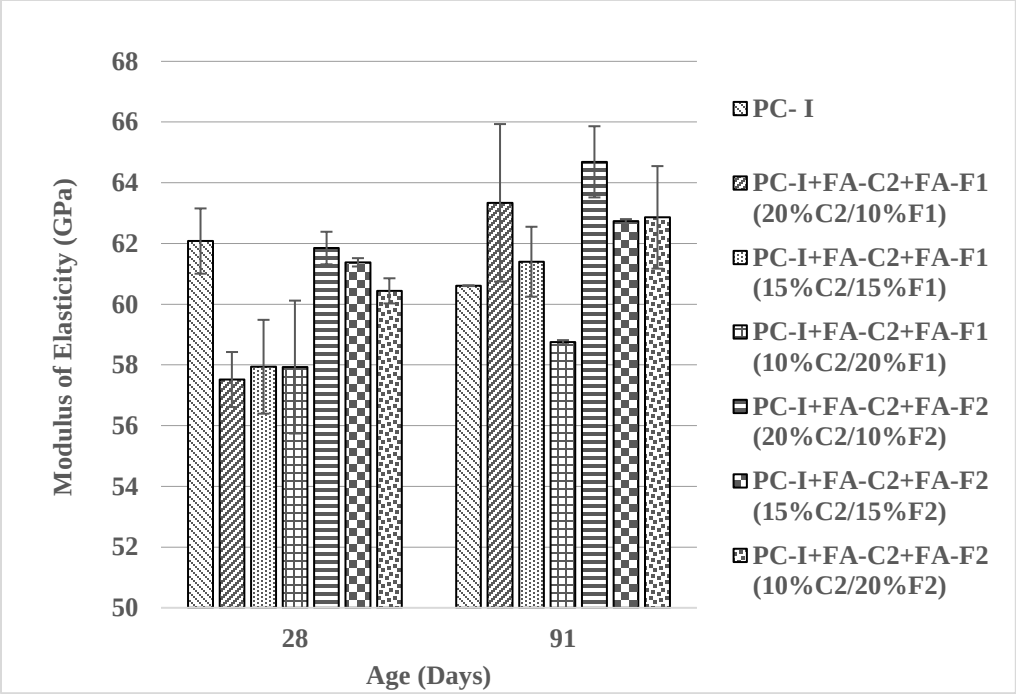

Figure 19. Modulus of Elasticity for Ternary Mixture at w/cm of 0.4

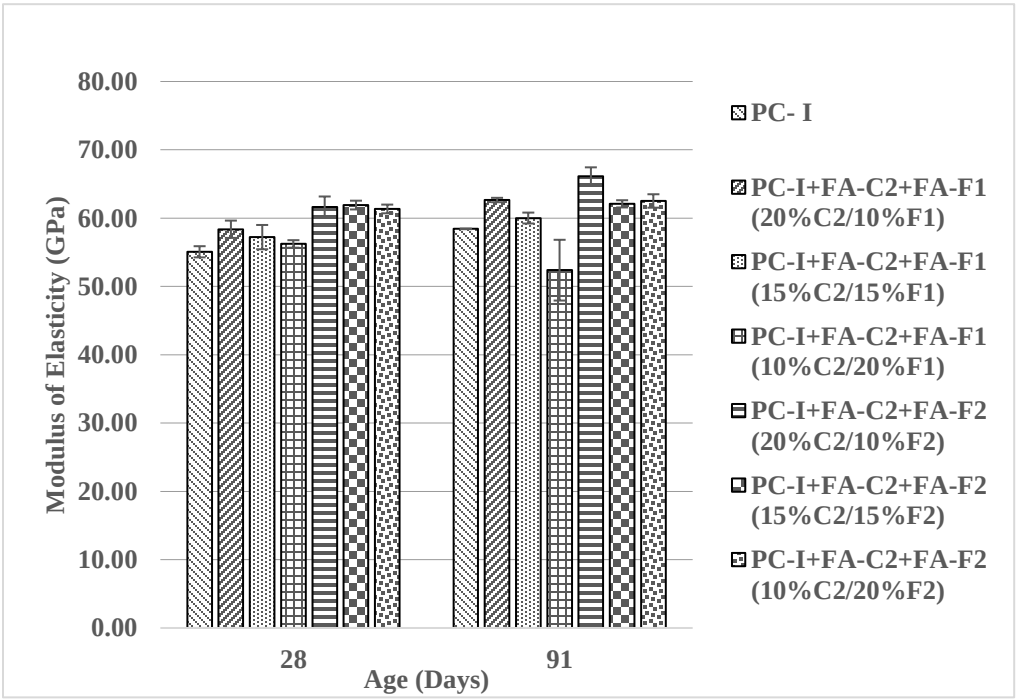

Figure 20. Modulus of Elasticity for Ternary Mixture at w/cm of 0.45

The modulus of elasticity of the binary mixture involving 30%C2 at w/cm ratio of 0.4 was lower than that of the control at day 28 but later exceeded the control at day 91 due to the pozzolanic reaction of fly ash C2. There was an increase in elastic modulus for all binary mixtures including control at a w/cm ratio 0.45 at day 91 with the binary mixture involving 30%F2 as the highest at day 91. All the binary mixtures at a w/cm ratio of 0.45 outperformed the control at day 28 and 91 except for the mixture involving 30%C3 at day 28 and that involving 20%F1 at day 91. This increase in elastic modulus observed in all fly ash binary mixtures was as a result of their pozzolanic reactions. For the ternary mixtures at w/cm of 0.4, the control exceeded the ternary mixtures at day 28. Though, the elastic modulus for the ternary mixtures involving 20%C2/10%F2, 10%C2/20%F2, and 15%C2/15%F2 came close to that of the control at day 28. This is likely due to enhancements in structure and strength of concrete associated with the use of fly ash C2 and F2. All the ternary mixtures at w/cm ratio of 0.4 outperformed the control at day 91 except for that involving 10%C2/20%F1. This low performance of the ternary mix involving 10%C2/20%F1 at day 91 was as a result of the low reactivity and strength gain of the Fly ash F1 which had the highest percentage replacement in the mix. The ternary mix involving 20%C2/10%F2 at w/cm ratio of 0.4 had the highest elastic modulus at day 91. All ternary mixtures at w/cm ratio of 0.45 outperformed the control at day 28 and 91 except for the ternary mixture involving 10%C2/20%F1 which reduced and became lesser than the control at day 91. This performance at day 91 for the ternary mixtures at w/cm ratio of 0.45 can be attributed to improvements due to the pozzolanic reactions of the various blends of fly ash used. The ternary mixtures involving 15%C2/15%F2 and

20%C2/10%F2 at w/cm ratio of 0.45 had the highest elastic modulus at day 28 and 91 respectively.

4.1.5 Drying shrinkage

The percentage drying shrinkage for all mixtures tested are given in Table 17. The drying shrinkage of the only fly ash binary mixture tested at w/cm ratio of 0.4 and the ternary mixtures at w/cm ratio of 0.4 are given in Figure 21 and Figure 22 respectively.

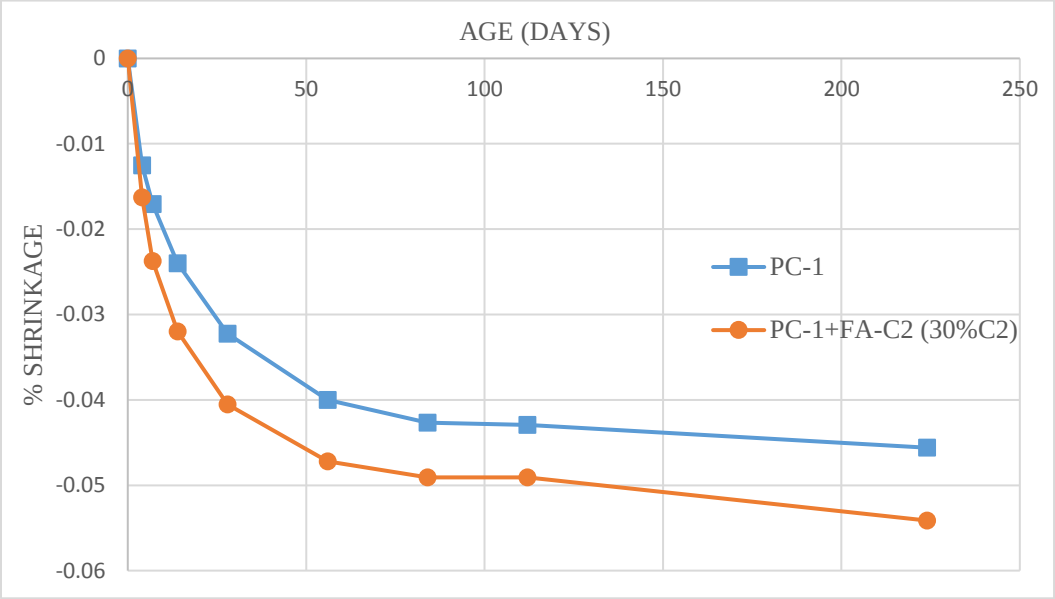

Figure 21. Percentage Drying Shrinkage for Binary Mixture at w/cm of 0.4

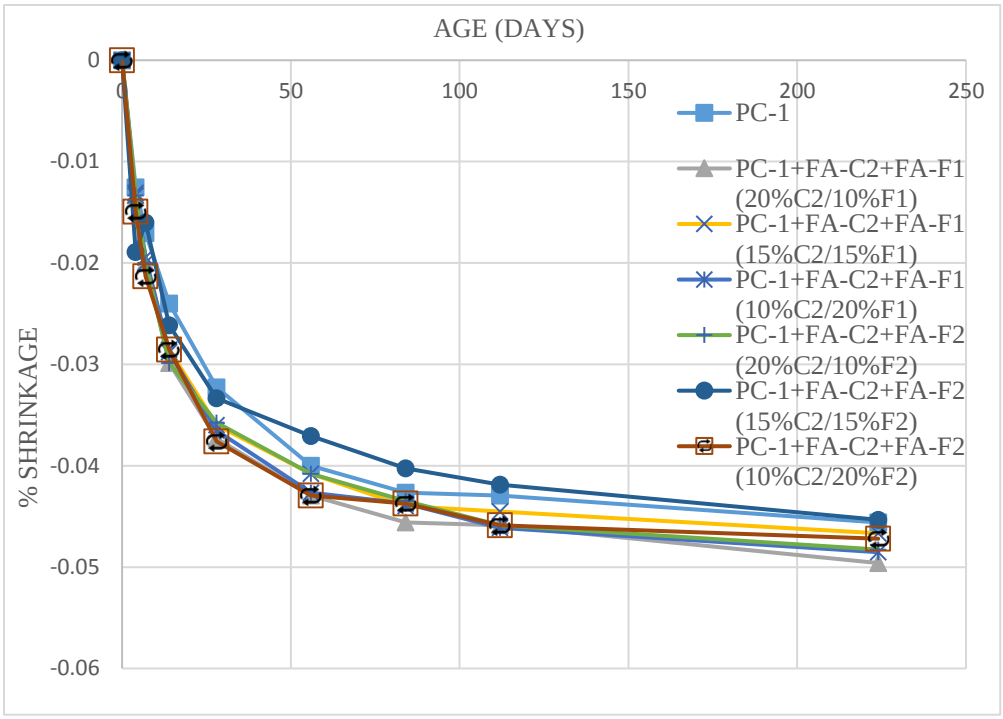

Figure 22. Percentage Drying Shrinkage for Ternary Mixture at w/cm of 0.4

Table 18. Drying Shrinkage Results for all Mixtures in Percent

W/CM =0.4								
AGE (DAYS):	**4**	**7**	**14**	**28**	**56**	**84**	**112**	**224**
MIXTURES	**(%)**	**(%)**	**(%)**	**(%)**	**(%)**	**(%)**	**(%)**	**(%)**
PC-1	-0.013	-0.017	-0.024	-0.032	-0.040	-0.043	-0.043	-0.046
PC-1+FA-C2 (30%C2)	-0.016	-0.024	-0.032	-0.041	-0.047	-0.049	-0.049	-0.054
PC-1+FA-C2+FA-F1 (20%C2/10%F1)	-0.013	-0.020	-0.030	-0.037	-0.043	-0.046	-0.046	-0.050
PC-1+FA-C2+FA-F1 (15%C2/15%F1)	-0.013	-0.020	-0.029	-0.036	-0.041	-0.044	-0.045	-0.047
PC-1+FA-C2+FA-F1 (10%C2/20%F1)	-0.013	-0.019	-0.029	-0.037	-0.043	-0.044	-0.046	-0.049
PC-1+FA-C2+FA-F2 (20%C2/10%F2)	-0.013	-0.020	-0.030	-0.036	-0.041	-0.043	-0.046	-0.048
PC-1+FA-C2+FA-F2 (15%C2/15%F2)	-0.019	-0.016	-0.026	-0.033	-0.037	-0.040	-0.042	-0.045
PC-1+FA-C2+FA-F2 (10%C2/20%F2)	-0.015	-0.021	-0.029	-0.038	-0.043	-0.044	-0.046	-0.047
W/CM = 0.45								
AGE(DAYS):	**4**	**7**	**14**	**28**	**56**	**84**	**112**	**224**
MIXTURES	**(%)**	**(%)**	**(%)**	**(%)**	**(%)**	**(%)**	**(%)**	**(%)**
PC-1	-0.012	-0.017	-0.024	-0.032	-0.041	-0.043	-0.043	-0.047
PC-1+FA-C1 (30%C1)	-0.015	-0.022	-0.033	-0.043	-0.051	-0.055	-0.055	-0.060
PC-1+FA-C2 (30%C2)	-0.009	-0.015	-0.023	-0.029	-0.037	-0.039	-0.040	-0.041
PC-1+FA-C3 (30%C3)	-0.016	-0.024	-0.032	-0.040	-0.049	-0.051	-0.052	-0.055
PC-1+FA-F1 (20%F1)	-0.008	-0.012	-0.020	-0.029	-0.039	-0.042	-0.045	-0.047
PC-1+FA-F2 (20%F2)	-0.007	-0.013	-0.020	-0.029	-0.036	-0.037	-0.039	-0.041
PC-1+FA-C2+FA-F1 (20%C2/10%F1)	-0.011	-0.017	-0.026	-0.033	-0.037	-0.040	-0.041	-0.043
PC-1+FA-C2+FA-F1 (15%C2/15%F1)	-0.012	-0.017	-0.027	-0.035	-0.040	-0.042	-0.045	-0.047
PC-1+FA-C2+FA-F1 (10%C2/20%F1)	-0.013	-0.019	-0.028	-0.038	-0.044	-0.046	-0.049	-0.050
PC-1+FA-C2+FA-F2 (20%C2/10%F2)	-0.021	-0.019	-0.029	-0.035	-0.040	-0.042	-0.044	-0.047
PC-1+FA-C2+FA-F2 (15%C2/15%F2)	-0.011	-0.018	-0.028	-0.036	-0.039	-0.042	-0.044	-0.047
PC-1+FA-C2+FA-F2 (10%C2/20%F2)	-0.010	-0.017	-0.027	-0.034	-0.037	-0.039	-0.041	-0.045

Figure 21 shows that drying shrinkage of the control was less than that of the binary mixture containing 30%C2 at a w/cm ratio of 0.4 all through the period considered. The percentage drying shrinkage for ternary mixtures at a w/cm ratio of 0.4 were more than the control except for the ternary mixture involving 15%C2/15%F2

which was more than the control at day 28 but later decreased to become lesser than the control in the remaining period considered. The ternary mixture involving 20%C2/10%F1 at w/cm ratio of 0.4 exhibited the most drying shrinkage. Figure 23, 24 and 25 shows the percentage drying shrinkage at a w/cm ratio of 0.45 for the binary mixtures of Class C fly ashes, binary mixtures of Class F fly ashes and ternary mixtures involving both Class C and Class F respectively.

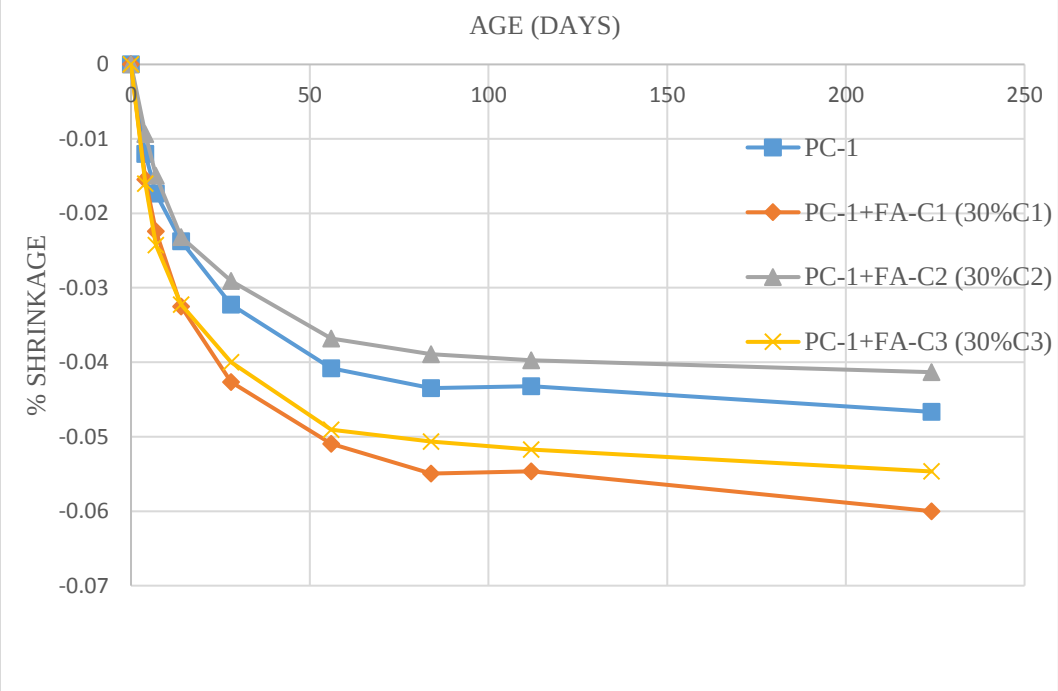

Figure 23. Percentage Drying Shrinkage for Fly Ash Class C Binary Mixtures at w/cm of 0.45

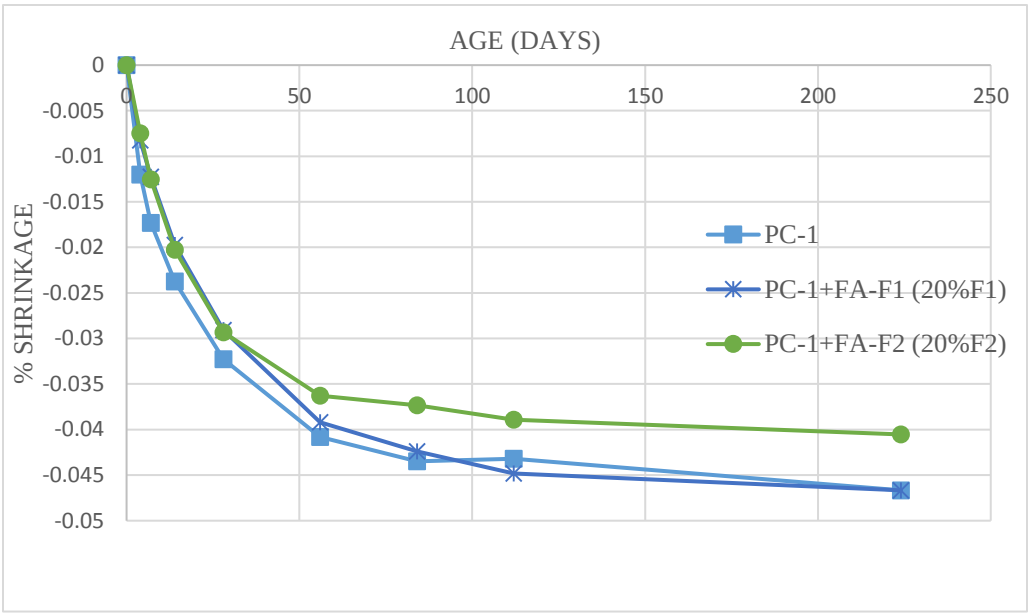

Figure 24. Percentage Drying Shrinkage for Fly Ash Class F Binary Mixtures at w/cm of 0.45

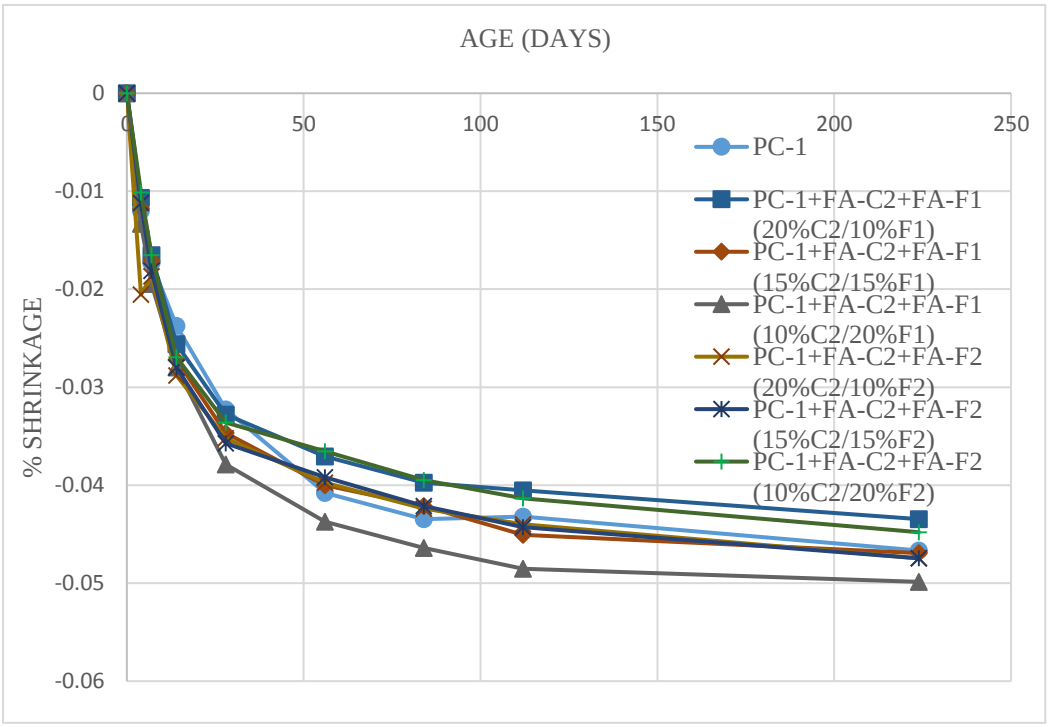

Figure 25. Percentage Drying Shrinkage for Ternary Mixtures at w/cm of 0.45

The percentage drying shrinkage for the Class C binary mixtures at a w/cm ratio of 0.45 were more than that of the control. The binary mixture involving 30%C1 had the most drying shrinkage due to its chemical composition and less reactivity compared to the other Class C fly ashes (C2 and C3). The Class F fly ashes performed better than the Class C fly ashes in reducing shrinkage at w/cm 0.45. The drying shrinkage of the Class F binary mixture involving 20%F2 at a w/cm ratio of 0.45 was lesser than that of the 20% F1 binary mixture and control. Hence, the binary mixtures involving 20%F2 and 30%C2 at a w/cm ratio of 0.45 performed better than the control and all other binary mixtures produced at the same w/cm ratio. Figure 25 shows that the ternary mixtures containing 20%C2/10%F1 and 10%C2/20%F2 at w/cm ratio of 0.45 had lesser percentage drying shrinkage than the control and other ternary mixtures. The ternary mixture with the highest percentage shrinkage at w/cm ratio of 0.45 was that containing 10%C2/20%F1.

4.1.6 Summary of mechanical testing

The mechanical properties test results affirmed the efficacy of fly ash in improving the mechanical properties of concrete. However, the extent to which these properties were improved depended on some factors that were considered in this test. Some of these factors are the Class and composition of fly ash, blending, percentage replacement, period of curing and water-cement ratio. The effect of curing period was evident in the compressive strength, splitting tensile, and elastic modulus test results. This was seen in the way the various mixtures tested increased in mechanical properties from day 1 through day 91. The Class C binary mixtures involving C1, C2, and C3 at 30% replacement performed remarkably well in improving the mechanical properties of concrete especially at early age. However, the Class C fly ash C2 outperformed the other

Class C fly ashes in improving the mechanical properties of concrete. The least in performance among the Class C fly ashes at 30% replacement was fly ash C1. The Class F fly ash F2 at 20% replacement showed an outstanding performance in improving the mechanical properties of concrete both at early age and later ages. Its performance can be attributed to fact that it was produced by burning 80% PRB coal and 20% Lignite causing the ash to possess chemical properties that are somewhat intermediate of a typical Class F and Class C. The Class F fly ash F1 at 20% replacement was not as reactive as the fly ash F2 and thus, was not very effective in improving mechanical properties at early age compared to fly ash F2. However, the Class fly ash F1 at 20% replacement still showed increase in mechanical properties at later age due to pozzolanic reactions. This low reactivity of fly ash F1 was due to its chemical composition. The ternary blends also performed well in improving the mechanical properties of concrete. However, the ternary blends involving C2/F2 outperformed that involving C2/F1 especially at the replacement levels 10%C2/20%F2, 20%C2/10%F2, and 15%C2/15%F2. The blends containing 20%C2/10%F1 also performed well in improving mechanical properties. This was due to the high percentage of the Class C fly ash C2 in the blend compensating for some of the weaknesses of the Class F fly ash F1. The effect of w/cm ratio was also obvious as some of the ternary mixtures performed better at a w/cm ratio of 0.4 than 0.45.

4.2 Heat of Hydration using Isothermal Calorimetry

The heat of hydration for both paste and mortar mixtures were computed per gram of cementitious material content for each mix. The results of the test as discussed in this section showed the peak heat of hydration per gram of cementitious material for each mix

and the corresponding time taken to attain the peak. Also, discussed was the influence of the various blends of fly ash and temperatures at which the test was conducted.

4.2.1 Hydration of blended fly ash paste mixtures

4.2.1.1 ***Influence of blended fly ash systems in paste mixtures at 5ºC.*** The peak heat of hydration per gram of cementitious material for binary and ternary paste mixtures at a temperature of 5ºC as well as the corresponding time taken to attain the peak heat are given in Table 19 and Table 20 respectively. This was also depicted graphically in Figure 26 and Figure 27.

Table 19. Heat of Hydration for Binary Paste Mixtures at 5ºC

Mixture ID	Average Peak Heat Flow (mW/g Cemm)	Average Time until Peak Heat Flow (min)
PC-I	2.29	9.82
PC-I+ FA-F1 (30% F1)	1.69	10.99
PC-I+ FA-F2 (30% F2)	1.27	24.94
PC-I+FA-C2 (30% C2)	1.54	29.99

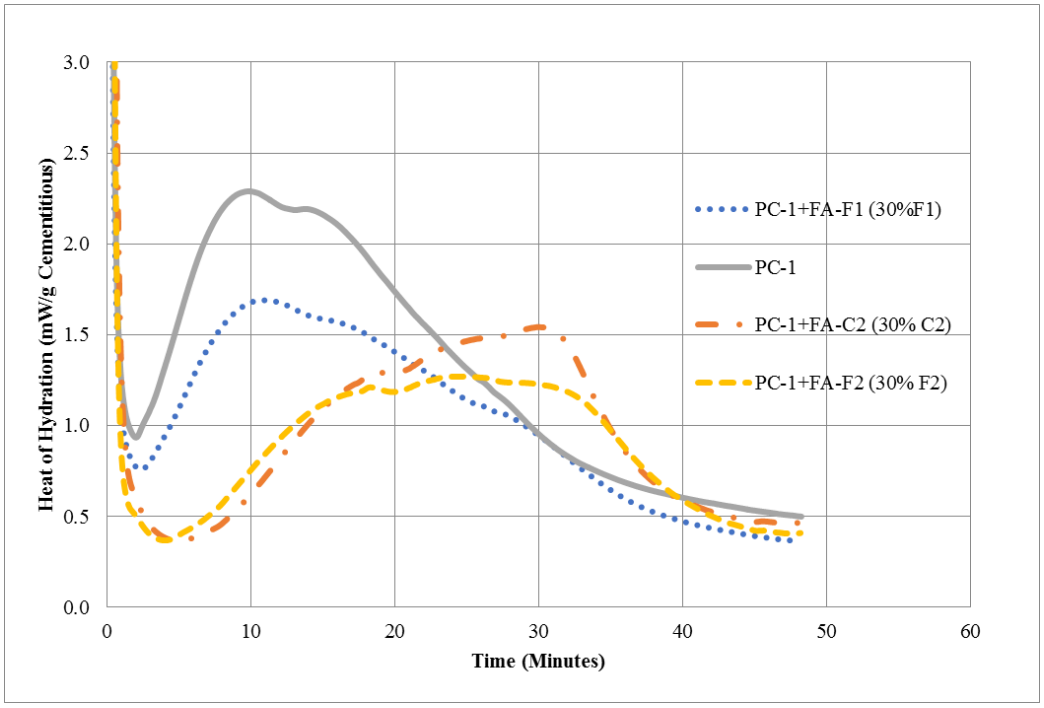

Figure 26. Heat of Hydration for Binary Paste Mixtures at 5°C

Table 20. Heat of Hydration for Ternary Paste Mixtures at 5°C

Mixture ID	Average Peak Heat Flow (mW/g Cemm)	Average Time until Peak Heat Flow (min)
PC-1	2.29	9.82
PC-1+FA-F1+FA-C2-(20%F1/10%C2)	1.21	22.54
PC-1+FA-F1+FA-C2 (15%F1/15%C2)	1.32	22.54
PC-1+FA-F1+FA-C2-(10%F1/20%C2)	1.25	23.23
PC-1+FA-F2+FA-C2 (20%F2/10%C2)	1.36	23.15
PC-1+FA-F2+FA-C2 (15%F2/15%C2)	1.41	24.69
PC-1+FA-F2+FA-C2 (10%F2/20%C2)	1.51	24.59

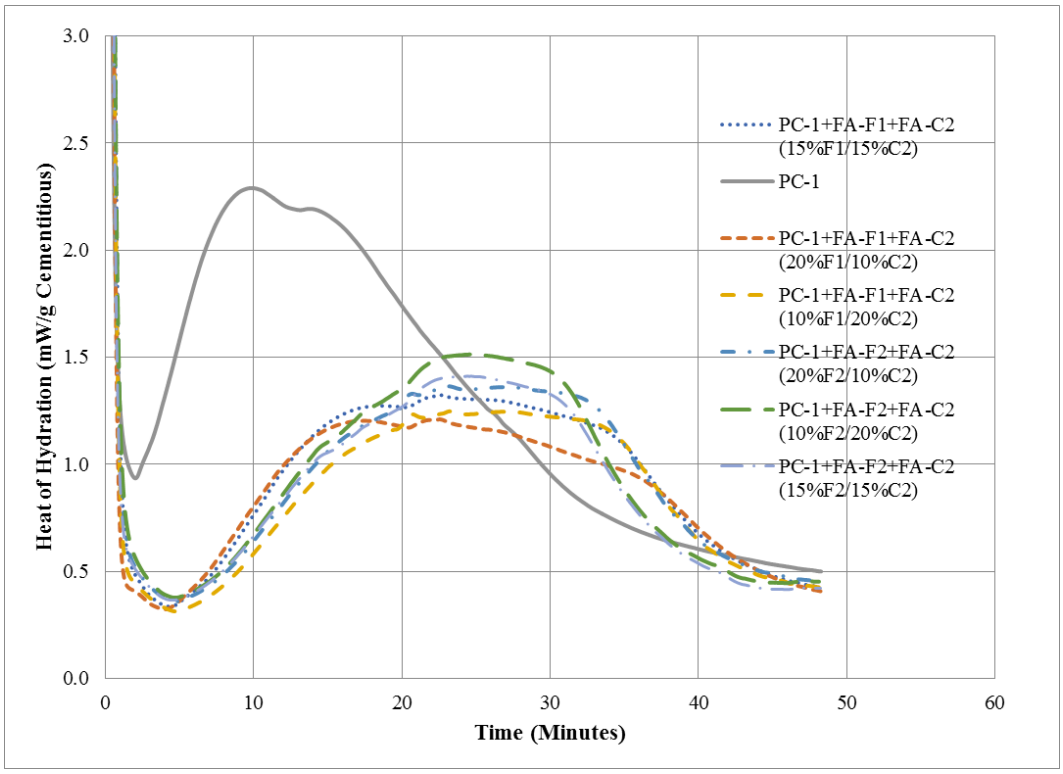

Figure 27. Heat of Hydration for Ternary Paste Mixtures at 5^{o}C

The results shows that the control mixture at 5^{o}C produced more heat than the fly ash mixtures (binary and ternary mixtures). This affirms the efficacy of mineral admixtures like fly ash to reduce the heat generated due to hydration. (Naik et al., 1998). The results also shows the effect of the temperature on all fly ash mixtures including the control as they all took more time to achieve a low heat peak. However, the binary mixture containing 30%F1 produced the highest heat at lesser time compared to the binary mixtures containing 30%C2 and 30%F2. This implies that the reactivity of the fly ash binary mixture containing 30%F1 was less affected by the low temperature (5^{o}C) compared to those containing 30%C2 and 30%F2. The binary mixture containing 30%C2 appeared to be the most affected by the low temperature (5^{o}C) as it attained a peak heat

of 1.54mW/g cementitious materials in approximately 30 minutes. This was followed by the binary mixture containing 30%F2 which attained a peak heat of 1.27mW/g of cementitious materials in approximately 25 minutes. The reactivity of the ternary mixtures were all affected by the low temperature (5^{o}C). This is seen in the amount of time taken to reach the peak heat. For instance, the ternary paste mixture containing 10%F2/20%C2 produced the highest peak heat compared to other ternary mixtures at 5^{o}C in 24.59 minutes. Also, the ternary paste mixture 20%F1/10%C2 which produced the lowest peak heat at 5^{o}C attained its peak heat in 22.54 minutes. This effect of temperature on the heat of hydration is in agreement with the results of Xiong and Van Breugel (2001).

4.2.1.2 ***Influence of blended fly ash systems in paste mixtures at 23^{o}C.*** The peak heat of hydration per gram of cementitious material for binary and ternary paste mixtures at a temperature of 23^{o}C as well as the corresponding time taken to attain the peak heat are given in Table 21 and Table 22 respectively. Figure 28 and 29 shows a graphical representation of the heat of hydration at 23^{o}C for binary and ternary paste mixtures respectively.

Table 21. Heat of Hydration for Binary Paste Mixtures at 23^{o}C

Mixture ID	Average Peak Heat Flow (mW/g Cemm)	Average Time until Peak Heat Flow (min)
PC-I	4.41	10.07
PC-I+ FA-F1 (30% F1)	3.25	10.64
PC-I+ FA-F2 (30% F2)	3.29	12.04
PC-I+FA-C2 (30% C2)	3.81	13.68

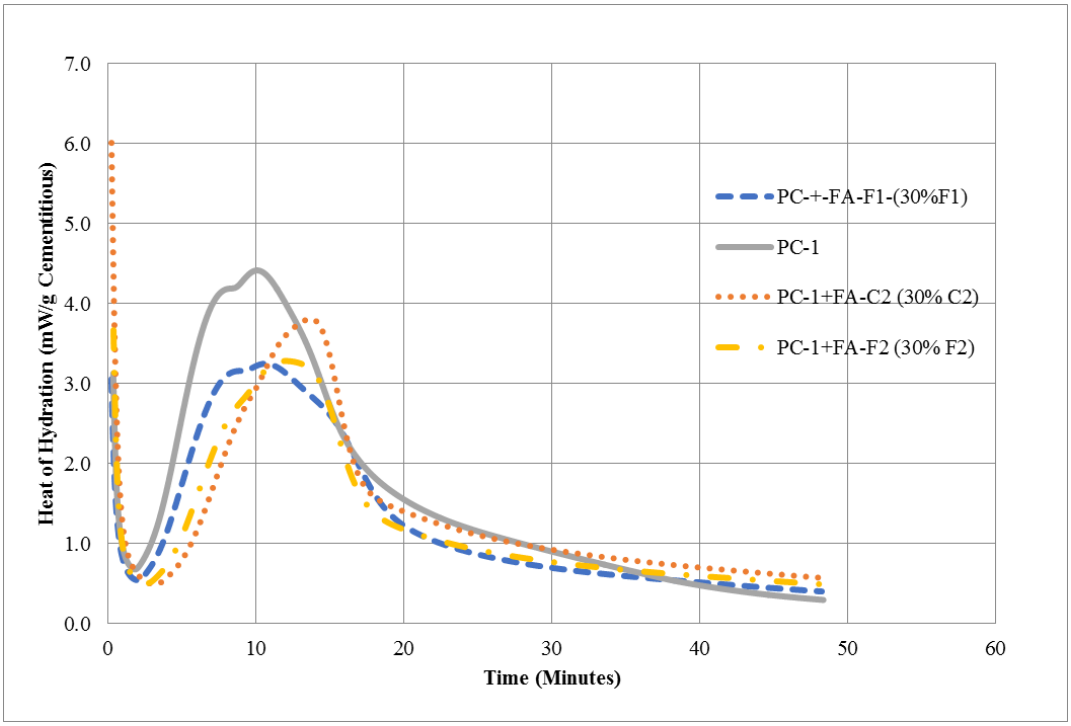

Figure 28. Heat of Hydration for Binary Paste Mixtures at 23ºC

Table 22. Heat of Hydration for Ternary Paste Mixtures at 23ºC

Mixture ID	Average Peak Heat Flow (mW/g Cemm)	Average Time until Peak Heat Flow (min)
PC-I	4.41	10.07
PC-1+FA-F1+FA-C2-(20%F1/10%C2)	3.10	11.88
PC-1+FA-F1+FA-C2 (15%F1/15%C2)	3.45	12.36
PC-1+FA-F1+FA-C2-(10%F1/20%C2)	3.33	13.20
PC-1+FA-F2+FA-C2 (20%F2/10%C2)	3.59	13.07
PC-1+FA-F2+FA-C2 (15%F2/15%C2)	3.45	13.44
PC-1+FA-F2+FA-C2 (10%F2/20%C2)	3.73	13.34

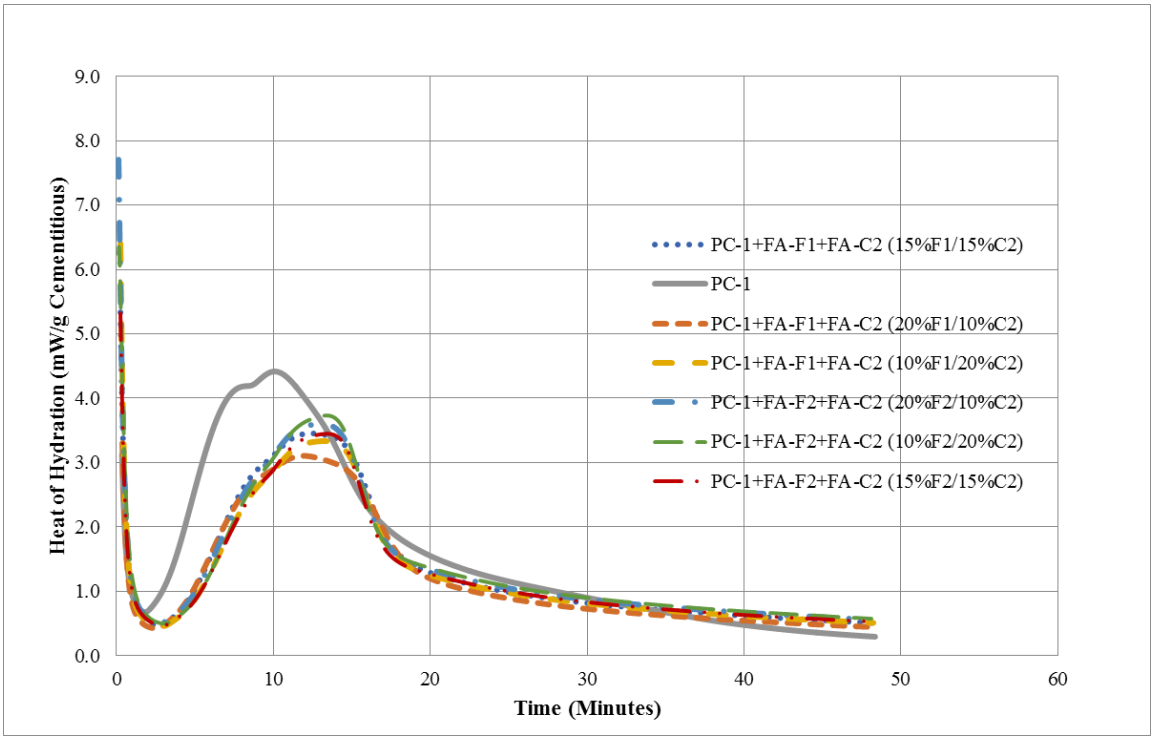

Figure 29. Heat of Hydration for Ternary Paste Mixtures at 23°C

The control mixture produced the highest peak heat at the lowest time compared to all other mixtures (binary and ternary) at 23°C. This confirms that the control was more reactive than the fly ash mixtures at 23°C. Table 21 and Figure 28 shows that the Class C fly ash binary mixture containing 30%C2 produced more heat than the Class F fly ashes containing 30%F1 and 30%F2. The least between the two binary Class F fly ash mixtures was that containing 30%F1 with a peak heat of 3.25mW/g of cementitious materials in 10.64 minutes. This implies that the Class C fly ash C2 was more reactive than the Class F fly ashes F2 and F1 at 23°C with the Class F fly ash F1 as the least of the three. The results for the ternary mixtures at 23°C shows that the ternary mixture containing 10%F2/20%C2 produced the highest heat followed by that containing 20%F2/10%C2. This is due to the high reactivity of the fly ashes C2 and F2 in the mixture. The least

among the ternary mixtures was that containing 20%F1/10%C2. Whereas, the ternary mixtures containing 15%C2/15%F1 and 15%C2/15%F2 produced heat that seemed to be midway between that highest and lowest heat produced. This further affirms the reactivity of the fly ashes C2, F2 and F1 as their amount in each ternary mixture were reflected in the heat produced.

4.2.1.3 ***Influence of blended fly ash systems in paste mixtures at 38°C.*** The peak heat of hydration per gram of cementitious material for binary and ternary paste mixtures at a temperature of 38°C as well as the corresponding time taken to attain the peak heat are given in Table 23 and Table 24 respectively. Figure 30 and 31 shows a graphical representation of the heat of hydration at 38°C for binary and ternary paste mixtures respectively.

Table 23. Heat of Hydration for Binary Paste Mixtures at 38°C

Mixture ID	Average Peak Heat Flow (mW/g Cemm)	Average Time until Peak Heat Flow (min)
PC-I	11.95	6.07
PC-I+ FA-F1 (30% F1)	8.17	6.70
PC-I+ FA-F2 (30% F2)	8.51	7.19
PC-I+FA-C2 (30% C2)	9.44	7.28

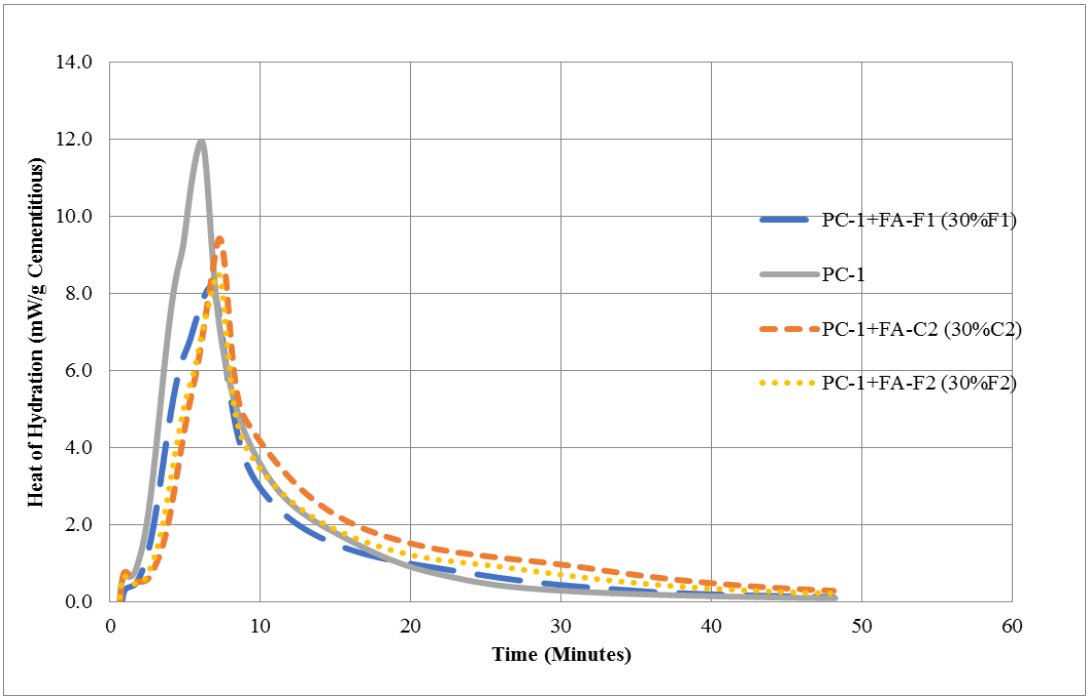

Figure 30. Heat of Hydration for Binary Paste Mixtures at 38°C

Table 24. Heat of Hydration for Ternary Paste Mixtures at 38°C

Mixture ID	Average Peak Heat Flow (mW/g Cemm)	Average Time until Peak Heat Flow (min)
PC-I	11.95	6.07
PC-1+FA-F1+FA-C2-(20%F1/10%C2)	8.01	7.00
PC-1+FA-F1+FA-C2 (15%F1/15%C2)	8.79	7.03
PC-1+FA-F1+FA-C2-(10%F1/20%C2)	8.01	7.89
PC-1+FA-F2+FA-C2 (20%F2/10%C2)	8.55	7.78
PC-1+FA-F2+FA-C2 (15%F2/15%C2)	8.46	7.81
PC-1+FA-F2+FA-C2 (10%F2/20%C2)	9.06	7.78

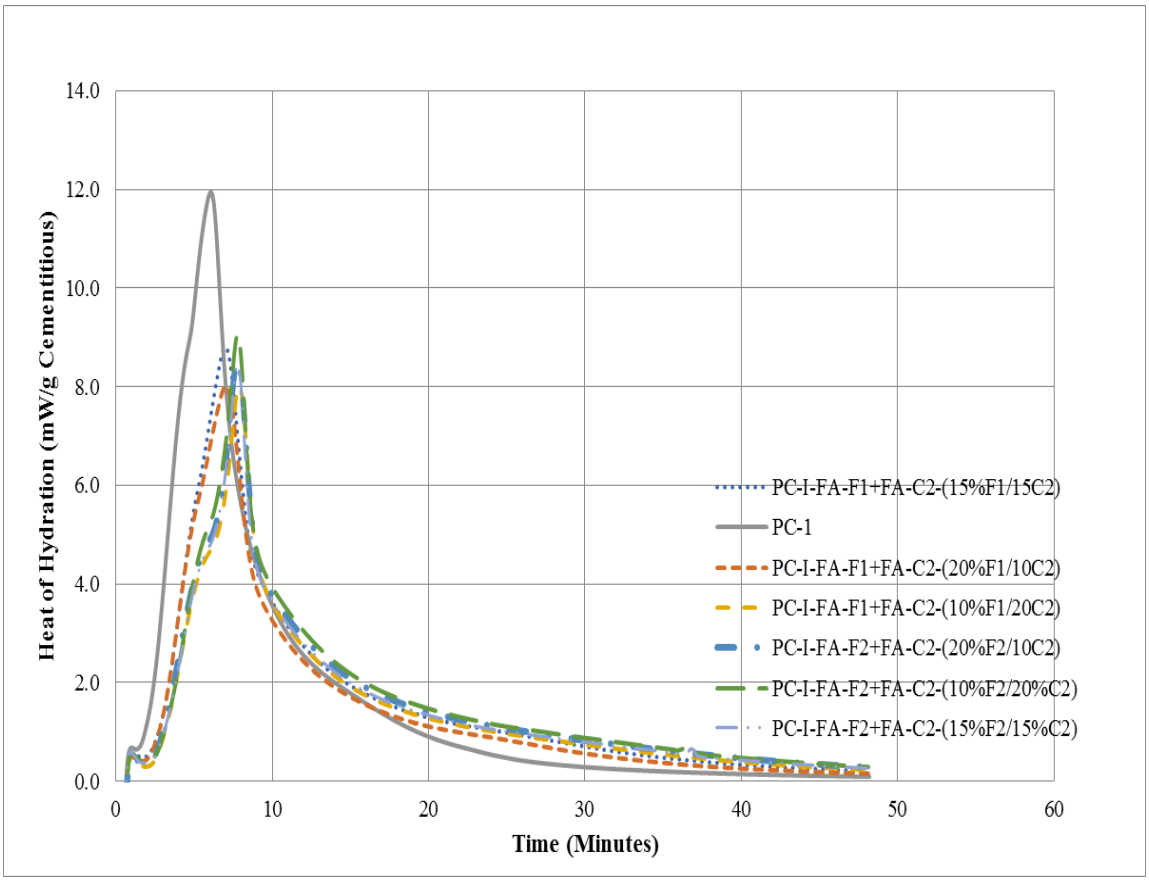

Figure 31. Heat of Hydration for Ternary Paste Mixtures at 38°C

The control mixture produced the highest heat at the least time compared to the fly ash mixtures at 38°C. This affirms the ability of fly ash to reduce the heat of hydration even at high temperature. The results shows that the high temperature of 38°C affected all fly ash mixtures including the control as they all attained higher peak heat values in less time compared to that at lower temperatures (5°C and 23°C). The binary paste mixture with 30%C2 cement replacement produced the highest peak heat at a higher amount of time compared to other binary paste mixtures. Following the binary paste mixture containing 30%C2 were the binary paste mixtures containing 30%F2 and 30%F1 with that

containing 30%F1 as the least of the three. This quantity of heat produced by the Class C fly ash C2 at 38^{o}C shows that the fly ash C2 was more reactive than the Class F ashes F1 and F2. However, considering the quantity of heat produced by the Class F fly ashes, the Class F ash F2 seemed to be more reactive than the Class F fly ash F1. As for the ternary paste mixtures at 38^{o}C, the ternary paste mixture containing 10%F2/20%C2 produced the highest amount of peak heat compared to other ternary paste mixtures at 38^{o}C. This still confirms the high reactivity of the Class C fly ash C2 followed by the Class F fly ash F2. The least heat were produced by the ternary paste mixtures containing 10%F1/20%C2 and 20%F1/10%C2. The ternary paste mixtures containing 15%F1/15%C2 and 15%F2/15%C2 produced peak heat values that seemed to be between the highest and lowest peak heat produced among the ternary paste mixtures at 38^{o}C.

4.2.2 Hydration of blended fly ash mortar mixtures

4.2.2.1 ***Influence of blended ash systems in mortar mixtures at 5^{o}C.*** The peak heat of hydration per gram of cementitious material for binary and ternary mortar mixtures at a temperature of 5^{o}C as well as the corresponding time taken to attain the peak heat are given in Table 25 and Table 26 respectively. Figure 32 and 33 shows a graphical representation of the heat of hydration at 5^{o}C for binary and ternary mortar mixtures respectively.

Table 25. Heat of Hydration for Binary Mortar Mixtures at 5°C

Mixture ID	Average Peak Heat Flow (mW/g Cemm)	Average Time until Peak Heat Flow (min)
PC-I+RS	0.97	22.90
PC-I+RS+ FA-F1 (30% F1)	0.49	25.33
PC-I+RS+ FA-F2 (30% F2)	0.47	30.13
PC-I+RS+FA-C2 (30% C2)	0.59	48.13

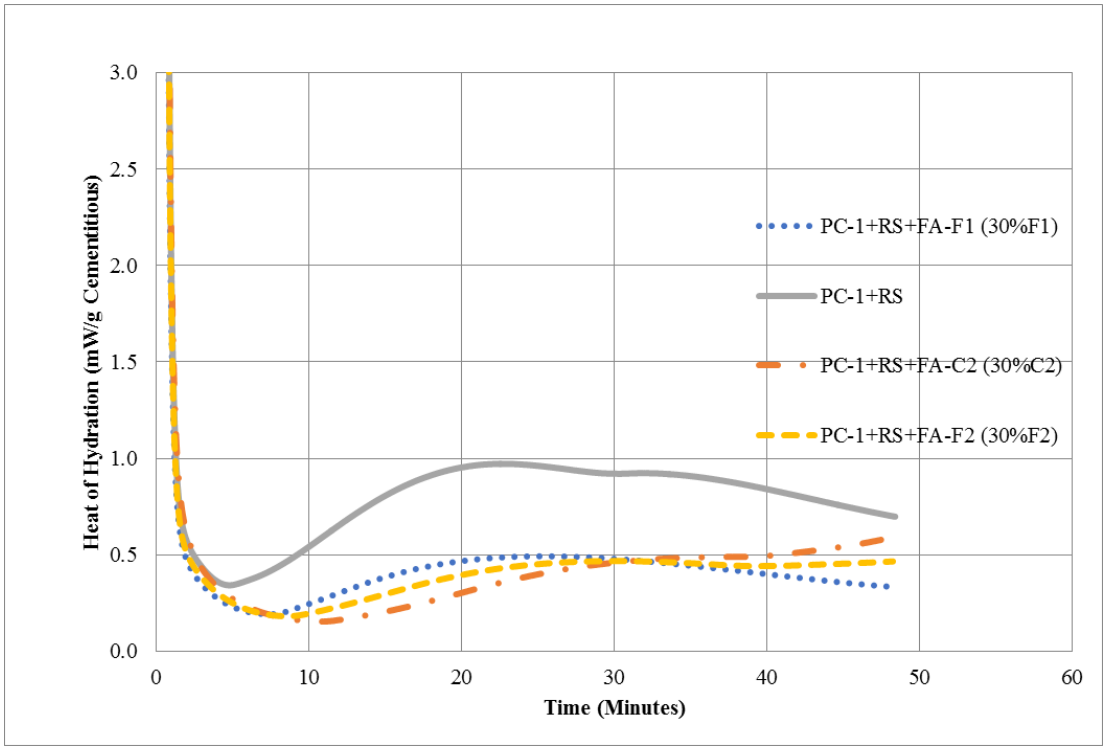

Figure 32. Heat of Hydration for Binary Mortar Mixtures at 5°C

Table 26. Heat of Hydration for Ternary Mortar Mixtures at 5°C

Mixture ID	Average Peak Heat Flow (mW/g Cemm)	Average Time until Peak Heat Flow (min)
PC-I+RS	0.97	22.90
PC-1+RS+FA-F1+FA-C2-(20%F1/10%C2)	0.47	29.64
PC-1+RS+FA-F1+FA-C2 (15%F1/15%C2)	0.53	31.15
PC-1+RS+FA-F1+FA-C2-(10%F1/20%C2)	0.55	48.28
PC-1+RS+FA-F2+FA-C2 (20%F2/10%C2)	0.70	48.14
PC-1+RS+FA-F2+FA-C2 (15%F2/15%C2)	0.75	48.12
PC-1+RS+FA-F2+FA-C2 (10%F2/20%C2)	0.75	48.12

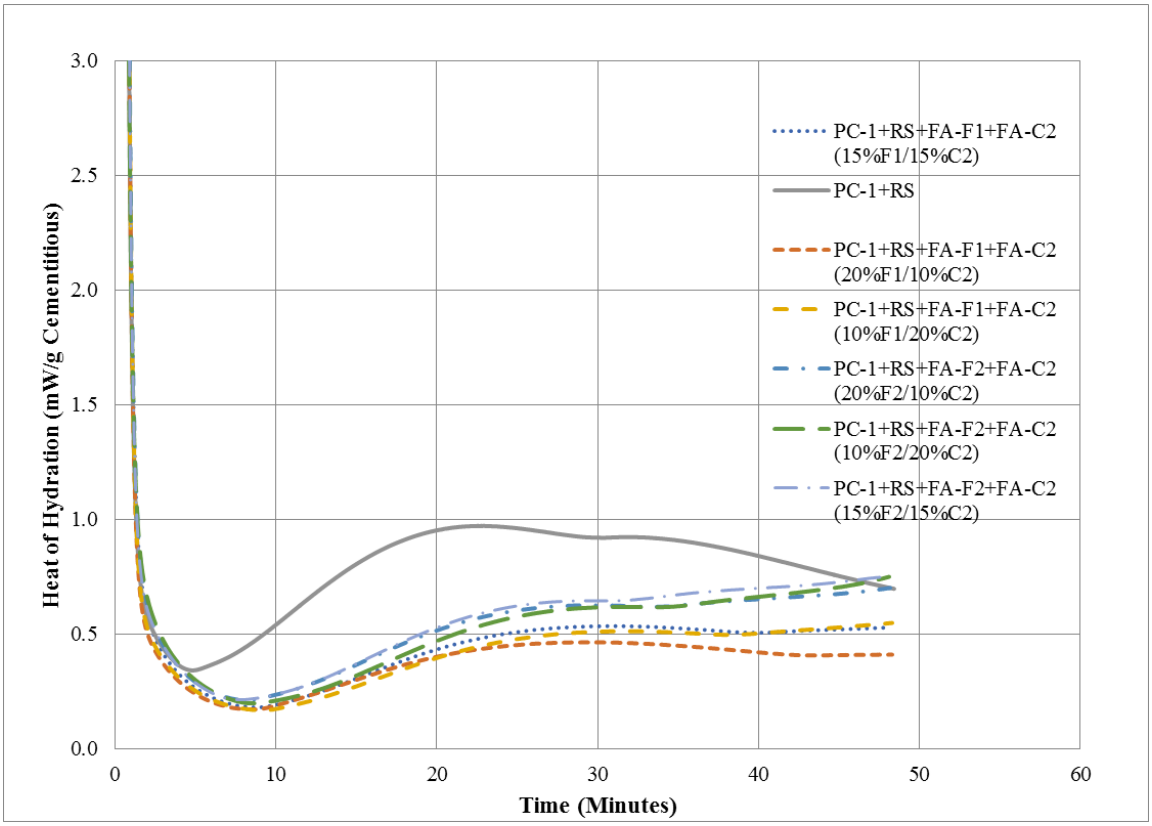

Figure 33. Heat of Hydration for Ternary Mortar Mixtures at 5°C

The results shows that the effect of the low temperature (5^{o}C) was more pronounced in the mortar mixtures compared to the paste mixtures. This is seen in the higher amount of time taken to achieve a low peak heat in all the mortar mixtures including the control. However, the control mortar mixture produced the highest peak heat at the least time compared to other fly ash mortar mixtures at 5^{o}C. This implies that the addition of fly ash to the mortar mixtures at 5^{o}C was able to reduce the heat of hydration produced in these mixtures. The binary mortar mixture containing 30%C2 produced the highest peak heat at the highest amount of time compared to the binary mixtures containing 30%F2 and 30% F1. The ternary mortar mixtures containing 10%F2/20%C2 and 15%C2/15%F2 produced the highest peak heat values compared to other ternary mortar mixtures. The ternary mortar mixture containing 20%F1/10%C2 produced the least peak heat compared to other ternary mortar mixtures.

4.2.2.2 ***Influence of blended ash systems in mortar mixtures at 23^{o}C.*** The peak heat of hydration per gram of cementitious material for binary and ternary mortar mixtures at a temperature of 23^{o}C as well as the corresponding time taken to attain the peak heat are given in Table 27 and Table 28 respectively. Figure 34 and 35 shows a graphical representation of the heat of hydration at 23^{o}C for binary and ternary mortar mixtures respectively.

Table 27. Heat of Hydration for Binary Mortar Mixtures at 23ºC

Mixture ID	Average Peak Heat Flow (mW/g Cemm)	Average Time until Peak Heat Flow (min)
PC-I+RS	3.23	8.34
PC-I+RS+ FA-F1 (30% F1)	2.53	8.77
PC-I+RS+ FA-F2 (30% F2)	3.10	14.56
PC-I+RS+FA-C2 (30% C2)	3.75	14.95

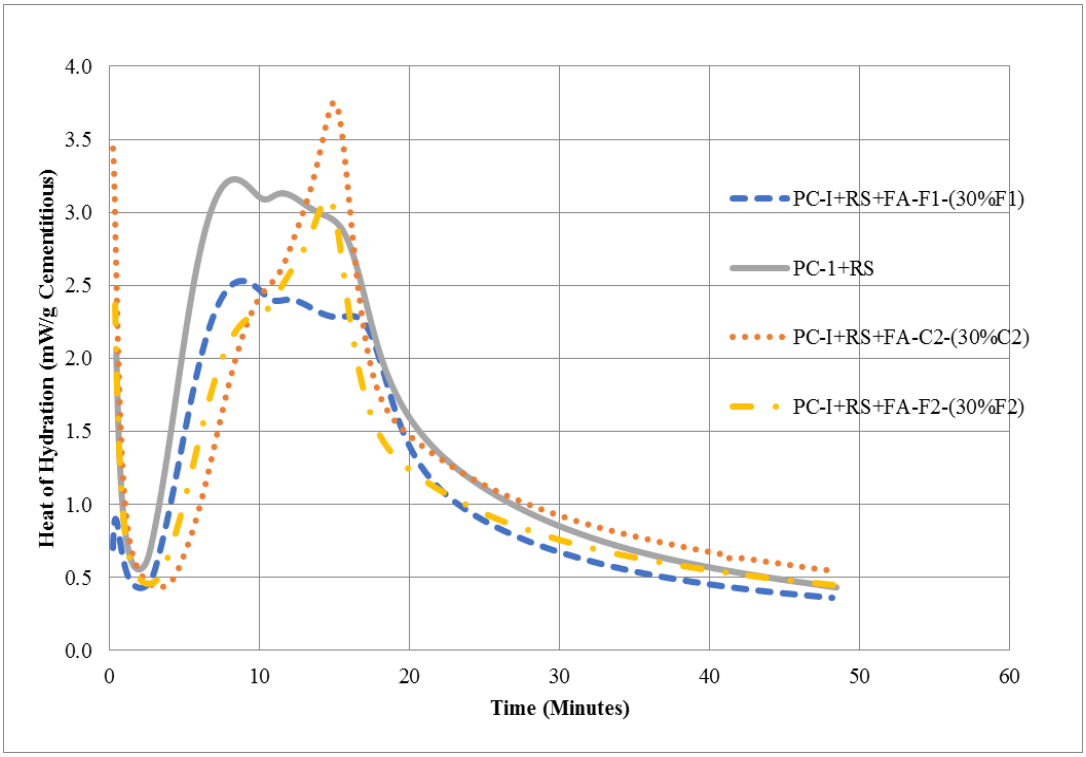

Figure 34. Heat of Hydration for Binary Mortar Mixtures at 23ºC

Table 28. Heat of Hydration for Ternary Mortar Mixtures at 23°C

Mixture ID	Average Peak Heat Flow (mW/g Cemm)	Average Time until Peak Heat Flow (min)
PC-I+RS	3.23	8.34
PC-1+RS+FA-F1+FA-C2-(20%F1/10%C2)	2.67	15.18
PC-1+RS+FA-F1+FA-C2 (15%F1/15%C2)	3.05	14.96
PC-1+RS+FA-F1+FA-C2-(10%F1/20%C2)	3.24	15.19
PC-1+RS+FA-F2+FA-C2 (20%F2/10%C2)	3.52	14.84
PC-1+RS+FA-F2+FA-C2 (15%F2/15%C2)	3.24	14.81
PC-1+RS+FA-F2+FA-C2 (10%F2/20%C2)	3.54	14.79

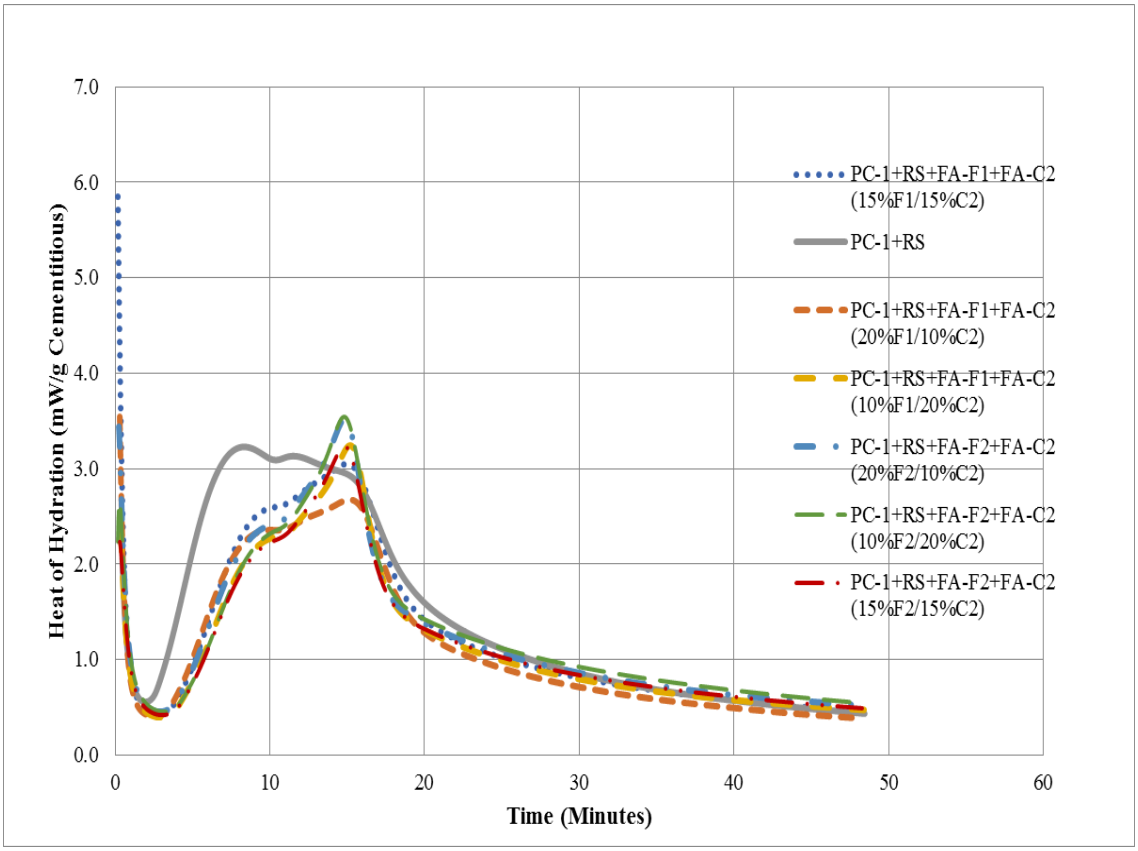

Figure 35. Heat of Hydration for Ternary Mortar Mixtures at 23°C

The result shows that the binary mortar mixture containing 30%C2 at 23^{o}C produced the highest peak heat compared to the control (cement and river sand) and other fly ash mortar mixtures. However, the binary mortar mixture containing 30%C2 took more time to achieve this high peak heat compared to the control and other binary mixtures. The least peak heat at 23^{o}C was produced by the binary mortar mixture containing 30%F1. As for the ternary mortar mixtures, the mixtures containing 10%F2/20%C2 and 20%F2/10%C2 produced the highest peak heat compared to the control and other ternary mixtures. Though this took more time to attain compared to the control mortar mixture. This high peak heat values attained at a higher time by the ternary mortar mixtures containing 10%F2/20%C2 and 20%F2/10%C2 shows that despite the reactivity of the fly ashes C2 and F2, this fly ashes were still able to reduce the rate at which the heat of hydration was generated in the ternary mortar mixtures at 23^{o}C. The ternary mortar mixture with the least peak heat value and time was that containing 20%F1/10%C2. This shows that the Class F fly ash F1 with a replacement level of 20% in the ternary mortar mixture exhibited less reactivity and hence reduced the heat of hydration produced in the ternary mortar mixture. The ternary mortar mixtures containing 15%F1/15%C2 and 15%F2/15%C2 produced peak heat values that seemed to be between the highest and lowest peak heat produced among the ternary mortar mixtures at 23^{o}C.

4.2.2.3 ***Influence of blended fly ash systems in mortar mixtures at 38^{o}C.*** The peak heat of hydration per gram of cementitious material for binary and ternary mortar mixtures at a temperature of 38^{o}C as well as the corresponding time taken to attain the peak heat are given in Table 29 and Table 30 respectively. Figure 36 and 37 shows a graphical

representation of the heat of hydration at 38ºC for binary and ternary mortar mixtures respectively.

Table 29. Heat of Hydration for Binary Mortar Mixtures at 38ºC

Mixture ID	Average Peak Heat Flow (mW/g Cemm)	Average Time until Peak Heat Flow (min)
PC-I+RS	10.80	6.38
PC-I+RS+ FA-F1 (30% F1)	7.90	7.00
PC-I+RS+ FA-F2 (30% F2)	8.68	6.90
PC-I+RS+FA-C2 (30% C2)	9.37	7.43

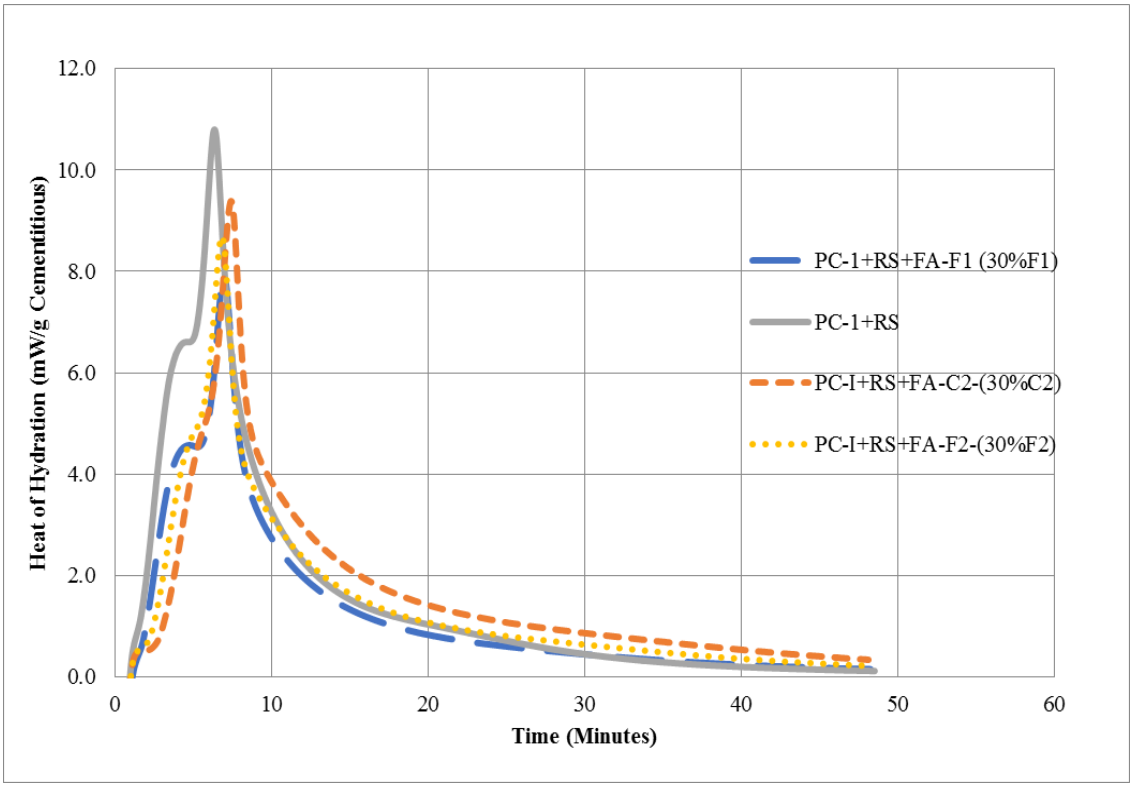

Figure 36. Heat of Hydration for Binary Mortar Mixtures at 38ºC

Table 30. Heat of Hydration for Ternary Mortar Mixtures at 38ºC

Mixture ID	Average Peak Heat Flow (mW/g Cemm)	Average Time until Peak Heat Flow (min)
PC-I+RS	10.80	6.38
PC-1+RS+FA-F1+FA-C2-(20%F1/10%C2)	8.12	7.19
PC-1+RS+FA-F1+FA-C2 (15%F1/15%C2)	8.71	7.25
PC-1+RS+FA-F1+FA-C2-(10%F1/20%C2)	7.93	7.47
PC-1+RS+FA-F2+FA-C2 (20%F2/10%C2)	8.89	7.14
PC-1+RS+FA-F2+FA-C2 (15%F2/15%C2)	8.80	6.98
PC-1+RS+FA-F2+FA-C2 (10%F2/20%C2)	9.26	6.97

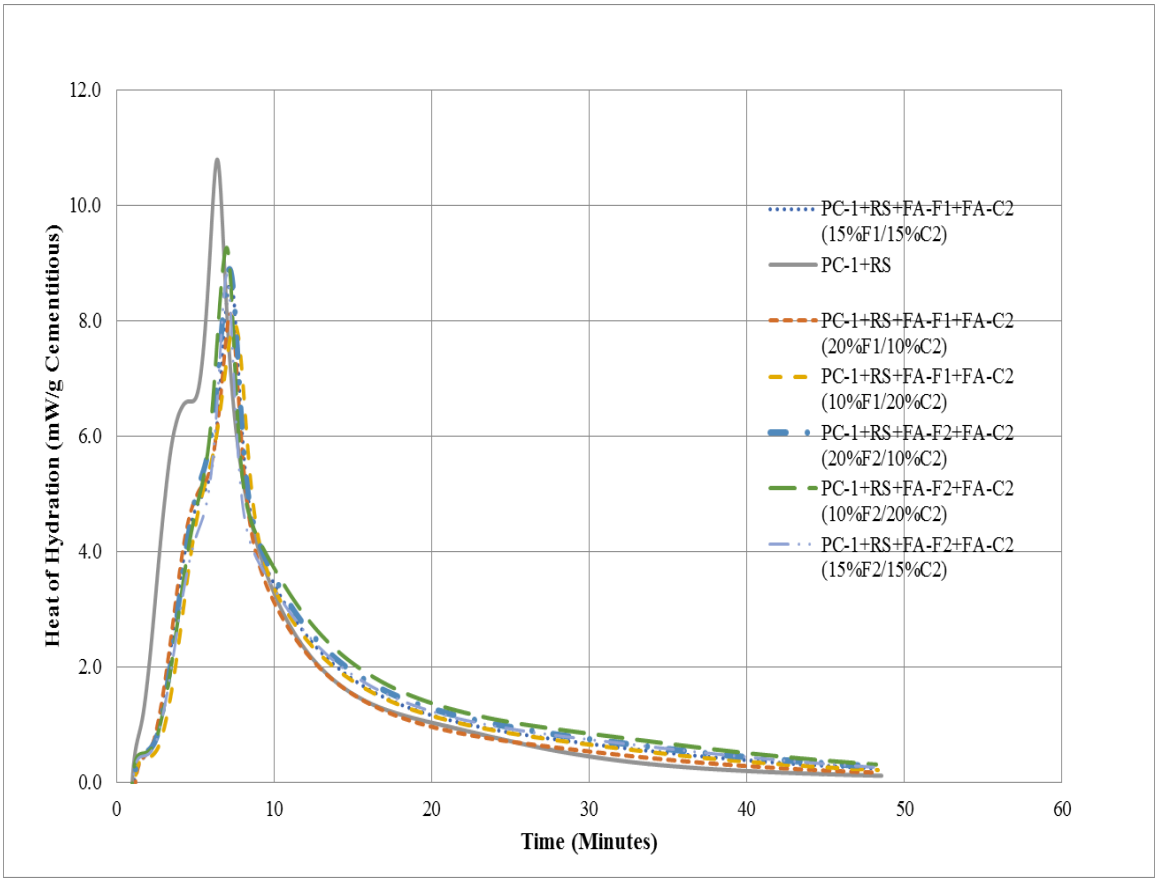

Figure 37. Heat of Hydration for Ternary Mortar Mixtures at 38ºC

The result shows that the control (cement and river sand) produced the highest peak heat at the least amount of time compared to the other mortar mixtures at 38^{o}C. The binary mortar mixture containing 30%C2 at 38^{o}C produced the highest peak heat compared to other binary mortar mixtures at 38^{o}C. Also, the binary mortar mixture containing 30%F2 produced a higher peak heat compared to that containing 30%F1. This variations in the peak heat produced by the Class C and F fly ash binary mortar mixtures at 38^{o}C depended on the reactivity of these fly ashes (C2, F2, and F1) and the extent to which they were able to reduce the heat of hydration in their respective mixtures. The ternary mortar mixtures involving the fly ashes F2 and C2 at 38^{o}C produced higher peak heat compared to those involving F1 and C2 at the same temperature. However, the ternary mortar mixture with the highest peak heat was that containing 10%F2/20%C2 while the least peak heat was attained by the ternary mortar mixture containing 10%F1/20%C2.

4.2.3 Summary of heat of hydration testing

The peak heat of hydration per gram of cementitious material for binary and ternary mixtures depended more on the fly ash type, replacement levels used and temperature at which the test was conducted. However, the mortar mixtures produced slightly less peak heat values at higher amount of time compared to the paste mixtures. The variation in temperature affected the peak heat of hydration generated in both paste and mortar mixtures as well as the time taken to attain the peak heat. The results shows an increase in the peak heat generated and a decrease in the corresponding time taken as the temperature increases from 5^{o}C to 23^{o}C and then 38^{o}C. The control paste and mortar mixtures exhibited higher peak heat at lesser time compared to the fly ash paste and mortar mixtures. As for the fly ash mixtures, the binary mixtures (paste and mortar) with

30%C2 replacement produced higher peak heat at higher amount of time compared to other binary paste and mortar mixtures. The binary paste and mortar mixtures with 30%F2 replacement produced higher peak heat at higher amount of time compared to that of 30%F1. The ternary paste and mortar mixtures involving 10%F2/20%C2 and 20%F2/10%C2 produced higher peak heat at higher amount of time compared to other paste and mortar ternary mixtures. The ternary paste and mortar mixtures involving 20%F1/10%C2 produced the least peak heat at lowest amount of time compared to other ternary paste and mortar mixtures. The ternary paste and mortar mixtures containing 15%F1/15%C2 and 15%F2/15%C2 produced peak heat values that seemed to be between the highest and lowest peak heat produced among the ternary paste and mortar mixtures. This high heat of hydration generated in the binary and ternary mixtures involving the Class C fly ash C2 shows that the Class C fly ash C2 was more reactive than the Class F fly ashes F2 and F1. However, the fly ash mixtures containing the Class F fly ash F2 exhibited higher peak heat compared to those of the Class F fly ash F1. This shows that the Class F fly ash F2 was more reactive than F1.

4.3 Alkali Silica Reactivity

The results of the Accelerated Mortar Bar Test (ASTM C1567/ASTM C1260), Concrete Prism Test (ASTM C1293) and the exposure concrete blocks are discussed in this section. Also, the results of the fresh property tests (slump, air content and unit weight) for the Concrete Prism Test (ASTM C1293) and the exposure concrete blocks mixtures are given in Table 31.

Table 31. Fresh Properties Tests Results for ASR Concrete Mixtures

Mixture	% Fly Ash		w/cm = 0.40		
	Class C	Class F	Slump (mm)	Air Content (%)	Unit Weight (Kg/m^3)
PC-1	Control		0.00	0.80	2302.75
PC-I+FA-C2	30	-	38.10	1.10	2324.53
PC-I+FA-F1	-	30	38.10	1.20	2392.45
PC-I+FA-F2	-	30	248.92	0.80	2302.75
PC-I+FA-C2+FA-F1	20	10	132.08	1.20	2283.53
PC-I+FA-C2+FA-F1	10	20	181.36	1.10	2268.15
PC-I+FA-C2+FA-F2	20	10	177.80	1.20	2301.47
PC-I+FA-C2+FA-F2	10	20	179.83	0.90	2295.06

4.3.1 Accelerated mortar bart test/Mortar bar test

The accelerated mortar bar test expansion data for binary and ternary mixtures are given in Table 32 and Table 33 respectively. The test results for Class C and Class F binary mixtures at 20% cement replacement are shown on Figure 38 and Figure 39 respectively. Whereas, the test results for Class C and Class F binary mixtures at 30% cement replacement are shown on Figure 40 and Figure 41 respectively.

Table 32. Accelerated Mortar Bar Test Expansion Data for Binary Mixtures

Mixture	% Fly Ash		% Expansion						
	Class C	Class F	Day 3	Day 5	Day 7	Day 10	Day 14	Day 21	Day 28
PC-1	Control		0.21	0.33	0.39	0.44	0.50	0.56	0.59
PC-1+FA-C1	20	-	0.24	0.32	0.35	0.39	0.42	0.45	
PC-1+FA-C1	30	-	0.27	0.27	0.30	0.33	0.36	0.40	0.43
PC-1+FA-C2	20	-	0.19	0.25	0.27	0.30	0.32	0.36	0.39
PC-1+FA-C2	30	-	0.05	0.08	0.08	0.12	0.14	0.17	0.20
PC-1+FA-C3	20	-	0.19	0.26	0.29	0.32	0.34	0.38	0.41
PC-1+FA-C3	30	-	0.07	0.09	0.12	0.15	0.18	0.22	0.25
PC-1+FA-C4	20	-	0.06	0.11	0.15	0.19	0.22	0.27	0.31
PC-1+FA-C4	30	-	0.01	0.02	0.05	0.07	0.11	0.16	0.19
PC-1+FA-F1	-	20	0.01	0.01	0.02	0.06	0.08	0.14	0.18
PC-1+FA-F1	-	30	0.01	0.0	0.01	0.01	0.02	0.03	0.05
PC-1+FA-F2	-	20	0.03	0.07	0.10	0.14	0.18	0.23	0.28
PC-1+FA-F2	-	30	0.02	0.02	0.03	0.05	0.07	0.12	0.15
PC-1+FA-F3	-	20	0.02	0.04	0.07	0.11	0.15	0.20	0.25
PC-1+FA-F3	-	30	0.01	0.01	0.02	0.03	0.06	0.10	0.13

Table 33: Accelerated Mortar Bar Test Expansion Data for Ternary Mixtures

Mixture	% Fly Ash		% Expansion						
	Class C	Class F	Day 3	Day 5	Day 7	Day 10	Day 14	Day 21	Day 28
PC-I	Control		0.21	0.33	0.39	0.44	0.50	0.56	0.59
PC-I+FA-C2+FA-F1	20	10	-	0.03	0.06	0.08	0.12	0.17	0.21
PC-I+FA-C2+FA-F1	15	15	-	0.02	0.03	0.05	0.08	0.14	0.18
PC-I+FA-C2+FA-F1	10	20	-	0.01	0.02	0.04	0.07	0.12	0.17
PC-I+FA-C2+FA-F2	20	10	0.03	0.07	0.12	0.16	0.19	0.24	0.28
PC-I+FA-C2+FA-F2	15	15	0.02	0.05	0.09	0.13	0.15	0.20	0.25
PC-I+FA-C2+FA-F2	10	20	0.02	0.04	0.07	0.09	0.13	0.16	0.20
PC-I+FA-C2+FA-F3	20	10	-	0.04	0.07	0.11	0.15	0.18	0.24
PC-I+FA-C2+FA-F3	15	15	-	0.02	0.04	0.07	0.12	0.16	0.22
PC-I+FA-C2+FA-F3	10	20	-	0.01	0.03	0.05	0.10	0.14	0.20

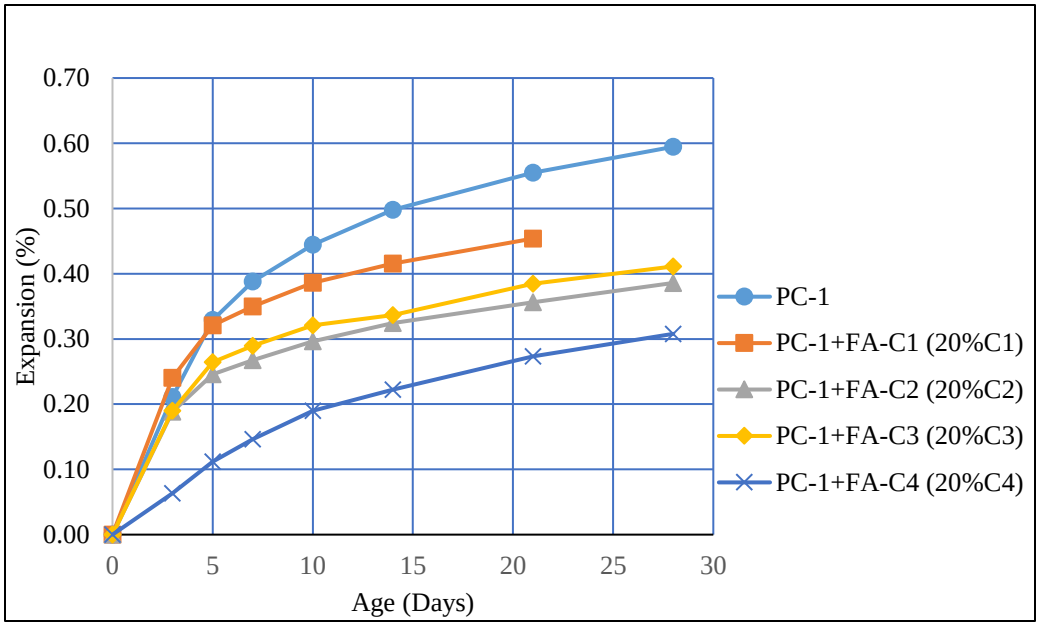

Figure 38. Accelerated Mortar Bar Test Results for Class C Fly Ash Binary Mixtures at 20% Replacement

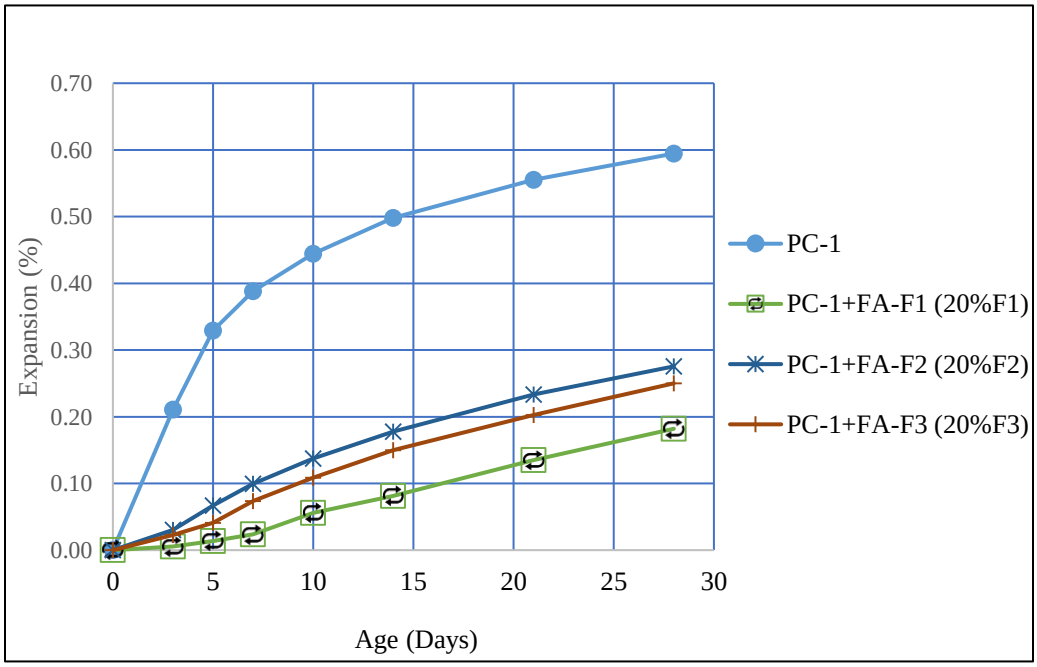

Figure 39. Accelerated Mortar Bar Test Results for Class F Fly Ash Binary Mixtures at 20% Replacement

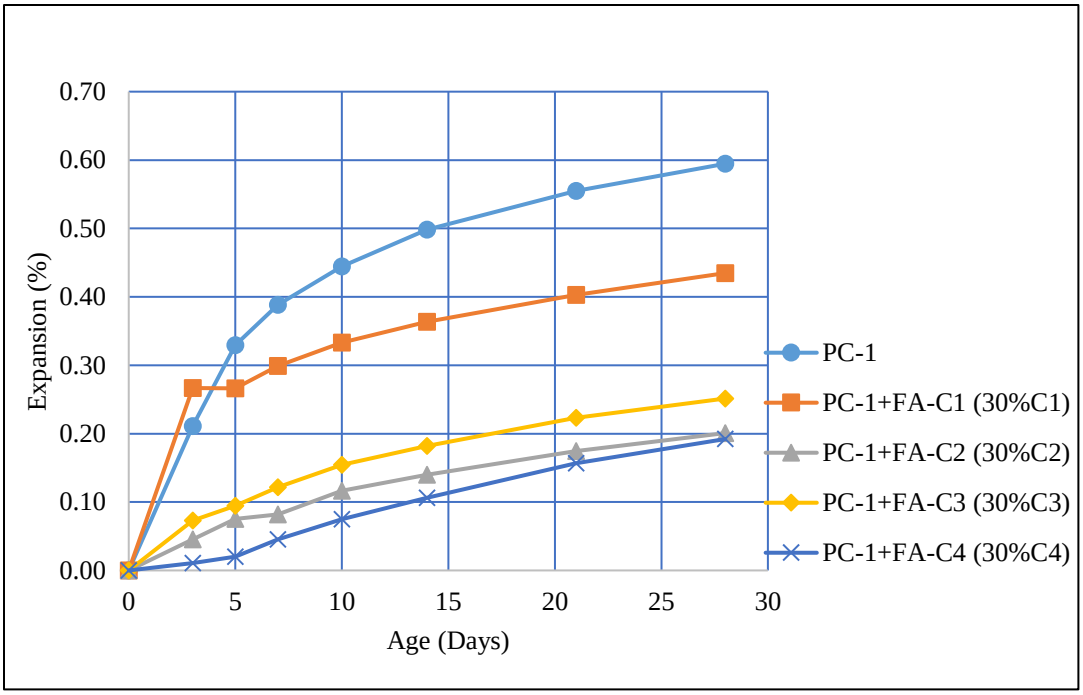

Figure 40. Accelerated Mortar Bar Test Results for Class C fly ash Binary Mixtures at 30% Replacement

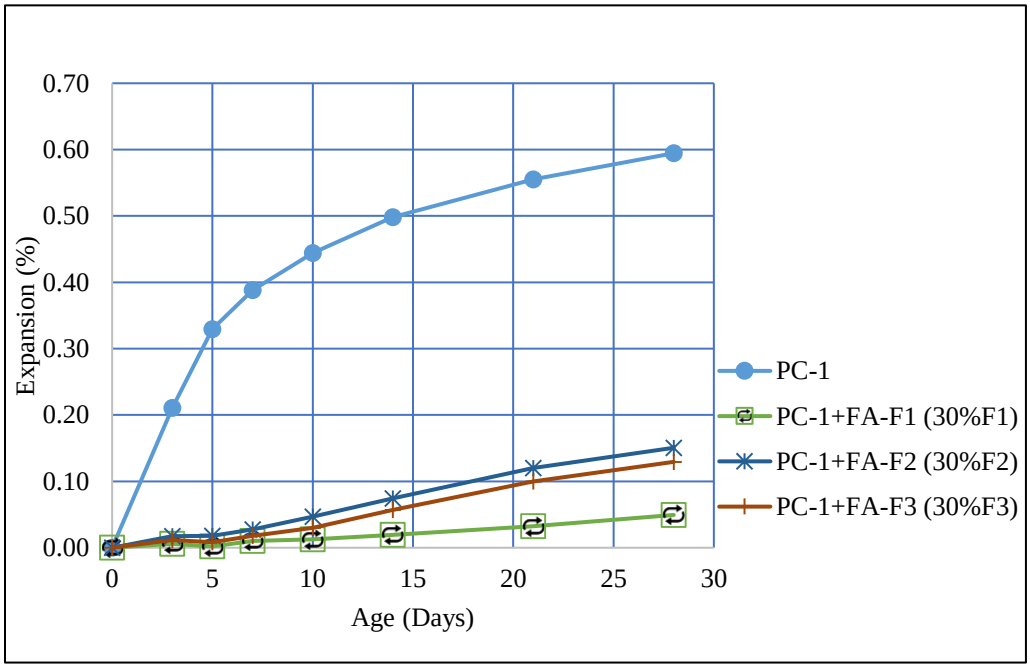

Figure 41. Accelerated Mortar Bar Test Results for Class F Fly Ash Binary Mixtures at 30% Replacement

All Class C binary mixtures at 20% replacement including control expanded beyond 0.10% at 16 days and according to ASTM C1567 this means that they are likely to produce a harmful expansion when used in concrete. However, the control had the highest expansion nearly at all ages considered followed by the mixtures containing 20%C1, 20%C3, 20%C2 and 20% C4. The Class C fly ash mixture with the least expansion at 20% replacement was that involving 20% C4. All the Class C fly ashes produced less expansion at 30% replacement than they did at 20% replacement. However, none of them produced an acceptable expansion of less or equal to 0.10% at 16 days. The binary mixture containing 30%C4 still produced the least expansion followed by binary mixtures containing 30%C2, 30%C3 and 30% C1. Among the Class F binary mixtures at 20% cement replacement, the binary mixture involving 20%F1 was the only Class F mixture with acceptable expansion of 0.10% at 16 days but later exceeded 0.10% expansion after 16 days. According to ASTM C1567, this means that the Class F fly ash F1 at 20% replacement is likely to produce and innocuous expansion in concrete. The control expanded far more than the other Class F fly ash mixtures involving 20%F2 and 20%F3, which had expansions that were above 0.10% at 16 days. All the Class F fly ashes at 30% replacement produced expansions that were less than 0.10% at 16 days. Though, the Class F fly ash F1 produced the least expansion which was below 0.10% all through the ages tested. This was followed by the Class F fly ash F3 and F2 at 30% replacement. The expansion results for ternary mixtures involving the fly ashes C2/F1, C2/F2, and C2/F3 are shown in the Figures 42, 43, and 44 respectively.

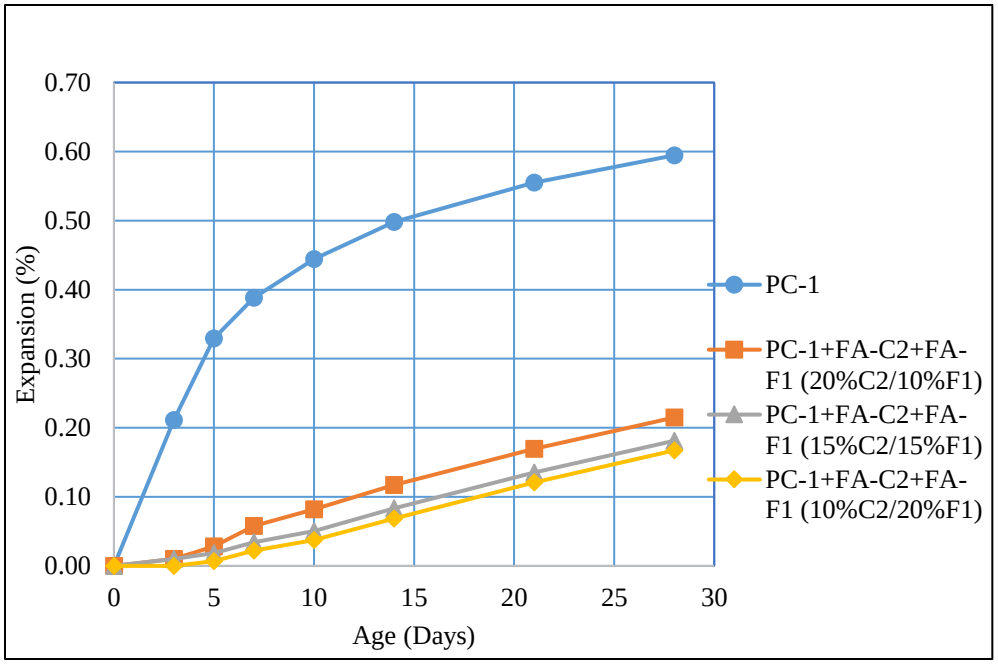

Figure 42. Accelerated Mortar Bar Test Results for Ternary Mixtures Involving Fly Ash C2 and F1

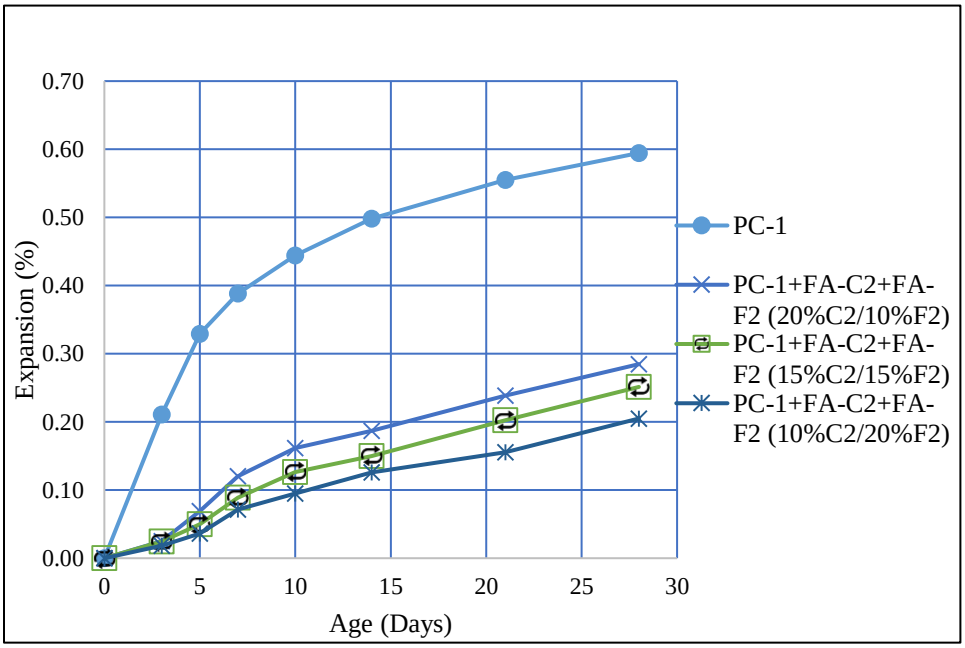

Figure 43. Accelerated Mortar Bar Test Results for Ternary Mixtures Involving Fly Ash C2 and F2

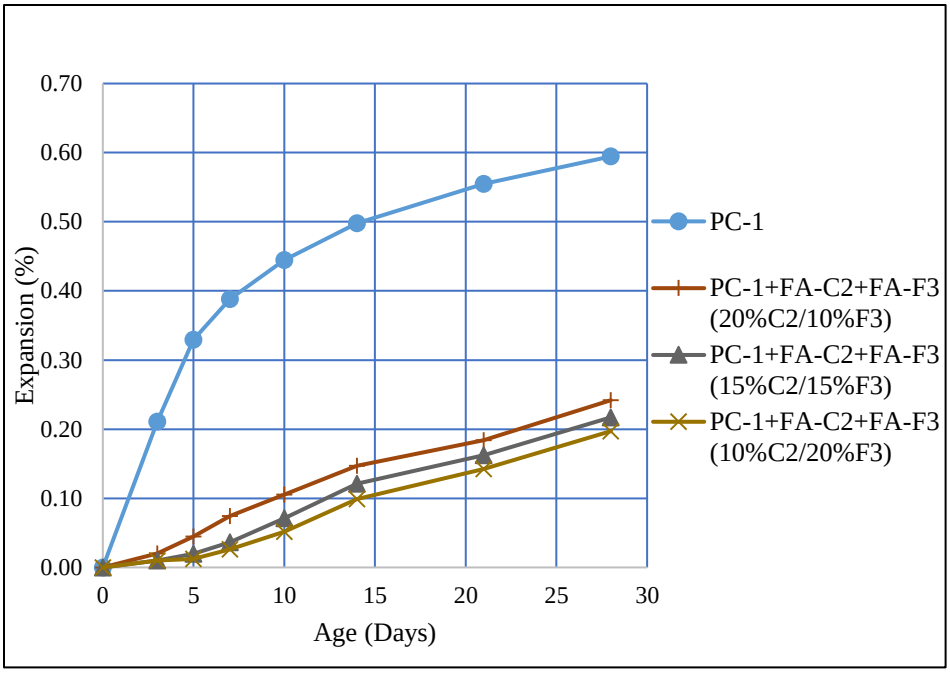

Figure 44. Accelerated Mortar Bar Test Results for Ternary Mixtures Involving Fly Ash C2 and F3

The ternary mixtures involving fly ash C2/F1 performed better than those involving C2/F2 and C2/F3 at the various percentage replacements used in this test. Among all the ternary mixtures, the ternary mixtures involving 15%C2/15%F1 and 10%C2/20%F1 were the only ternary mixtures that produced expansions that were below 0.10% at 16 days. According to ASTM C1567, this means that the ternary blends involving 15%C2/15%F1 and 10%C2/20%F1 are likely to produce a harmless expansion when used in concrete. The ternary mixture involving 20%C2/10%F1 exceeded 0.10% expansion at 16 days. This probably was due to the higher percentage replacement of the Class C fly ash C2.

4.3.2 Concrete prism test (ASTM C1293)

The one-year expansion data for the concrete prism test is given in Table 34. The percentage expansion of the binary and ternary mixtures are shown in Figure 45 and Figure 46 respectively.

Table 34. One Year Expansion Data for Concrete Prism Test

Mixture	**Day 7**	**Day 28**	**Day 56**	**Day 91**	**Day 182**	**Day 273**	**Day 365**
PC-1	0.001%	0.008%	0.041%	0.135%	0.329%	0.372%	0.383%
PC-I+FA-C2 (30%C2)	0.002%	0.002%	0.012%	0.012%	0.016%	0.025%	0.031%
PC-I+FA-F1 (30%F1)	-0.003%	0.002%	0.005%	0.012%	0.014%	0.020%	0.023%
PC-I+FA-F2 (30%F2)	0.001%	0.000%	0.010%	0.011%	0.013%	0.020%	0.019%
PC-I+FA-C2+FA-F1 (20%C2/10%F1)	0.003%	-0.001%	0.008%	0.007%	0.012%	0.019%	0.023%
PC-I+FA-C2+FA-F1 (10%C2/20%F1)	0.003%	0.001%	0.012%	0.010%	0.014%	0.018%	0.017%
PC-I+FA-C2+FA-F2 (20%C2/10%F2)	0.002%	-0.004%	0.006%	0.006%	0.009%	0.016%	0.023%
PC-I+FA-C2+FA-F2 (10%C2/20%F2)	0.002%	-0.002%	0.008%	0.009%	0.012%	0.017%	0.011%

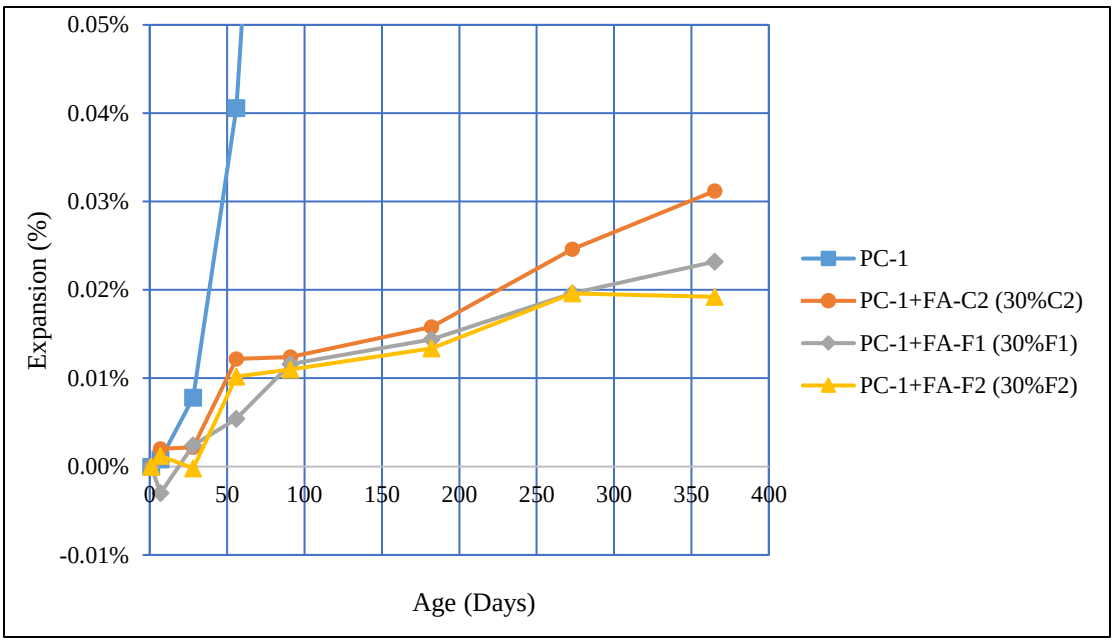

Figure 45. Concrete Prism Test Expansion for Binary Mixtures

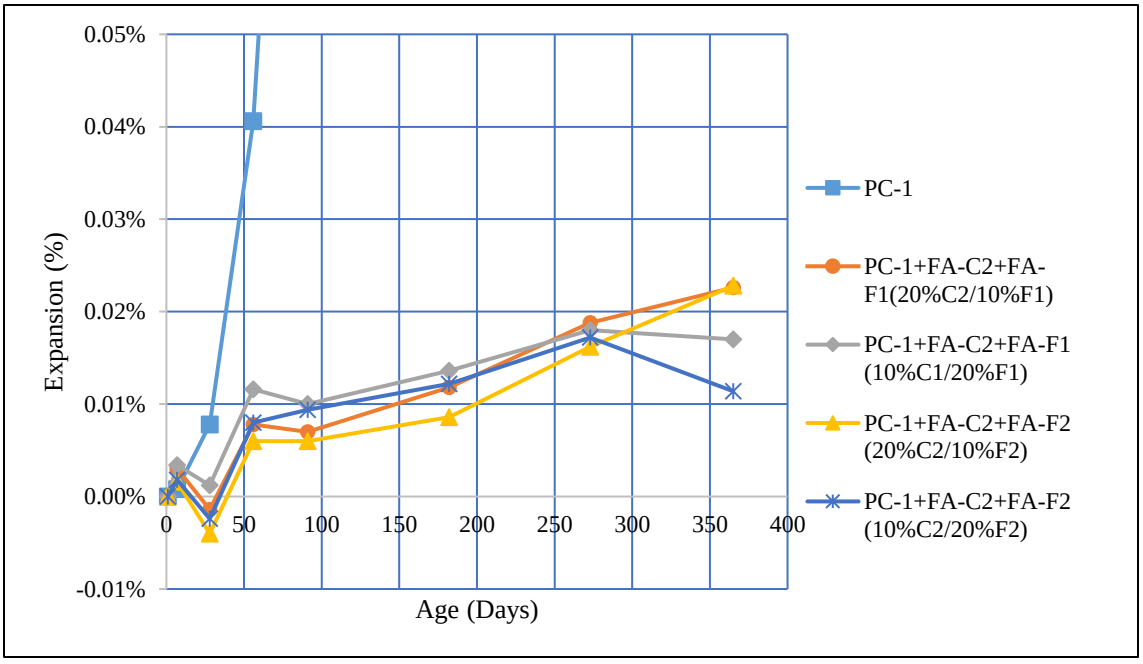

Figure 46. Concrete Prism Test Expansion for Ternary Mixtures

The control expanded up to 0.38% at day 365 which is far more than the 0.04% limit prescribed by ASTM C1293. This affirmed the presence of a deleterious reactive aggregate in the mixtures. The fly ash binary and ternary mixtures exhibited expansions that were less than 0.04% from day 1 through day 365 and hence, confirmed the ability of fly ash to prevent excessive expansion in concrete. However, a more conclusive result on the performance of these fly ash binary and ternary mixtures in preventing excessive expansion would be determined at two years according to ASTM C1293. Among the binary mixtures, the fly ash mixtures containing 30%F1 and 30%F2 performed better than the Class C fly ash C2 at 30% replacement in preventing harmful expansion due to alkali silica reaction. As for the ternary mixtures, the mixture involving 10%C2/20%F2 seemed to have performed better than the rest at day 365 followed by the mixtures involving 10%C2/20%F1, 20%C2/10%F2, and 20%C2/10%F1.

4.3.3 Concrete exposure blocks

The expansion data for the concrete blocks are given in Table 35. The graphical representation of the expansion for the binary and ternary mixtures are shown in Figure 47 and Figure 48 respectively.

Table 35. One Year Expansion Data for Concrete Exposure Blocks

Mixtures	Day 21	Day 49	Day 84	Day 175	Day 266	Day 358
	(%)	(%)	(%)	(%)	(%)	(%)
PC-1	-0.0031	0.0002	0.0018	0.0036	0.0046	0.0057
PC-1+FA-F1 (30%F1)	-0.0032	0.0009	-0.0010	-0.0006	-0.0006	-0.0005
PC-1+FA-F2 (30%F2)	0.0014	0.0012	0.0000	0.0001	0.0004	0.0006
PC-1+FA-C2 (30%C2)	-0.0007	0.0011	-0.0006	0.0005	0.0010	0.0011
PC-1+FA-C2-FA-F1 (20%C2/10%F1)	0.0012	0.0015	-0.0002	0.0000	0.0004	0.0008
PC-1+FA-C2-FA-F1 (10%C2/20%F1)	-0.0009	0.0008	-0.0018	-0.0017	-0.0015	-0.0013
PC-1+FA-C2-FA-F2 (20%C2/10%F2)	-0.0017	0.0015	-0.0023	-0.0020	-0.0017	-0.0013
PC-1+FA-C2-FA-F2 (10%C2/20%F2)	-0.0010	0.0022	-0.0016	-0.0019	-0.0016	-0.0011

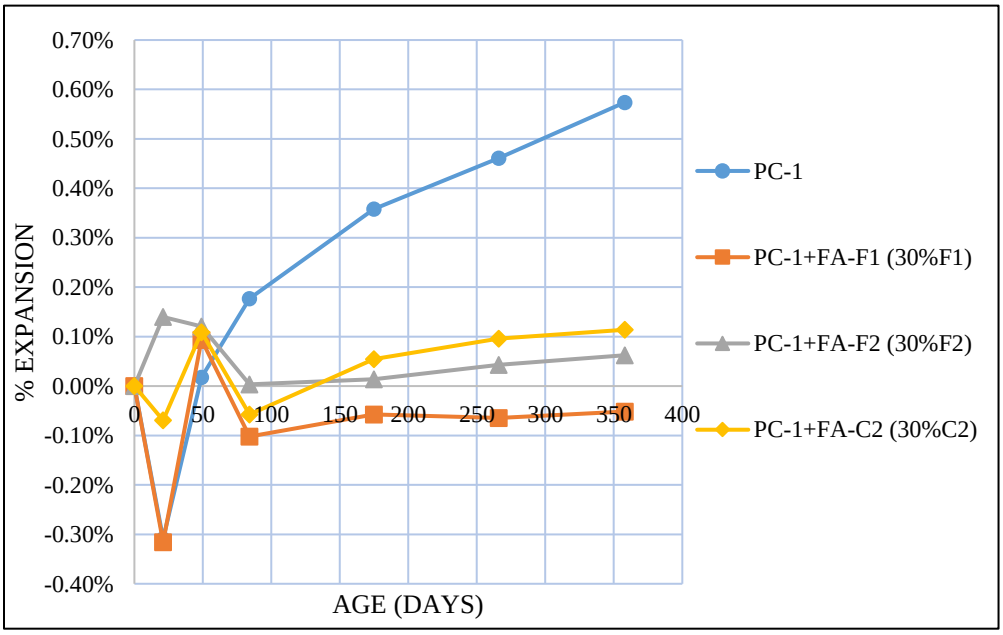

Figure 47. Exposure Blocks Expansion for Binary Mixtures

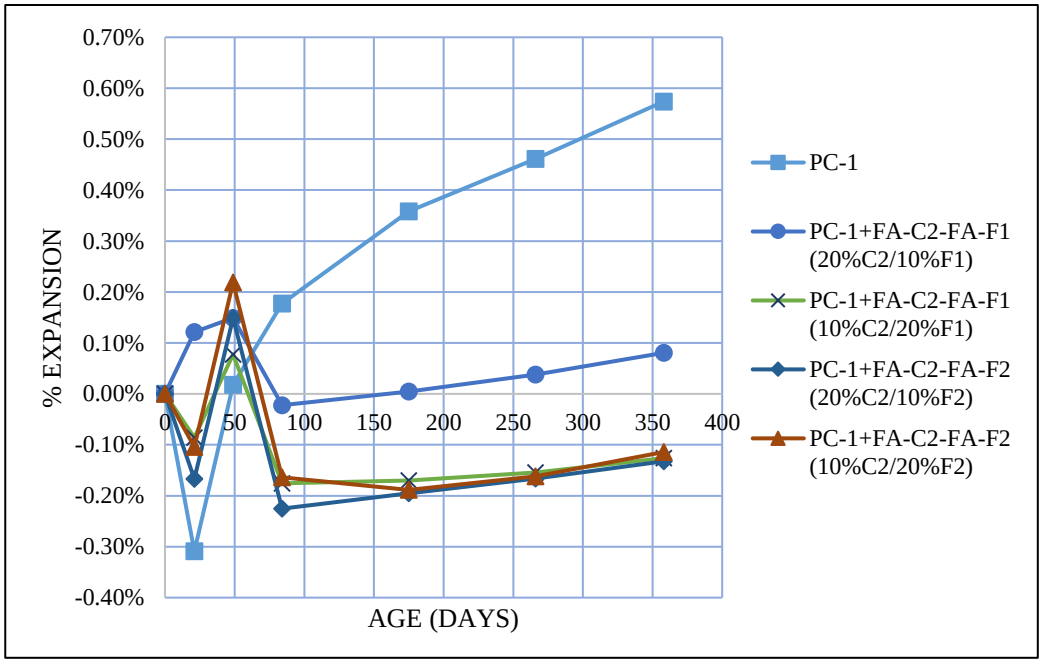

Figure 48. Exposure Blocks Expansion for Ternary Mixtures

As expected, the control block expanded more than the fly ash blocks with an expansion of 0.57% at one year. This high expansion of the control block above the limit 0.04% confirmed the presence of a deleterious reactive aggregate in the mixtures. The fly ash mixtures exhibited an outstanding performance in preventing harmful expansion due to alkali silica reaction. However, there were some observed differences in their ability to prevent harmful expansion due to ASR. Among the blocks produced with binary mixtures that which was produced with 30% F1 outperformed the rest with no expansion at one year. Following the block produced with 30%F1 was that produced with 30% F2 which had an expansion of 0.06% at year one. The block produced with the Class C fly ash C2 at 30% replacement had an expansion of 0.11% at year one and was the highest compared to other binary mixture blocks at one year. Aside the block produced with the ternary mixture containing 20%C2/10% F1, all other ternary mixture blocks had no

expansion at year one. The block produced with the ternary mixture containing 20%C2/10% F1 had an expansion of 0.13% at year one and hence, was the highest among other ternary mixture blocks. Despite the remarkable performance of some of these fly ash mixtures in preventing harmful expansion at one year, a more conclusive result on the performance of these fly ash binary and ternary mixtures in preventing excessive expansion would be determined at two years according to ASTM C1293. Figure 49 shows the pictures of the exposure blocks and rating of cracks observed on each block. The rating starts from 0 through 5, where 0 signifies no crack and 5 the maximum crack observed.

30%F1 (Crack Rating 0)

Control (Crack Rating 5)

30%C2 (Crack Rating 2)

30%F2 (Crack Rating 0)

10%C2/20%F2 (Crack Rating 0)

20%C2/10%F2 (Crack Rating 0)

20%C2/10%F1 (Crack Rating 2)

10%C2/20%F1 (Crack Rating 0)

Figure 49. Rate of Crack Observed on Each Block

4.2.3 Summary of ASR testing

The accelerated mortar bar test result for binary mixtures shows that the Class F fly ashes (F1, F2 and F3) performed better than the Class C fly ashes (C1, C2, C3 and C4) in preventing harmful expansion due to ASR. However, the performance of these fly ashes in preventing harmful expansion due to ASR increased as their replacement levels increased from 20% to 30%. None of the Class C fly ashes produced acceptable expansion at both 20% and 30% replacement levels. The Class F fly ash F1 was the only fly ash among the Class F fly ashes to produce acceptable expansion at a replacement of 20%. However, all the Class F fly ashes (F1, F2 and F3) at 30% replacement level were able to keep expansion within acceptable limit. The effect of blending was also seen in the ternary mixtures containing 15%C2/15% F1 and 10%C2/20%F1 as both were able to keep expansion within acceptable limits at 16 days. The ternary mixtures involving fly ash C2/F1 performed better than those involving C2/F2 and C2/F3 at the various percentage replacements used in this test

The concrete prism test results shows that all binary and ternary mixtures were able to keep expansion below the acceptable limit of 0.04% all through the first year. Though the ternary mixtures appeared to have performed better than the binary mixtures in preventing deleterious expansion due to ASR. As for the binary mixtures, the Class F fly ash binary mixtures involving F1 and F2 performed better that involving the Class C fly ash C2 in preventing harmful expansion due to ASR.

The exposure blocks expansion data for binary mixtures shows that the Class fly ash F1 performed better than the fly ashes F2 and C2 with no expansion at one year. The

ternary mixtures exhibited an outstanding performance with no expansion at one year except for that containing 20%C2/10%F1. Despite the amazing performance exhibited by these fly ashes in CPT and Exposure Blocks Test, a more conclusive result on their performance in preventing excessive expansion due to ASR would be determined at two years according to ASTM C1293.

5. CONCLUSIONS AND RECOMMENDATIONS

5.1 Mechanical Properties

5.1.1 Compressive strength

1. The effect of w/cm ratio on compressive strength was observed from the results as all mixtures tested exhibited higher compressive strength at w/cm ratio of 0.4 compared to their corresponding compressive strengths at a w/cm ratio of 0.45.
2. The effect of curing age was evident as the compressive strength of virtually all mixtures at both w/cm ratio of 0.4 and 0.45 increased as the curing age increased.
3. The efficacy of fly ash in increasing compressive strength was also evident as the fly ash mixtures (binary and ternary) started off with compressive strengths that were lesser than the control but later surpassed the control as they aged due to pozzolanic reactions. The Class C fly ashes C2 and C3 as well as the Class F fly ash F2 exhibited an outstanding performance in compressive strength as they aged both at w/cm ratio of 0.4 and 0.45. This was due to their to their reactivity and high CaO content.
4. The binary mixtures involving fly ashes C2, C3 and F2 exhibited high early strengths at day 7 and continued to increase as their curing age increased. Though the quality of early compressive strength is peculiar to Class C fly ashes, the Class F fly ash F2 exhibited the same quality due to its chemical composition and thus can be applied in cases where early strength is required and a Class F is to be used. However, the Class F fly ash F1 exhibited low compressive strength at early

age and hence can be applied in cases were early strength isn't a challenge, but the heat generated due to high reactivity and early strength gain.

5. The effect of blending on the compressive strength of concrete was also observed as the ternary mixtures containing the more reactive fly ashes C2 and F2 at all tested cement replacement levels and w/cm ratios (0.4 and 0.45) outperformed those containing C2 and F1 which was less reactive.

5.1.2 Splitting tensile strength

1. The effect of curing age was evident as the splitting tensile strengths of virtually all mixtures at both w/cm ratio of 0.4 and 0.45 increased as the curing age increased from day 28 to 91 due to pozzolanic reactions.
2. The performance of the fly ash mixtures in the splitting tensile strength test validates the efficacy of fly ash in improving the splitting tensile strength of concrete due to pozzolanic reaction. For instance. the fly ash binary mixture involving 30%C2 at w/cm ratio of 0.4 exhibited higher splitting tensile strength than the control at day 28 but was exceeded by the control at day 91. Also, the binary mixtures involving 30%C2 and 30%F2 at a w/cm ratio of 0.45 exhibited higher splitting tensile strengths compared to the control at day 28. However, at day 91 the binary mixtures involving 30%C2, 30%C3 and 30% F1 outperformed the control. The fly ash binary mixture with the highest splitting tensile strength at day 91 and w/cm ratio of 0.45 was that involving 30%C2 followed by that containing 30%C3 and 30%F1.
3. Compared to the control mixture, the ternary mixtures showed better splitting tensile strengths at w/cm ratio of 0.45 than they did at w/cm of 0.4. The ternary

mixtures involving 10%C2/20%F2, 15%C2/15%F2 and 20%C2/10%F1 at w/cm ratio of 0.45 exhibited remarkable splitting tensile strength at late age (28 and 91).

5.1.3 Elastic modulus

1. The effect of curing age was evident as the modulus of elasticity of virtually all mixtures at both w/cm ratio of 0.4 and 0.45 increased as the curing age increased from day 28 to 91 due to pozzolanic reactions. The binary mixture involving 30%C2 at w/cm 0.4 exceeded the control at day 91. Also, all binary mixtures at w/cm ratio of 0.45 exceeded the control at day 91 except that involving 20%F1.
2. The blending of the Class C fly ash C2 with the Class F fly ashes F1 and F2 in the ternary mixtures showed remarkable improvements in modulus of elasticity especially in those mixes that involved the reactive fly ashes C2 and F2. For instance, all ternary mixtures at w/cm ratio of 0.4 and 0.45 outperformed the control except that involving 10%C2/20%F1. This was due to the low reactivity and late strength gain of the fly ash F1 which had the highest percentage replacement in the mix. The fly ash ternary mixture involving 20%C2/10%F2 at w/cm of 0.4 exhibited the highest tensile strength at day 91 while that involving 15%C2/15%F2 and 20%C2/10% F2 at w/cm ratio of 0.45 exhibited the highest splitting tensile strength at day 28 and 29 respectively.

5.1.4 Drying shrinkage

1. The drying shrinkages for all ternary mixtures and the binary mixture involving 30%C2 at w/cm ratio of 0.4 were more than the control except for the ternary mixture containing 15%C2/15%F2.

2. The binary mixtures involving 30%C2 and 20%F2 at w/cm ratio of 0.45 exhibited lesser shrinkage compared to the control and other binary mixtures at the same w/cm ratio. This means that these fly ashes could be applied to reduce drying shrinkage in concrete
3. The ternary mixtures involving 20%C2/10%F1 and 10%C2/20%F2 at w/cm ratio of 0.45 exhibited lesser shrinkage compared to the control and other ternary mixtures at the same w/cm ratio.

5.2 Heat of Hydration

1. The variation in temperature affected the peak heat of hydration generated in both paste and mortar mixtures as well as the time taken to attain the peak heat. This was observed in the way the peak heat increased while the corresponding time decreased as the temperature increased from 5^{o}C to 23^{o}C and then 38^{o}C.
2. The control paste and mortar mixtures exhibited higher peak heat at lesser time compared to the fly ash paste and mortar mixtures. This validates the ability of fly ash to reduce the heat of hydration in concrete.
3. The binary mixtures (paste and mortar) containing 30%C2 produced more heat than those containing 30%F2 and 30% F1. However, the binary mixtures containing 30% F2 produced more heat than those containing 30%F1. This indicates the order of reactivity of the fly ashes from the most reactive C2, then F2 and F1 as the least reactive.
4. The ternary paste and mortar mixtures involving a higher percent replacement of the reactive fly ashes C2 and F2 produced more heat compared to those that had a high percent replacement of least reactive fly ash F1. This was seen in the way

the ternary paste and mortar mixtures involving 10%F2/20%C2 and 20%F2/10%C2 produced the most heat compared to other ternary paste and mortar mixtures. The least heat was produced by the ternary paste and mortar mixtures involving 10%C2/20%F1.

5. The ternary paste and mortar mixtures involving 15%C2/15%F1 and 15%C2/15%F2 produced heat that seemed to be between the highest and lowest peak heat produced among the ternary paste and mortar mixtures.

5.3 Alkali Silica Reactivity

5.3.1 Accelerated mortar bar test/Mortar bar test

1. The Class F fly ashes F1, F2 and F3 outperformed the Class C fly ashes C1, C2, C3, and C4 in preventing deleterious expansion due to ASR both at 20% and 30% replacement levels.
2. The binary mixture containing fly ash F1 at 20% replacement was the only binary mixture at 20% replacement that produced acceptable expansion at 16 days. This means that the Class F fly ash F1 at 20% cement replacement is likely to produce and innocuous expansion if used in concrete.
3. The ability of the fly ash binary mixtures in preventing harmful expansion due to ASR was enhanced as the replacement levels increased from 20% to 30%. This was observed in the way all Class F fly ash binary mixtures at 30% replacement produced acceptable expansion of less than 0.10% at 16 days with the Class F fly ash F1 as the most effective. Also, the expansion of the Class C fly ash mixtures due to ASR was reduced at 30% cement replacement.

4. The ternary mixtures involving C2/F1 performed better than those involving C2/F2 and C2/F3. The results shows that the only ternary mixtures that produced acceptable expansions were those involving 15%C2/15%F1 and 10%C2/20%F2. Hence, such proportion could be adopted in cases of insufficiency where blending is required to meet required amount.

5.3.2 Concrete prism test

1. The fly ash binary and ternary mixtures exhibited expansions that were below 0.04% from day 1 through one year. Whereas, the control mixture expanded up to 0.38% at year one. This affirmed the presence of a deleterious reactive aggregate in the concrete as well as the efficacy of fly ashes in preventing harmful expansion due to ASR. However, a two-year expansion data is required to make conclusive assertions as to the performance of these fly ash mixtures in preventing harmful expansions due to ASR.

2. The Class F binary mixtures containing 30%F2 and 30% F1 performed better than the Class C fly ash binary mixture containing 30%C2 in preventing harmful expansions due to ASR. Since the outcome of the CPT is in an agreement with the results of the Accelerated Mortar Bar Test, this Class F fly ashes (F1 and F2) at 30% cement replacement can be used to prevent harmful expansion due to ASR in concrete.

3. The ternary mixture involving 10%C/20%F2 performed better than other ternary mixtures at year one.

5.3.3 Concrete exposure blocks

1. Among the blocks produced with binary mixtures, the block produced with 30% F1 had no expansion at year one. Whereas those produced with 30%F2 and 30%C2 had expansions of 0.06% and 0.11% respectively at year one. The fly ash F1 at 30% replacement was the most effective in preventing harmful expansions due to ASR. This was followed by the Class F fly ash F2 at 30% replacement.
2. All blocks produced with ternary mixtures had no expansion at year one except that containing 20%C2/10%F1 which had an expansion of 0.13% at year one. This higher expansion exhibited by the ternary mixture containing 20%C2/10%F1 was as result of the higher percent replacement of the Class C fly ash C2 in the mix. This also means that in achieving a ternary blend for application to mitigate ASR, the blend involving 20%C2/10%F1 should be avoided. However, a two-year expansion data is also required to make conclusive assertions as to the performance of these fly ash mixtures in preventing harmful expansions due to ASR.

5.4 Recommendation for Future Work

Additional work could be carried out to evaluate the reactivity and performance of the various fly ashes in improving mechanical properties and mitigating ASR by blending them with other SCMs like slag, silica fume, metakaolin etc. Also, higher percentage replacement levels and extended test periods could be implemented for the CPT and large exposure concrete blocks to ascertain the long term performance of the fly ashes due pozzolanic reactions.

REFERENCES

Ahmaruzzaman, M. (2010). A review on the utilization of fly ash. *Progress in Energy and Combustion Science*, 327-363.

Antiohos, S. K., Papadakis, V. G., Chaniotakis, E., & Tsimas, S. (2007). Improving the performance of ternary blended cements by mixing different types of fly ashes. *Cement and Concrete Research, 37*, 877-855.

ASTM International. (2013). *ASTM C1567-13 Standard Test Method for Determining the Potential Alkali-Silica Reactivity of Combinations of Cementitious Materials and Aggregate (Accelerated Mortar-Bar Method).* Retrieved from https://doi-org.libproxy.txstate.edu/10.1520/C1567-13

ASTM International. (2014). *ASTM C469/C469M-14 Standard Test Method for Static Modulus of Elasticity and Poisson's Ratio of Concrete in Compression.* Retrieved from https://doi-org.libproxy.txstate.edu/10.1520/C0469_C0469M-14

ASTM International. (2014). *ASTM C1260-14 Standard Test Method for Potential Alkali Reactivity of Aggregates (Mortar-Bar Method).* Retrieved from https://doi-org.libproxy.txstate.edu/10.1520/C1260-14

ASTM International. (2015). *ASTM C143/C143M-15a Standard Test Method for Slump of Hydraulic-Cement Concrete.* Retrieved from https://doi-org.libproxy.txstate.edu/10.1520/C0143_C0143M-15A

ASTM International. (2015*). ASTM C617/C617M-15 Standard Practice for Capping Cylindrical Concrete Specimens.* Retrieved from https://doi-org.libproxy.txstate.edu/10.1520/C0617_C0617M-15

ASTM International. (2016). *ASTM C109/C109M-16a Standard Test Method for Compressive Strength of Hydraulic Cement Mortars (Using 2-in. or [50-mm] Cube Specimens)*. Retrieved from https://doi-org.libproxy.txstate.edu/10.1520/C0109_C0109M-16A

ASTM International. (2016). *ASTM C192/C192M-16a Standard Practice for Making and Curing Concrete Test Specimens in the Laboratory*. Retrieved from https://doi-org.libproxy.txstate.edu/10.1520/C0192_C0192M-16A

ASTM International. (2016). *ASTM C1697-16 Standard Specification for Blended Supplementary Cementitious Materials.* Retrieved from https://doi-org.libproxy.txstate.edu/10.1520/C1697-16

ASTM International. (2017). *ASTM C138/C138M-17a Standard Test Method for Density (Unit Weight), Yield, and Air Content (Gravimetric) of Concrete.* Retrieved from https://doi-org.libproxy.txstate.edu/10.1520/C0138_C0138M-17A

ASTM International. (2017). *ASTM C157/C157M-17 Standard Test Method for Length Change of Hardened Hydraulic-Cement Mortar and Concrete*. Retrieved from https://doi-org.libproxy.txstate.edu/10.1520/C0157_C0157M-17

ASTM International. (2017). *ASTM C231/C231M-17a Standard Test Method for Air* Content of Freshly Mixed Concrete by the Pressure Method. Retrieved from https://doi-org.libproxy.txstate.edu/10.1520/C0231_C0231M-17A

ASTM International. (2017). *ASTM C496 /C496M-17 Standard Test Method for Splitting Tensile Strength of Cylindrical Concrete Specimens.* Retrieved from https://doi-org.libproxy.txstate.edu/10.1520/C0496_C0496M-17

ASTM International. (2017). *ASTM C618-17 Standard Specification for Coal Fly Ash and Raw or Calcined Natural Pozzolan for Use in Concrete.* Retrieved from https://doi-org.libproxy.txstate.edu/10.1520/C0618-17

ASTM International. (2017). *ASTM C1679-17 Standard Practice for Measuring Hydration Kinetics of Hydraulic Cementitious Mixtures Using Isothermal Calorimetry.* Retrieved from https://doi-org.libproxy.txstate.edu/10.1520/C1679-17

ASTM International. (2018). *ASTM C39/C39M-18 Standard Test Method for Compressive Strength of Cylindrical Concrete Specimens.* Retrieved from https://doi-org.libproxy.txstate.edu/10.1520/C0039_C0039M-18

ASTM International. (2018). *ASTM C1293-18a Standard Test Method for Determination of Length Change of Concrete Due to Alkali-Silica Reaction.* Retrieved from https://doi-org.libproxy.txstate.edu/10.1520/C1293-18A

ASTM International. (2019). *ASTM C125-19 Standard Terminology Relating to Concrete and Concrete Aggregates.* Retrieved from https://doi-org.libproxy.txstate.edu/10.1520/C0125-19

Aughenbaugh, K. L., Stutzman, P., & Juenger, M. C. G. (2016). Identifying Glass Compositions in Fly Ash. *Frontiers in Materials*, *3*(1). doi:10.3389/fmats.2016.00001

Aydin, S., Karatay, C., & Baradan, B. (2010). The effect of grinding process on mechanical properties and alkali-silica reaction resistance of fly ash incorporated cement mortars. *Powder Technology, 197,* 68-72.

Chen, J. (2016). A study on the properties of high performance concrete with compound mineral admixtures. 17, 48.41-48.49.

Deboucha, W., Leklou, N., Khelidj, A., & Oudjit, M. N. (2017). Hydration development of mineral additives blended cement using thermogravimetric analysis (TGA): Methodology of calculating the degree of hydration. *Construction and Building Materials, 146*, 687-701. doi: https://doi.org/10.1016/j.conbuildmat.2017.04.132

Dhole, R., Thomas, M. D. A., Folliard, K. J., & Drimalas, T. (2011). Sulfate resistance of mortar mixtures of high-calcium fly ashes and other pozzolans. *ACI Materials Journals, 108*, 645-654.

Diaz-Loya, I., Juenger, M., Seraj, S., & Minkara, R. (2017). Extending supplementary cementitious material resources: Reclaimed and remediated fly ash and natural pozzolans. *Cement and concrete composites*. doi:https://doi.org/10.1016/j.cemconcomp.2017.06.011

Drimalas, T., Ideker, I. H., Bentivegna, A. F., Folliard, K. J., Fournier, B., & Thomas, M. D. A. (2012). The long-term monitoring of large-scale concrete specimens containing lithium salts to mitigate alkali-silica reaction. *ACI Materials Journals, 289*, 1-17.

Erdem, T. K., & Kirca, O. (2008). Use of binary and ternary blends in high strength concrete. *Construction and Building Materials, 22*, 1477-1483.

Fly Ash Supply. (2010). *Technical Advisory- Texas Department of Transportation*.

Folliard, K., Hover, K., Harris, N., Ley, T. M., & Naranjo, A. (2009). *Effects of Texas fly ash on air-entrainment in concrete: comprehensive report*. Retrieved from http://ctr.utexas.edu/wp-content/uploads/pubs/0_5207_1.pdf

García-Lodeiro, I., Palomo, A., & Fernández-Jiménez, A. (2007). Alkali–aggregate reaction in activated fly ash systems. *Cement and Concrete Research, 37*, 175-183.

Gudmundsson , G., & Olafsson, H. (1999). Alkali-silica reactions and silica fume 20 years of experience in Iceland. *Cement and Concrete Research, 29*, 1289-1297.

Ichikawa, T. (2009). Alkali–silica reaction, pessimum effects and pozzolanic effect. *Cement and Concrete Research, 39*(8), 716-726.

Kadasamy, S., & Shehata, M. H. (2014). The capacity of ternary blends containing slag and high-calcium fly ash to mitigate alkali silica reaction. *Cement and concrete composites, 49*, 92-99.

Kocak, Y., & Nas, S. (2014). The effect of using fly ash on the strength and hydration characteristics of blended cements. *Construction and Building Materials, 73*, 25-32. doi:https://doi.org/10.1016/j.conbuildmat.2014.09.048

Kovler, K., & Roussel, N. (2011). Properties of fresh and hardened concrete. *Cement and Concrete Research, 41*(7), 775-792.

Kruse, K., Jasso, A., Folliard, K., Ferron, R., Juenger, M., & Drimalas, T. (2013). *Characterizing Fly Ash* (FHWA/TX-13/0-6648-1). Retrieved from https://library.ctr.utexas.edu/ctr-publications/0-6648-1.pdf

Lane, D. S., & Ozyildirim, C. (1999). Preventive measures for alkali-silica reactions (binary and ternary systems). *Cement and Concrete Research, 29*, 1281-1288.

Latifee, E. R. (2016). State-of-the-art report on alkali silica reactivity mitigation effectiveness using different types of fly ashes. *Journal of Materials*, 2016, 1-7.

Latifee, E. R., & Rangaraju, P. R. (2015). Miniature Concrete Prism Test: Rapid Test Method for Evaluating Alkali-Silica Reactivity of Aggregates. *Journal of Materials in Civil Engineering, 27*(7), 04014215. doi:doi:10.1061/(ASCE)MT.1943-5533.0001183

Marinković, S., & Dragaš, J. (2018). 11 - Fly ash. In R. Siddique & P. Cachim (Eds.), *Waste and Supplementary Cementitious Materials in Concrete* (pp. 325-360): Woodhead Publishing.

Mather, B. (1999). How to make concrete that will not suffer deleterious alkali-silica reaction. *Cement and Concrete Research, 29*, 1277-1280.

Mele, C. (2018). What Is Coal Ash and Why Is It Dangerous?

Mindess, S., Young, F. J., & Darwin, D. (2003). *Concrete*. New Jersey: Prentice Hall.

Monteagudo, S. M., Moragues, A., Gálvez, J. C., Casati, M. J., & Reyes, E. (2014). The degree of hydration assessment of blended cement pastes by differential thermal and thermogravimetric analysis. Morphological evolution of the solid phases. *Thermochimica Acta, 592*, 37-51. doi:https://doi.org/10.1016/j.tca.2014.08.008

Naik, T. R., Singh, S. S., & Ramme, B. W. (1998). Mechanical properties and durability of concrete made with blended fly ash. *Materials Journal, 95*(4), 454-462.

Nath, P., & Sarker, P. (2011). Effect of Fly Ash on the Durability Properties of High Strength Concrete. *Procedia Engineering, 14*, 1149-1156. doi:https://doi.org/10.1016/j.proeng.2011.07.144

Neville, A. M. (2011). *Properties of Concrete* (Fifth ed.). Harlow, England: Pearson.

Pandey, V. C., & Singh, N. (2010). Impact of fly ash incorporation in soil systems. *Agriculture, ecosystems & environment, 136*(1-2), 16-27.

Ramezanianpour, A. A. (2014). Fly Ash. In *Cement Replacement Materials: Properties, Durability, Sustainability* (pp. 47-156). Berlin, Heidelberg: Springer Berlin Heidelberg.

Ramme, B. W., & Tharaniyil, M. P. (2013). *Coal combustion product utilization handbook*. Wisconsin: We Energies.

Rashad, A. M. (2015). A brief on high-volume Class F fly ash as cement replacement – A guide for Civil Engineer. *International Journal of Sustainable Built Environment, 4*(2), 278-306. doi:https://doi.org/10.1016/j.ijsbe.2015.10.002

Ritter, S. K. (2016). A New Life For Coal Ash. *94*(7), 10-14.

Saha, A. K. (2018). Effect of class F fly ash on the durability properties of concrete. *Sustainable Environment Research, 28*(1), 25-31. doi:https://doi.org/10.1016/j.serj.2017.09.001

Shafaatian, S. M. H., Akhavan , A., Maraghechi, H., & Rajabipour, F. (2013). How does fly ash mitigate alkali-silica reaction (ASR) in acceletrated mortar bar test (ASTM C1567)? *Cement & Cocncrete Composites, 37*, 143-153.

Shaheen, S. M., Hooda, P. S., & Tsadilas, C. D. (2014). Opportunities and challenges in the use of coal fly ash for soil improvements – A review. *Journal of Environmental Management, 145*, 249-267. doi:https://doi.org/10.1016/j.jenvman.2014.07.005

Shaikh, F. U. A., & Supit, S. W. M. (2015). Compressive strength and durability properties of high volume fly ash (HVFA) concretes containing ultrafine fly ash (UFFA). *Construction and Building Materials, 82*, 192-205. doi:https://doi.org/10.1016/j.conbuildmat.2015.02.068

Skaropoulou, A., Sotiriadis, K., Kakali, G., & Tsivilis, S. (2013). Use of mineral admixtures to improve the resistance of limestone cement concrete against thaumasite form of sulfate attack. *Cement and concrete composites, 37*, 267-275.

Tang, S. W., Cai, X. H., He, Z., Shao, H. Y., Li, Z. J., & Chen, E. (2016). Hydration process of fly ash blended cement pastes by impedance measurement. *Construction and Building Materials, 113*, 939-950. doi:https://doi.org/10.1016/j.conbuildmat.2016.03.141

Thomas, M., Fournier, B., Folliard, K., Ideker, J., & Shehata, M. (2006). Test methods for evaluating preventive measures for controlling expansion due to alkali–silica reaction in concrete. *Cement and Concrete Research, 36*(10), 1842-1856.

Thomas, M. D. A., Shehata, M. H., Shashiprakash, S. G., Hopkins, D. S., & Cail, K. (1999). Use of ternary cementitious systems containing silica fume and fly ash in concrete. *Cement and Concrete Research, 29*, 1207-1214.

Wadsö, L. (2001). *Isothermal calorimetry for the study of cement hydration*. Retrieved from https://lucris.lub.lu.se/ws/files/4471618/4388332.pdf

Wang, X. Y., & Park, K. B. (2015). Analysis of compressive strength development of concrete containing high volume fly ash. *Construction and Building Materials, 98*, 810-819. doi:https://doi.org/10.1016/j.conbuildmat.2015.08.099

WeatherUnderground. (2019). Local Weather History. Retrieved June 23, 2019 https://www.wunderground.com/history/monthly/us/tx/san-marcos/KAUS/date/2019-6?cm_ven=localwx_history

Where Has the Fly Ash Gone? (2012). *Construction and Materials Tips - Texas Department of Transportation*.

Xiong, X., & Van Breugel, K. (2001). Isothermal calorimetry study of blended cements and its application in numerical simulations. *Heron, 46*(3), 150-159.

Zeng, Q., Li, K., Fen-chong, T., & Dangla, P. (2012). Determination of cement hydration and pozzolanic reaction extents for fly-ash cement pastes. *Construction and Building Materials, 27*(1), 560-569. doi:https://doi.org/10.1016/j.conbuildmat.2011.07.007